AD NUMBER

AD813324

LIMITATION CHANGES

TO:

Approved for public release; distribution is unlimited.

FROM:

**Distribution authorized to U.S. Gov't. agencies and their contractors;
Administrative/Operational Use; APR 1967. Other requests shall be referred to Arnold Engineering Development Center, Arnold AFS, TN.**

AUTHORITY

AEDC ltr, 12 Oct 1972

AEDC-TR-67-59

cy 1

WIND TUNNEL STUDY OF THE EFFECT OF MOL PROTUBERANCES ON STATIC-STABILITY AND PRESSURE DISTRIBUTION CHARACTERISTICS FOR SMALL-SCALE MODELS OF THE TITAN III/MOL LAUNCH VEHICLE

Charles D. Riddle and Tommy O. Shadow
ARO, Inc.

April 1967

PROPULSION WIND TUNNEL FACILITY
ARNOLD ENGINEERING DEVELOPMENT CENTER
AIR FORCE SYSTEMS COMMAND
ARNOLD AIR FORCE STATION, TENNESSEE

NOTICES

When U. S. Government drawings specifications, or other data are used for any purpose other than a definitely related Government procurement operation, the Government thereby incurs no responsibility nor any obligation whatsoever, and the fact that the Government may have formulated, furnished, or in any way supplied the said drawings, specifications, or other data, is not to be regarded by implication or otherwise, or in any manner licensing the holder or any other person or corporation, or conveying any rights or permission to manufacture, use, or sell any patented invention that may in any way be related thereto.

Qualified users may obtain copies of this report from the Defense Documentation Center.

References to named commercial products in this report are not to be considered in any sense as an endorsement of the product by the United States Air Force or the Government.

ERRATA

AEDC-TR-67-59, April 1967
(UNCLASSIFIED REPORT)

WIND TUNNEL STUDY OF THE EFFECT OF MOL PROTUBERANCES ON STATIC-STABILITY AND PRESSURE DISTRIBUTION CHARACTERISTICS FOR SMALL-SCALE MODELS OF THE TITAN III/MOL LAUNCH VEHICLE

Charles D. Riddle and Tommy O. Shadow, ARO, Inc.

Arnold Engineering Development Center
Air Force Systems Command
Arnold Air Force Station, Tennessee

pp. 86-87 Pressure coefficients plotted in Fig. 55 are partially in error. Specifically, coefficients at x/D stations 2.82 and 3.65 are incorrect for the 270-deg and 334-deg rays at Mach numbers 0.60 through 1.40. Figure 55 a and b should be replaced by the figures on the reverse of this page.

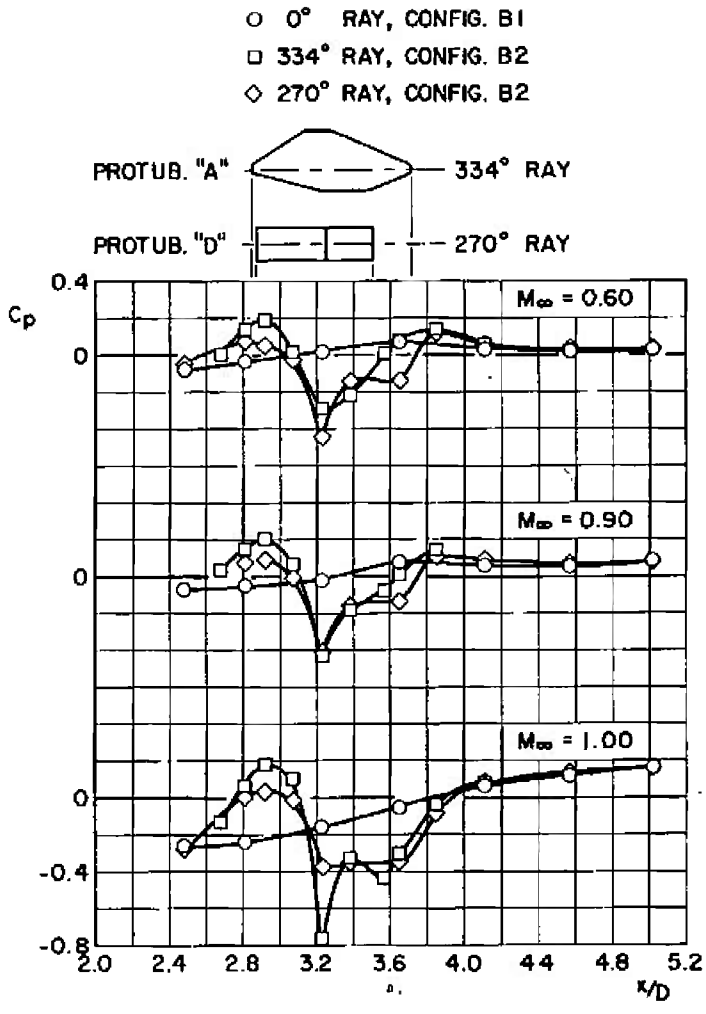
○ 0° RAY, CONFIG. B1
□ 334° RAY, CONFIG. B2
◇ 270° RAY, CONFIG. B2
PROTUB. "A"
334° RAY
PROTUB. "D"
270° RAY
C_p
0.4
0
0
0
-0.4
-0.8
M_∞ = 0.60
M_∞ = 0.90
M_∞ = 1.00
2.0
2.4
2.8
3.2
3.6
4.0
4.4
4.8
5.2
x/D
a.

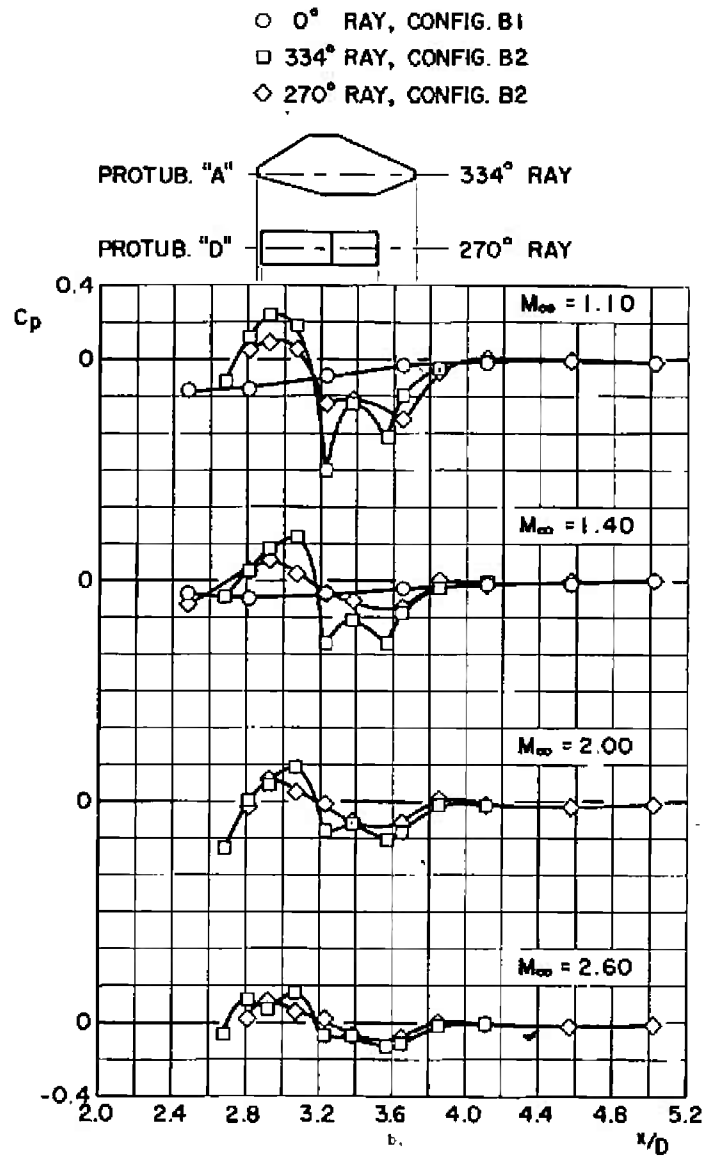
○ 0° RAY, CONFIG. B1
□ 334° RAY, CONFIG. B2
◇ 270° RAY, CONFIG. B2
PROTUB. "A"
334° RAY
PROTUB. "D"
270° RAY
C_p
0.4
0
0
0
-0.4
M_∞ = 1.10
M_∞ = 1.40
M_∞ = 2.00
M_∞ = 2.60
2.0
2.4
2.8
3.2
3.6
4.0
4.4
4.8
5.2
x/D
b.

WIND TUNNEL STUDY OF THE EFFECT OF MOL PROTUBERANCES ON STATIC-STABILITY AND PRESSURE DISTRIBUTION CHARACTERISTICS FOR SMALL-SCALE MODELS OF THE TITAN III/MOL LAUNCH VEHICLE

Charles D. Riddle and Tommy O. Shadow
ARO, Inc.

AF - AEDC
Arnold AFS Tenn

FOREWORD

The work reported herein was done at the request of the Space Systems Division (SSD), Air Force Systems Command (AFSC), for the Aerospace Division of the Martin-Marietta Corporation under Program Elements 63409404 /632A and 64409094/624A.

The test results presented were obtained by ARO, Inc. (a subsidiary of Sverdrup & Parcel and Associates, Inc.), contract operator of the Arnold Engineering Development Center (AEDC), AFSC, Arnold Air Force Station, Tennessee, under Contract AF40(600)-1200. The test was conducted under ARO Project No. PT0753 from December 6 to 30, 1966. The manuscript was submitted for publication on March 3, 1967.

Information in this report is embargoed under the Department of State International Traffic in Arms Regulations. This report may be released to foreign governments by departments or agencies of the U. S. Government subject to approval of the Space Systems Division (SSBDM), or higher authority within the Department of the Air Force. Private individuals or firms require a Department of State export license.

This technical report has been reviewed and is approved.

Richard W. Bradley
Lt Col, USAF
AF Representative, PWT
Directorate of Test

Leonard T. Glaser
Colonel, USAF
Director of Test

ABSTRACT

Force, pressure, and acoustical data were obtained for the Titan III/MOL (Manned Orbiting Laboratory) launch vehicle in Tunnels 16T and 16S of the Propulsion Wind Tunnel Facility. The primary objective of the test was to determine the effect of MOL protuberances on stability and axial-force coefficients and on surface pressure distributions. The force data were measured using three balances which sensed aerodynamic loads separately on the MOL-Gemini section, on the composite vehicle, and on one solid rocket motor. Mach number was varied from 0.60 to 3.00. Protuberance variations produced measurable changes in stability and axial-force characteristics for the MOL-Gemini section only. Surface pressures near the protuberances returned to protuberance-free trends within approximately 0.5-core diameters downstream of a protuberance trailing edge. (AFR 310-2, Stmt. 2)

CONTENTS

APPENDIXES

I. ILLUSTRATIONS

Figure

Page

II. TABLES

NOMENCLATURE

C_A	Total axial-force coefficient, $\frac{\text{measured axial force}}{q_\infty S}$
$C_{A,b}$	Base axial-force coefficient, $\sum_i \left(\frac{p_\infty - p_{b_i}}{q_\infty}\right) \frac{S_i}{S}$ (see Section 2.3)
$C_{A,F}$	Forebody axial-force coefficient, $C_A - C_{A,b}$
C_ℓ	Rolling-moment coefficient, $\frac{\text{measured rolling moment}}{q_\infty SD}$
C_m	Pitching-moment coefficient (see Fig. 7 for moment reference locations), $\frac{\text{measured pitching moment}}{q_\infty SD}$
C_{m_α}	Pitching-moment curve slope, rate of change of pitching-moment coefficient with angle of attack $(dC_m/d\alpha)$ evaluated at $\alpha = 0$ deg, per degree
C_N	Normal-force coefficient, $\frac{\text{measured normal force}}{q_\infty S}$
C_n	Yawing-moment coefficient, $\frac{\text{measured yawing moment}}{q_\infty SD}$
C_{n_β}	Yawing-moment curve slope, rate of change of yawing-moment coefficient with sideslip angle $(dC_n/d\beta)$ evaluated at $\beta = 0$ deg, per degree
C_p	Pressure coefficient, $\frac{p_\ell - p_\infty}{q_\infty}$
C_Y	Side-force coefficient, $\frac{\text{measured side force}}{q_\infty S}$
D	Core diameter (reference diameter), 0.535 ft
M_∞	Free-stream Mach number

p_{b_i}	Average base pressure for the i-th section, psf
p_ℓ	Static pressure measured on the pressure model, psf
p_∞	Free-stream static pressure, psf
q_∞	Free-stream dynamic pressure, psf
Re/ft	Reynolds number per foot, V_∞/ν_∞
S	Core cross-sectional area (reference area), 0.225 ft^2
S_i	Effective base area of the i-th section, ft^2
V_∞	Free-stream velocity, ft/sec
x	Distance of pressure model orifices from model nose, ft
x_{np_α}	Longitudinal neutral-point location measured in reference diameters from the moment reference point (see Fig. 7), dC_m/dC_n at α = 0 deg, positive forward
x_{np_β}	Lateral neutral-point location measured in reference diameters from the moment reference point (see Fig. 7), dC_n/dC_Y at β = 0 deg, positive forward
α	Model angle of attack with respect to the tunnel centerline, deg
β	Model sideslip angle with respect to the tunnel centerline, deg
ν_∞	Kinematic viscosity of the free stream, ft^2/sec
θ	Roll orientation of surface pressure orifices (see Fig. 6), deg

SUBSCRIPTS

2	MOL-Gemini
3	Composite model
4	Left SRM

SECTION I
INTRODUCTION

Force, pressure, and acoustical data were obtained for models of the Titan III/MOL launch vehicle in the Propulsion Wind Tunnels, Supersonic (16S) and Transonic (16T) of the Propulsion Wind Tunnel Facility (PWT). The models consisted of the Titan III/MOL launch vehicle supporting either a basic or a modified Gemini capsule. The subject investigation was an extension of a previous test reported in Ref. 1. The present models differed from those tested previously in that several protuberances were added to the MOL (Manned Orbiting Laboratory) section.

The purpose of the present entry was to assess the effects of the additional protuberances on vehicle stability and on steady and unsteady surface pressure environments. Component forces and moments were measured at Mach numbers from 0.60 to 3.00. Pressure data were obtained at Mach numbers from 0.60 to 2.60.

SECTION II
APPARATUS

2.1 TEST FACILITIES

Tunnel 16T is a variable density wind tunnel capable of operation from Mach numbers 0.55 to 1.6. The test section is 16 ft square in cross section and is lined with perforated plates to allow continuous operation with minimum wall interference.

Tunnel 16S is a variable density wind tunnel capable of operation between Mach numbers 1.7 to 3.2. The test section is 16 ft square in cross section.

Details of the test sections showing model location and support strut arrangement are presented in Fig. 1. A more extensive description of each tunnel is given in Ref. 2.

2.2 MODEL GEOMETRY

The Titan III/MOL launch vehicle combines a Titan III 120-in.-diam core and two 120-in.-diam, strap-on solid rocket motors (SRM's) with the MOL. The MOL consists of a 120-in.-diam cylinder and is mounted

aft of a Gemini capsule. Separate, 0.0535-scale force and pressure models were tested. Each model consisted of the launch vehicle with either basic or modified external geometry for the Gemini capsule. Details of the launch vehicle with a basic Gemini shape are shown in Fig. 2. Variations of Gemini shape and MOL protuberance orientation defined a total of five configurations for which data were obtained. A sketch of the two Gemini versions and configuration photographs are shown in Fig. 3. Excepting protuberance orientation, the launch vehicle aft of the Gemini section was unchanged for the five configurations. The protuberances are described in Fig. 4 and were of two types. These were (1) the four geometrically identical attitude control rockets and (2) the five faired protuberances labeled A through E. Protuberances A through E are sketched in the normal launch position in Fig. 4a. The following table identifies and describes the five configurations:

Config.	Gemini Version	Protuberances					Protub. Position	Attitude Control Rockets
		A	B	C	D	E		
B1	Basic	Off	Off	Off	Off	Off	-	On
B2	↓	On	On	On	On	On	Normal	↓
B3	↓	↓	↓	↓	↓	↓	Rotated 180 deg	↓
M1	Modified	Off	Off	Off	Off	Off	-	Off
M2	↓	↓	↓	↓	On	On	Normal	On

Configuration B1 was tested both during the present entry and during the Ref. 1 investigation. The external geometry of configuration B1 differed slightly for the two entries, in that the Ref. 1 configuration included a horizon sensor protuberance, whereas the most recent version of configuration B1 was tested without this protuberance. Details and location of the horizon sensor protuberance are shown in Fig. 4c.

2.3 INSTRUMENTATION

The force model was instrumented with three internally-mounted strain-gage balances for the measurement of component aerodynamic loads. Figure 5 shows the locations of the balances plus the 15 base and cavity orifices used to measure base pressures for the determination of base axial-force coefficients. The total base axial-force

coefficient, $C_{A,b}$, for each balance was the sum of $C_{A,b}$ values for rearward-facing model areas affecting that balance. For example, $C_{A,b}$ for the composite model (balance 3) included, in addition to $C_{A,b}$ for the effective core base and cavity areas, sums of $C_{A,b}$ from the thrust vector control bottles and from the solid rocket motors. The model centerbody was separated by a gap at the MOL-core interface such that balance 2 sensed loads only on the MOL-Gemini section. Balance 3 was used to measure composite model loads, and the left SRM loads were sensed by balance 4. Balance 1, used to measure Gemini loads in the Ref. 1 tests, was not used in the present test.

The pressure model was instrumented with 361 surface pressure orifices for the measurement of steady-state pressures. Five microphones were flush-mounted to the pressure model in Tunnel 16T and were used to record fluctuating pressures. Microphone and orifice locations are shown in Fig. 6.

SECTION III
TEST DESCRIPTION

3.1 PROCEDURE

Angles of attack (α) and sideslip (β) were obtained by pitching and rolling the sting to pre-calculated angles corresponding to the scheduled α-β combinations. The orientation of moments and forces and the moment reference locations for the force model are shown in Fig. 7.

Data were recorded by holding Mach number constant while α and β were varied from -11 to +11 deg. Mach number for the force model was varied from 0.60 to 1.40 in Tunnel 16T and from 1.80 to 3.00 in Tunnel 16S. Data were recorded for the pressure model at Mach numbers from 0.60 to 1.40 in Tunnel 16T and from 1.80 to 2.60 in Tunnel 16S. A summary of Mach numbers at which the various configurations were tested is shown in Table I (see Appendix II). Reynolds number variations are shown in Fig. 8.

3.2 PRECISION OF MEASUREMENTS

The estimated precision of measurements for pertinent test conditions is as follows:

Angle of attack or sideslip		±0.10 deg
Mach number	0.60 to 1.10	±0.003
	1.20 to 1.40	±0.010
	1.80 to 3.00	±0.020
Dynamic pressure	$M_\infty \leq 1.40$	±4 psf
	$M_\infty > 1.40$	±3 psf

The uncertainties quoted for Mach number relate to the variation of Mach number in the vicinity of the test article. The uncertainty in setting Mach number varied from ±0.003 to ±0.010 with increasing Mach number.

The calculated coefficient uncertainties, shown in Table II, are categorized as calibration and total uncertainties. Uncertainties within the calibration category are based on deviations in balance or transducer output observed during the most recent calibration. These output deviations were composed chiefly of random scatter, permitting the use of a statistical method to determine the calibration uncertainties quoted in Table II. These values are based on a 95-percent confidence level and a normal error distribution.

The total uncertainties include calibration uncertainties and balance or transducer output shifts. The output shifts were indicated by a discrepancy between wind-off outputs recorded before a data run and those recorded afterwards. The output shift uncertainty for a data channel was assumed equal to the largest observed shift between pre-run and post-run wind-offs for that particular channel.

Balance output shifts characteristically occur slowly relative to the acquisition time for a set of pitch or yaw data. An output shift consequently has a minimal effect on the slope of a coefficient as a function of pitch or yaw angle, and a slope uncertainty is adequately described by the calibration uncertainty for the coefficient in question. A coefficient magnitude would obviously be affected by both scatter and shift, and the corresponding uncertainty is best described within the total uncertainty category of Table II.

SECTION IV
RESULTS

4.1 FORCE PHASE

Launch vehicle force data are presented in Figs. 9 through 37 for the modified Gemini configurations and in Figs. 38 through 54 for the basic Gemini versions. The basic Gemini configuration without faired protuberances (configuration B1) was tested previously as reported in Ref. 1. Additional data were obtained for a slightly different version of configuration B1 (see Section 2.2) at selected Mach numbers during the latest entry to check the data reported in Ref. 1. Differences between the two sets of data were within the accuracies of measurement. All data reported herein for configuration B1 were obtained during the previous investigation and are presented for comparison purposes only. In view of the extensive reporting of basic Gemini force data in Ref. 1, data presentations for the basic Gemini configurations in the present report are limited chiefly to an assessment of protuberance effects on stability and axial-force characteristics. Force data are presented in more complete detail for the modified Gemini model, since no force configuration of this model had previously been tested.

4.1.1 Configurations with the Modified Gemini Shape

The two modified Gemini configurations (see Section 2.2) were defined as configurations M1 (without MOL protuberances) and M2 (with MOL protuberances). Data are presented in sequence for the MOL-Gemini section, the composite vehicle, and the left SRM.

Pitching-moment coefficients, C_m, for the MOL-Gemini section of configurations M1 and M2 are varied with angle of attack, α, for angles of sideslip, β, of 0, +8, and -8 deg in Fig. 9. Normal-force coefficient, C_N, is similarly presented in Fig. 10. Configuration M2 displayed slopes of C_m and C_N with α which were slightly larger than those exhibited by configuration M1. Yawing-moment coefficient, C_n, and side-force coefficient, C_Y, are shown as functions of β at α = 0, +8, and -8 deg for the MOL-Gemini section in Figs. 11 and 12. Measured differences in the trends of C_n or C_Y between the two configurations are insignificant. The effects of configuration change on the longitudinal and lateral coefficients are consistent with the protuberance locations. As shown in Figs. 3 and 4, four of the six MOL protuberances on configuration M2 were located along either side of the model, and removal of the six protuberances should effect a greater change in the longitudinal coefficients than in the lateral coefficients.

Variations of MOL-Gemini forebody axial-force coefficient, $C_{A,F}$, with α at $\beta = 0$ are compared for configurations M1 and M2 in Fig. 13. Configuration M2 consistently exhibited larger magnitudes of $C_{A,F}$. Trends of base axial-force coefficient, $C_{A,b}$, with α are shown in Fig. 14. No significant differences in MOL-Gemini $C_{A,b}$ values were observed for the two configurations. Variations of MOL-Gemini $C_{A,F}$ and $C_{A,b}$ with Mach number at α, $\beta = 0$ are compared for the two modified configurations in Figs. 15 and 16. A maximum value of $C_{A,b}$ occurred at Mach number 1.20 for both configurations.

Variations of C_m and C_N with α at $\beta = 0$, +8, and -8 deg are compared for configurations M1 and M2 of the composite model in Figs. 17 and 18. The two configurations exhibited no measurable differences in C_m or C_N. Figures 19 and 20 show variations of C_n and C_Y with β at $\alpha = 0$, +8, and -8 deg and, again, no significant differences between the two configurations were observed. The pitching-moment curve slope, C_{m_α}, and the yawing-moment curve slope, C_{n_β}, are varied with Mach number in Figs. 21 and 22. Longitudinal and lateral neutral-point locations are varied with Mach number in Fig. 23. The longitudinal neutral point, x_{np_β}, showed little response to changes in Mach number and displayed a maximum travel of less than one core diameter. The lateral neutral point, x_{np_β}, revealed a more definitive trend with a most forward location at Mach number 0.90 and a maximum travel in excess of two diameters.

Variations of $C_{A,F}$ and $C_{A,b}$ with α for the composite model, comparing configurations M1 and M2, are presented in Figs. 24 and 25. The values of $C_{A,F}$ and $C_{A,b}$ at α, $\beta = 0$ are plotted as functions of Mach number in Figs. 26 and 27. Configuration M2 produced slightly larger magnitudes of $C_{A,F}$ at Mach numbers from 1.00 to 1.40. The differences indicated were, however, only slightly larger than predicted uncertainties (see Section 3.2) and therefore are probably not significant. The values of $C_{A,b}$ did not differ for the two configurations.

Trends of C_m and C_N with α for $\beta = 0$, +8, and -8 deg are presented in Figs. 28 and 29 for the left SRM in the presence of configurations M1 and M2. Figures 30 and 31 show variations of C_n and C_Y with β at $\alpha = 0$, +8, and -8 deg. The SRM moment and force coefficients were insensitive to changes in MOL geometry caused by protuberances. The differences indicated in Figs. 28 through 31 were consistently less than the estimated uncertainties.

Variations of SRM $C_{A,F}$ with α at $\beta = 0$ deg and with β at $\alpha = 0$ deg are presented in Figs. 32 and 33. Corresponding variations of $C_{A,b}$

are presented in Figs. 34 and 35. Trends of $C_{A,F}$ and $C_{A,b}$ with Mach number at α, $\beta = 0$ are presented in Figs. 36 and 37. Configuration M1 displayed somewhat larger values of $C_{A,F}$ but again, the differences were of magnitudes approximately equal to predicted uncertainties. Maximum $C_{A,F}$ and $C_{A,b}$ occurred, respectively, at Mach numbers near 1.20 and 1.10.

4.1.2 Configurations with the Basic Gemini Shape

The three basic Gemini configurations (see Section 2.2) included the launch model without the five faired protuberances (configuration B1) and the model with the protuberances in the normal position (configuration B2) and in a position rotated 180 deg from the normal location (configuration B3). The 180-deg rotation of the MOL protuberances from the configuration B2 position to the configuration B3 position corresponded geometrically to rolling the composite model 180 deg. Therefore, the external geometries of the MOL-Gemini section and of the composite model were essentially unaffected by a change from configuration B2 to B3. The effect of protuberances on the aerodynamic characteristics of the MOL-Gemini section and of the composite model are consequently presented for configurations B1 and B2 only. The SRM data are compared for all three configurations, as each configuration afforded a unique protuberance orientation relative to the left SRM. It should be noted that the proximity of the left SRM of configuration B3 to the MOL protuberances was identical to that of the right SRM for configuration B2 and that, in fact, the purpose of testing configuration B3 was to determine the MOL protuberance effects on the right SRM of configuration B2. Variations of C_{m_α} and C_{N_α} with Mach number are presented for the MOL-Gemini section of configurations B1 and B2 in Figs. 38 and 39. Configuration B2 exhibited consistently more positive slopes of both C_{m_α} and C_{N_α}. Similarly, Figs. 40 and 41 show more negative values of C_{n_β} and C_{Y_β} for configuration B2. However, the differences indicated in Figs. 38 through 41 are near the predicted uncertainties, and therefore cannot be considered conclusive.

Variations of $C_{A,F}$ and $C_{A,b}$ with Mach number at α, $\beta = 0$ are presented for the MOL-Gemini section in Figs. 42 and 43. Configuration M2 data are included to achieve a comparison between configurations B2 and M2 as representative launch configurations of the basic and modified Gemini payloads. Configurations B1 and B2 did not exhibit consistently measurable differences in $C_{A,F}$. Values of $C_{A,F}$ varied significantly between configurations B2 and M2 at Mach numbers 1.80, 2.00, and 2.20, where configuration M2 displayed the larger magnitudes. Configuration M2 exhibited values of $C_{A,b}$ larger than those for configuration B2 at all Mach numbers for which data were compared.

Of the basic models, configuration B1 displayed slightly larger values of MOL-Gemini $C_{A,b}$ except at Mach number 1.40.

Trends of C_{m_α} and C_{n_β} with Mach number are compared for composite configurations B1 and B2 in Figs. 44 and 45. The longitudinal and lateral neutral-point locations are varied with Mach number for composite configurations B1, B2, and M2 in Fig. 46. The x_{np_α} for the basic configurations was relatively invariant with Mach number and displayed a maximum travel of approximately one core diameter, whereas x_{np_β} varied approximately 2.5 core diameters with Mach number and was most forward at Mach number 0.90. Configuration M2 exhibited values of neutral-point location similar to those of configuration B2 with no significant differences.

Forebody and base axial-force coefficients are varied with Mach number for composite configurations B1, B2, and M2 in Figs. 47 and 48. No consistent differences in magnitude of $C_{A,F}$ or $C_{A,b}$ were observed among the three configurations. Maximum $C_{A,F}$ occurred near Mach number 1.30 with a maximum $C_{A,b}$ near Mach number 1.20.

Variations of SRM C_m and C_N with α are compared for configurations B1, B2, and B3 in Figs. 49 and 50. Variations of C_n and C_Y with β are shown in Figs. 51 and 52. The longitudinal coefficients for the three configurations indicate differences in magnitude at various Mach numbers; however, these differences are probably caused by unusually large shifts in balance output. No significant differences in C_n or C_Y were observed.

Variations of SRM $C_{A,F}$ and $C_{A,b}$ with Mach number at α, $\beta = 0$ are presented for configurations B1, B2, and B3 in Figs. 53 and 54. Differences in magnitude of $C_{A,F}$ or $C_{A,b}$ are not significant for the three configurations.

4.2 PRESSURE PHASE

Surface pressures were measured at approximately 400 model locations (Fig. 6) for configurations M1, M2, B2, and B3. The pressure data reported in Ref. 1 were obtained at similar model locations for configuration B1 and for a modified Gemini configuration with attitude control rockets but without the faired protuberances. A comparison of present results with those reported in Ref. 1 showed reasonable agreement of C_p trends and magnitudes for similar configurations except in the model vicinity where protuberance changes were made.

The protuberance effects on surface pressure distributions are typified in Fig. 55, which compares distributions of C_p along the 0-deg ray of configuration B1 with C_p variations along the 270-deg and 334-deg rays of configuration B2. These data are presented for α and β = 0 deg. The data plotted for the 270- and 334-deg rays of configuration B2 include distributions across protuberances D and A, respectively. The configuration B1 data represent a protuberance-free distribution. The ray orientations, model stations, and protuberance locations are identified in Fig. 4a. Figure 55 shows a predictable distortion of C_p distributions across the protuberances. However, these C_p variations return to a protuberance-free trend within 0.5-core diameters downstream of the trailing edge of either protuberance.

SECTION V
SUMMARY OF RESULTS

The data results are summarized as follow:

1. The deletion of protuberances from the MOL portion of the modified and basic Gemini models effected measurable changes in force and moment characteristics for the MOL-Gemini section only. For the modified Gemini, C_{m_α}, C_{N_α}, and $C_{A,F}$ for the MOL-Gemini section decreased. Results for the MOL-Gemini section of the basic Gemini model showed C_{m_α} and C_{N_α} decreased after protuberance removal, whereas positive increments in C_{n_β} and C_{Y_β} occurred.

2. Typical surface pressure distributions across the faired protuberances reached protuberance-free values within 0.5-core diameters downstream of the protuberance trailing edge.

REFERENCES

1. Riddle, C. D., Shadow, T. O., and Black, J. A. "Wind Tunnel Investigations to Determine Static Stability and Pressure Distribution Characteristics of Small-Scale Models of the Titan III/MOL Launch Configuration at Mach Numbers from 0.60 to 3.10." AEDC-TR-66-202 (AD80173), November 1966.

2. Test Facilities Handbook (6th Edition). "Propulsion Wind Tunnel Facility, Vol. 5." Arnold Engineering Development Center, November 1966.

APPENDIXES

I. ILLUSTRATIONS

II. TABLES

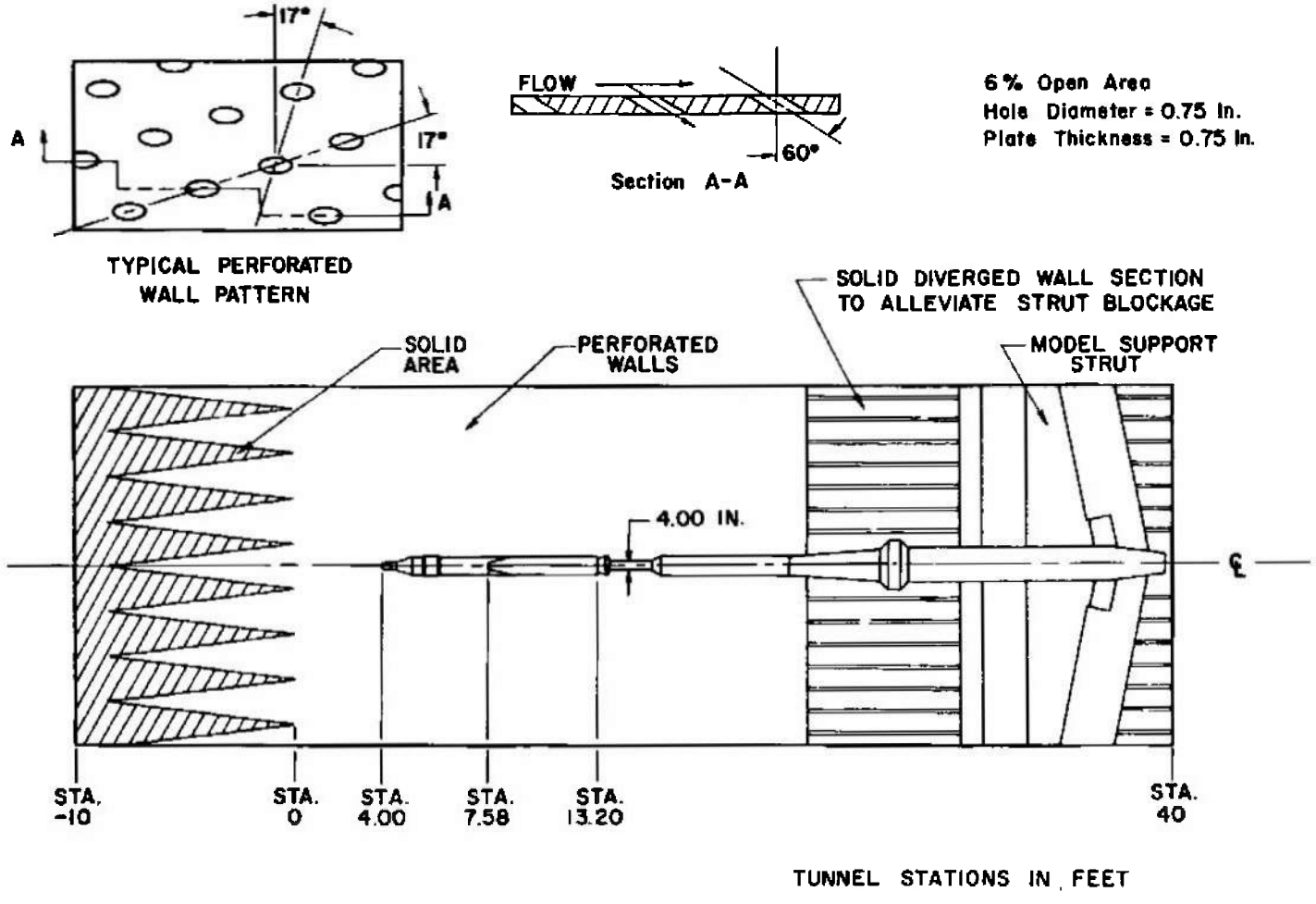

a. Sketch of the 16T Installation

Fig. 1 Installation of the Titan III/MOL Launch Vehicle Model in Tunnels 16T and 16S

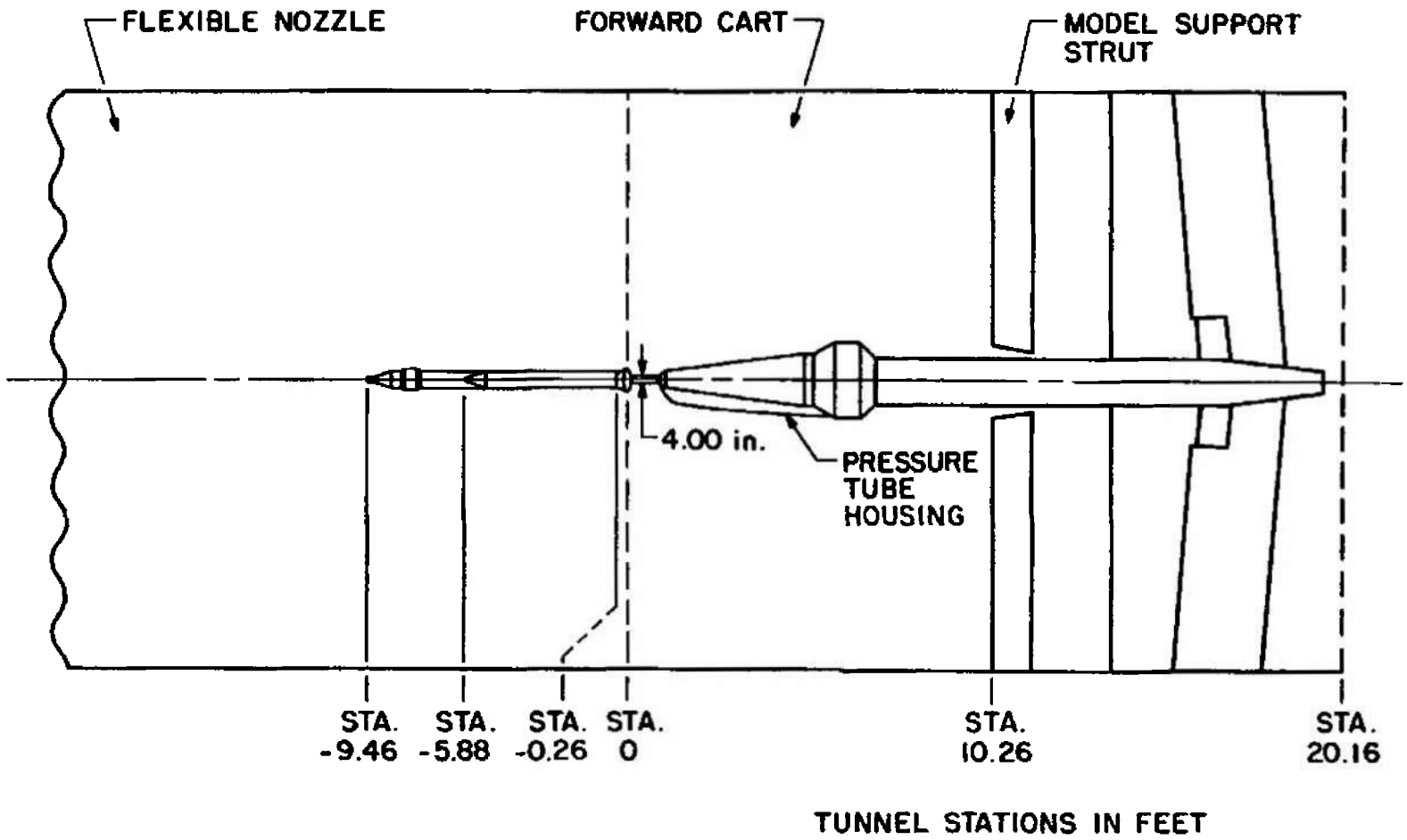

b. Sketch of the 16S Installation

Fig. 1 Continued

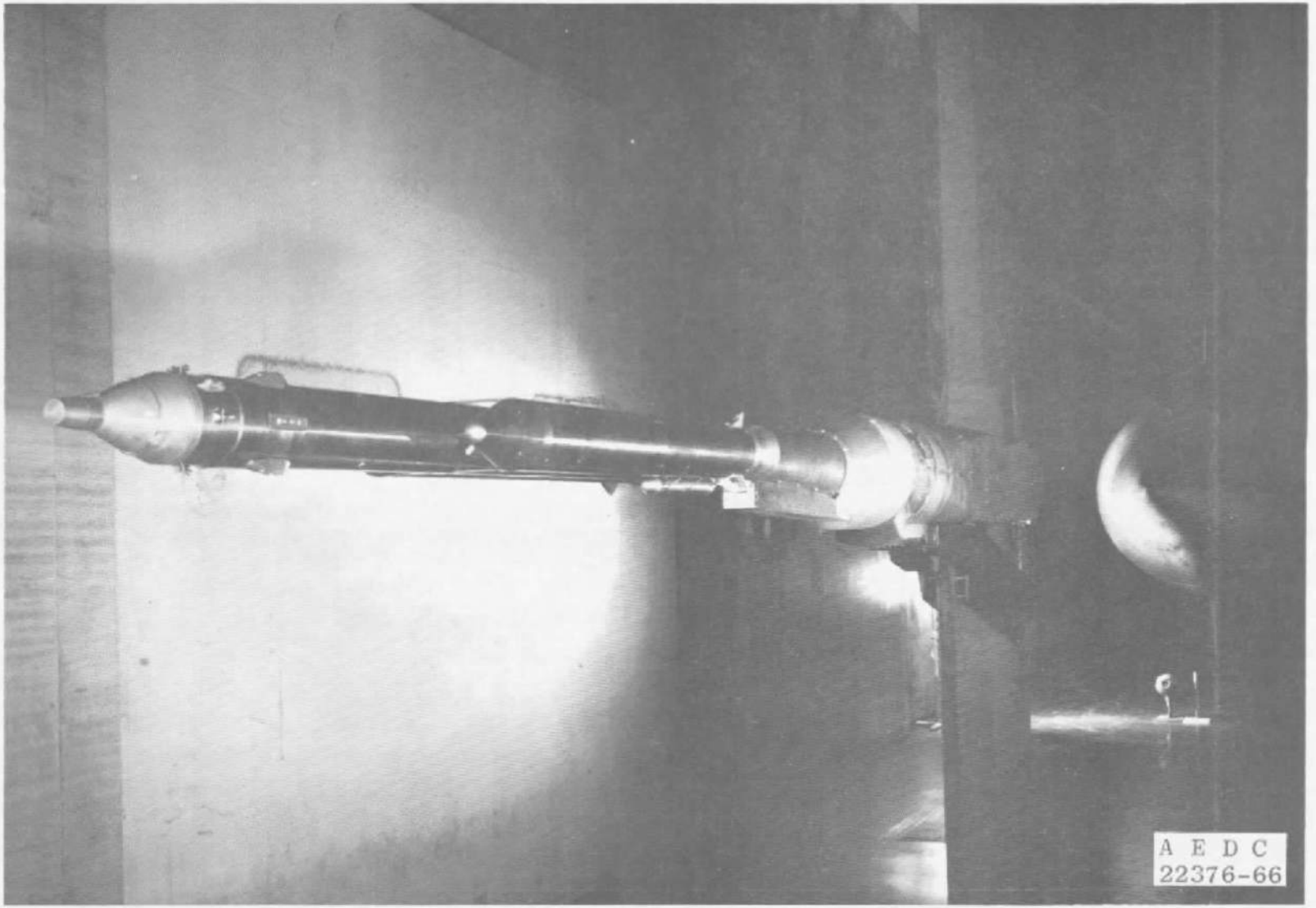

c. Photograph Showing the Installation of the Force Model in 16S

Fig. 1 Concluded

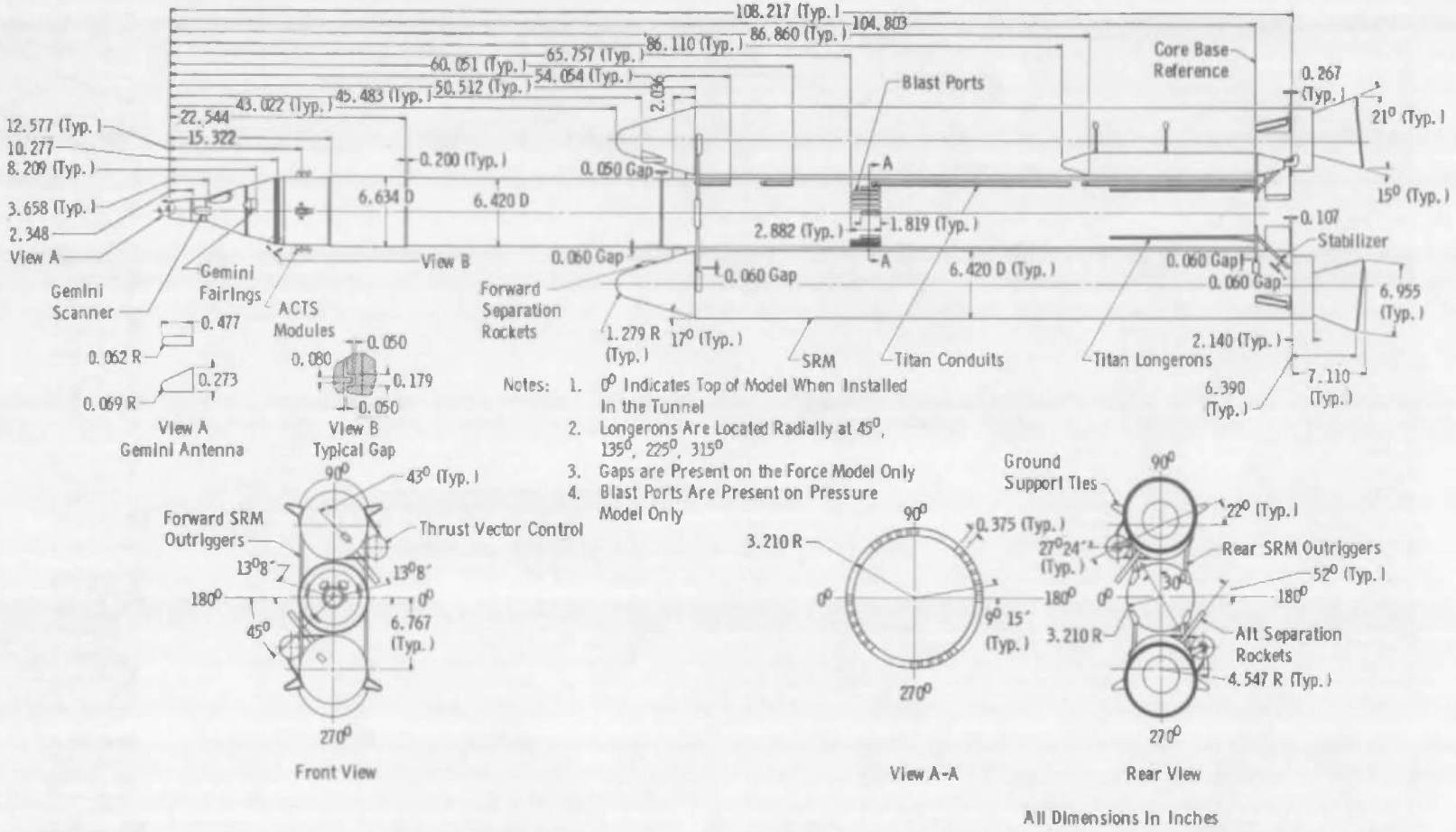

Fig. 2 Launch Vehicle Geometry

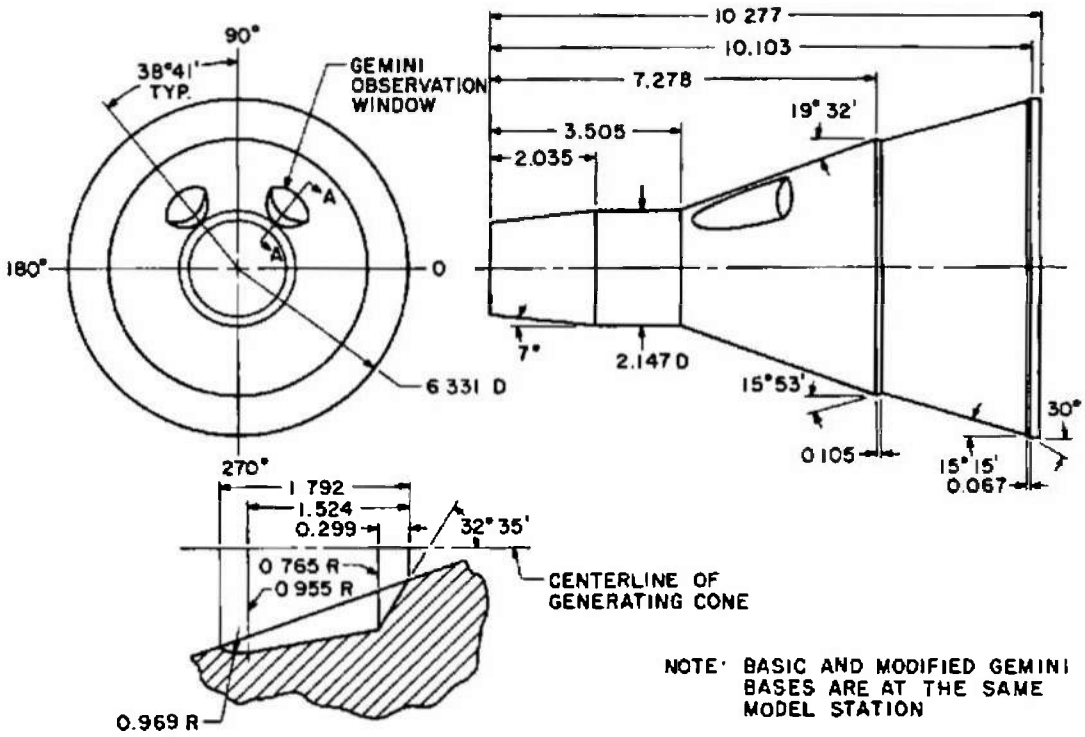

BASIC GEMINI DETAILS

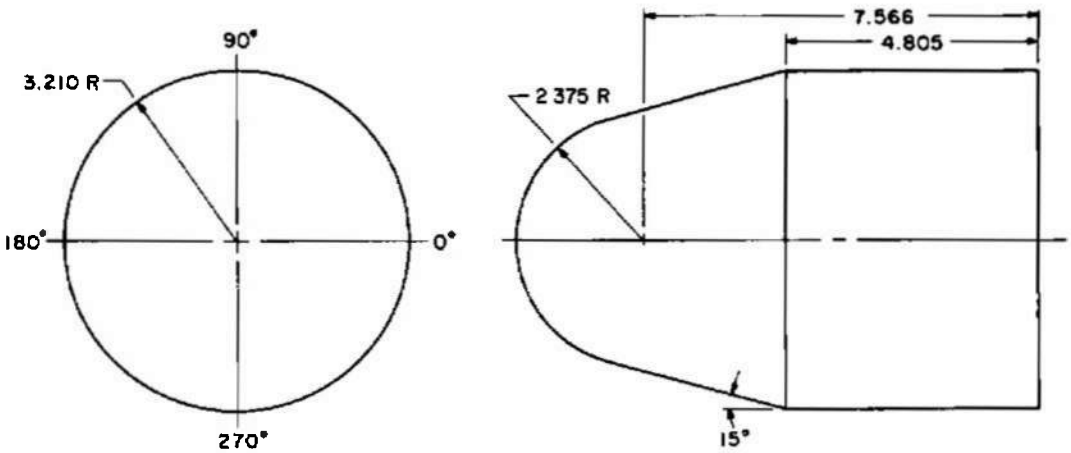

MODIFIED GEMINI DETAILS

ALL DIMENSIONS IN INCHES

a. Gemini Details

Fig. 3 Configuration Description

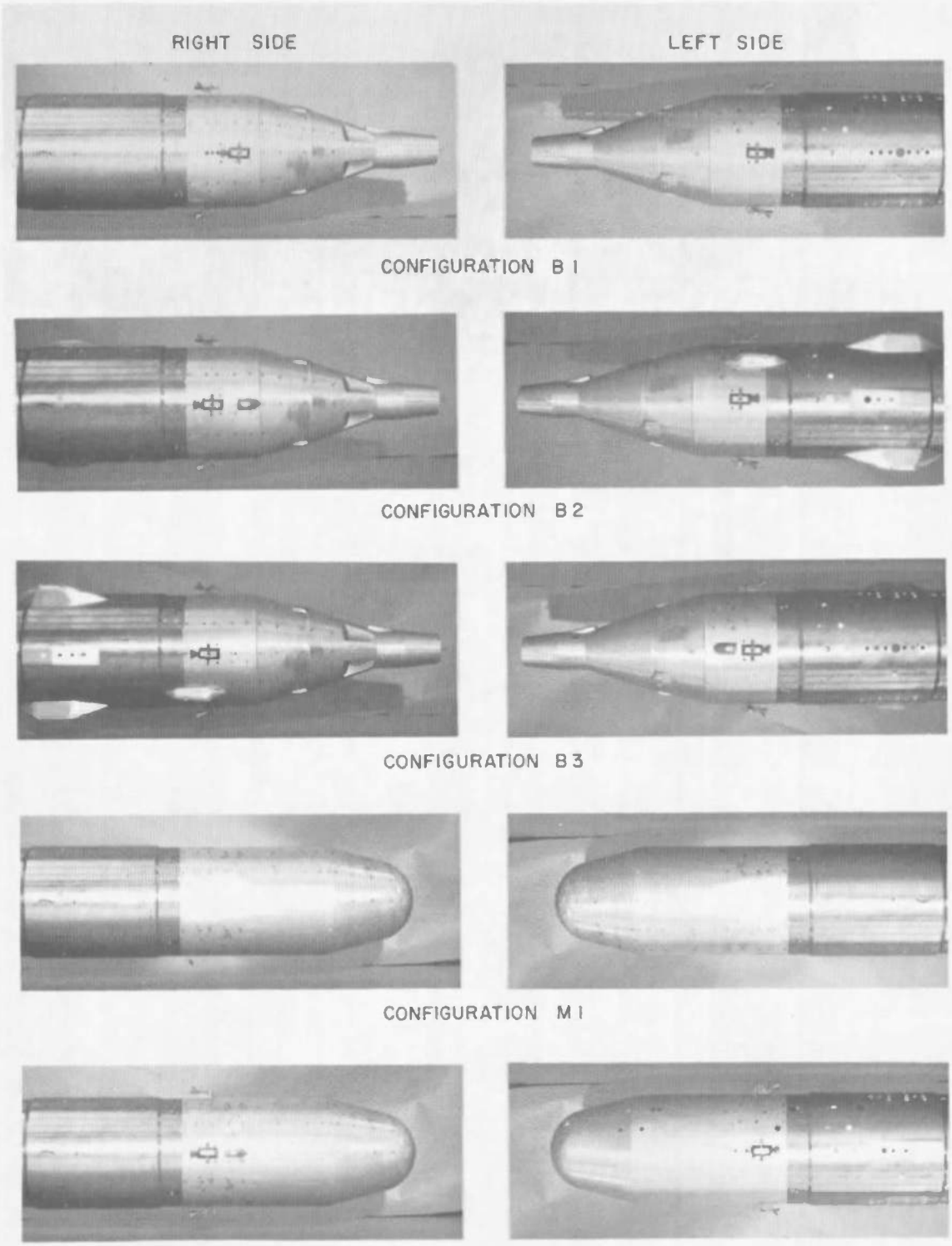

b. Configurotion Photographs

Fig. 3 Concluded

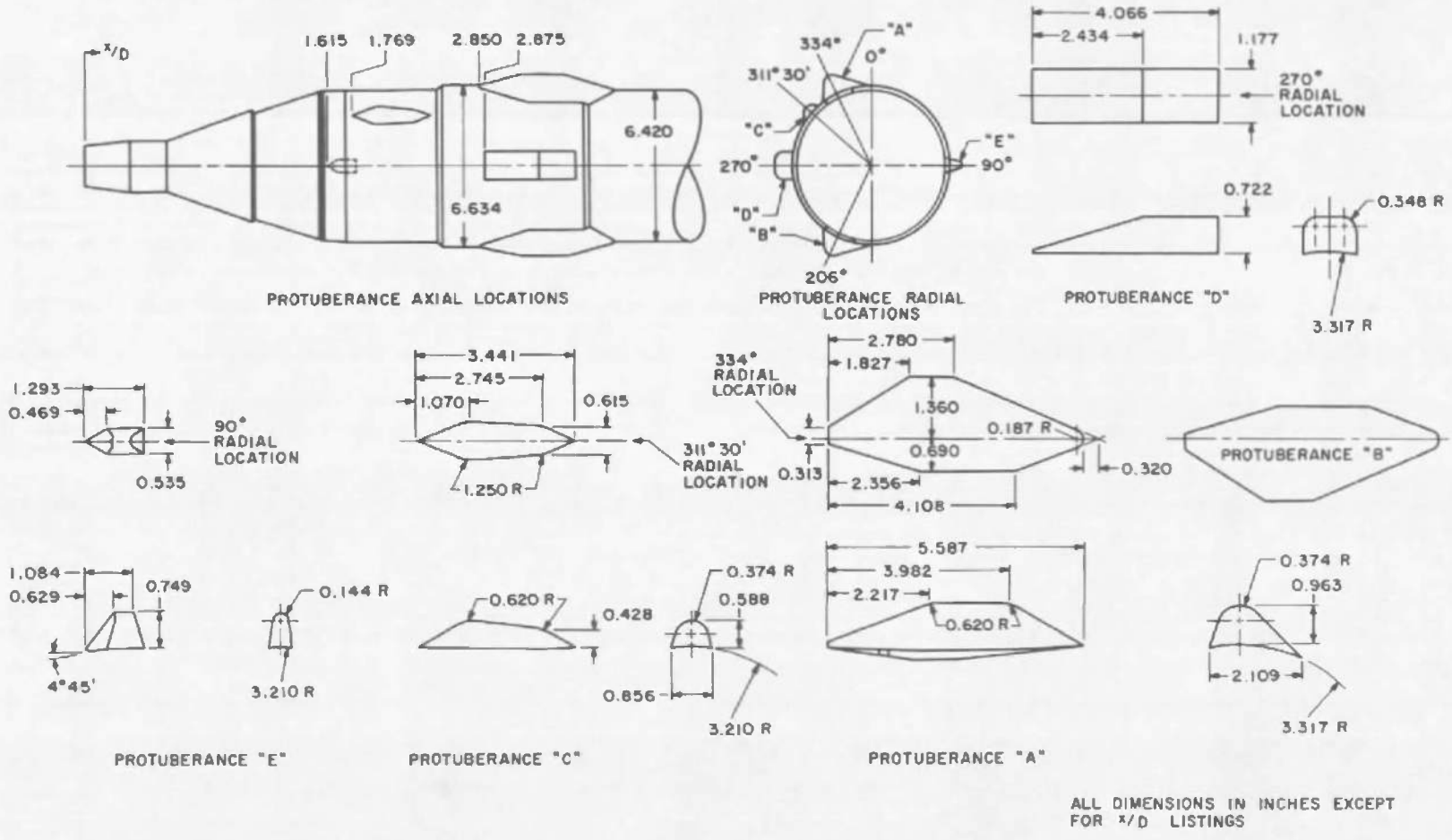

a. Sketch of Protuberances A-E

Fig. 4 Protuberance Details

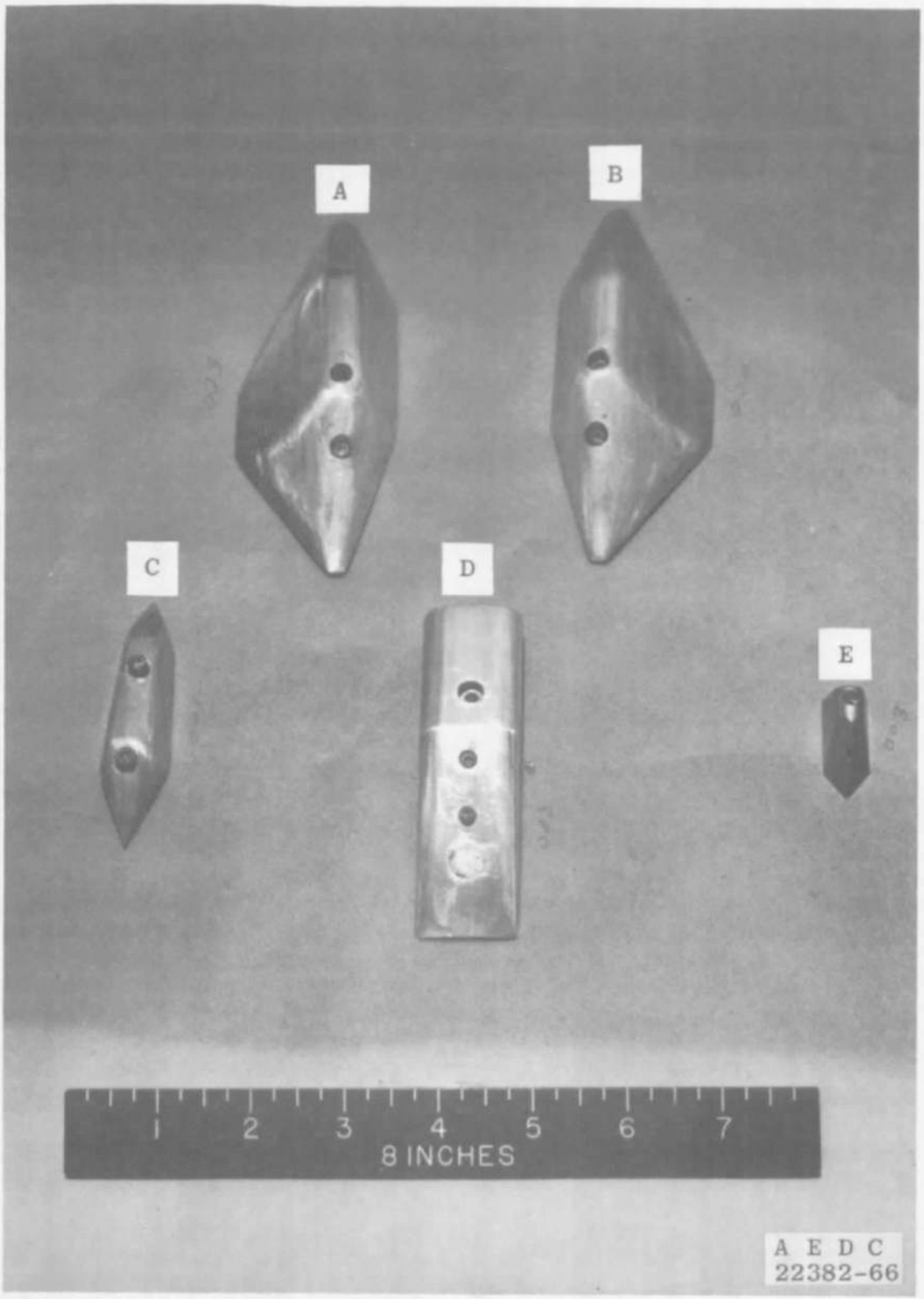

b. Photograph of Protuberances A-E

Fig. 4 Continued

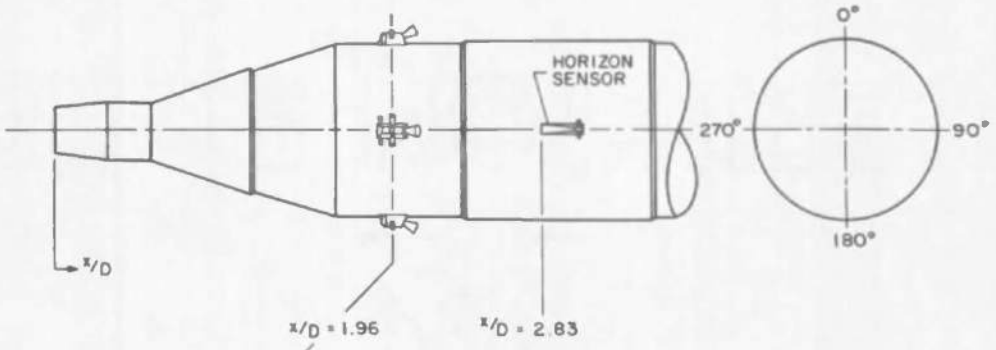

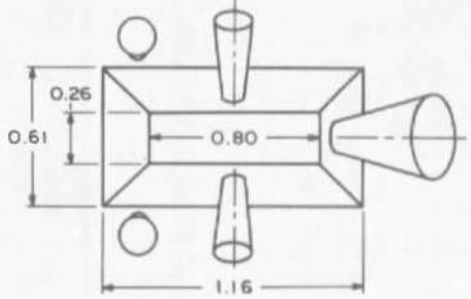

NOTES:

1. ALL DIMENSIONS IN INCHES EXCEPT x/D LISTINGS
2. ATTITUDE CONTROL ROCKETS POSITIONED AT 0, 90, 180 AND 270 DEG
3. HORIZON SENSOR LOCATED AT 270 DEG; PRESENT DURING REF. 1 TESTING ONLY

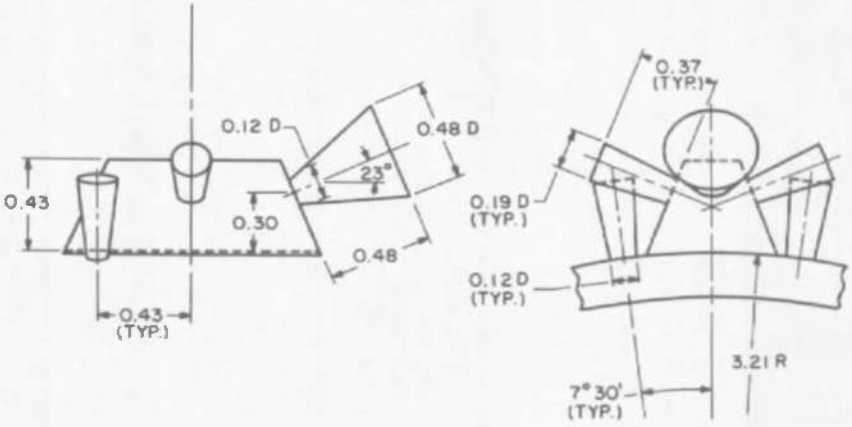

ATTITUDE CONTROL ROCKET

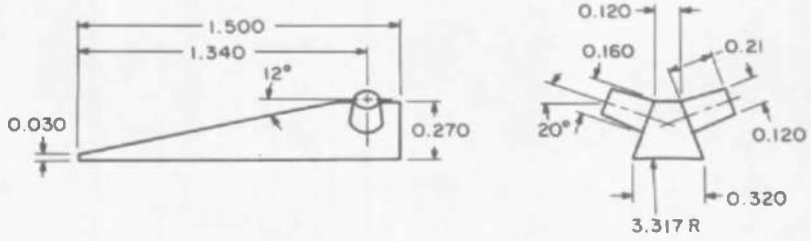

HORIZON SENSOR

c. Sketch of Attitude Control Rockets and Horizon Sensor

Fig. 4 Concluded

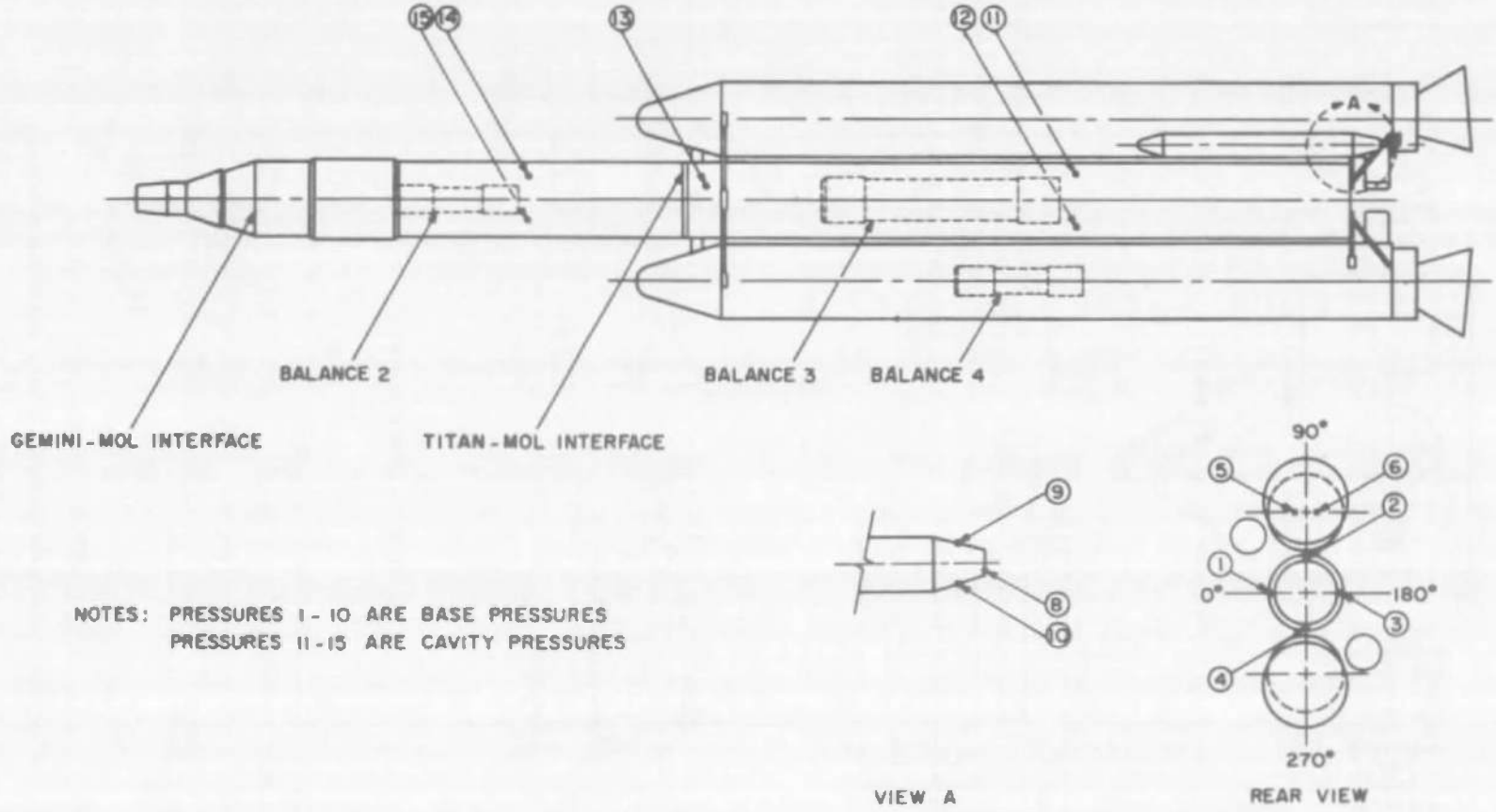

NOTES: PRESSURES 1 - 10 ARE BASE PRESSURES
PRESSURES 11 - 15 ARE CAVITY PRESSURES

Fig. 5 Sketch of Force Model Showing Balance and Pressure Orifice Location

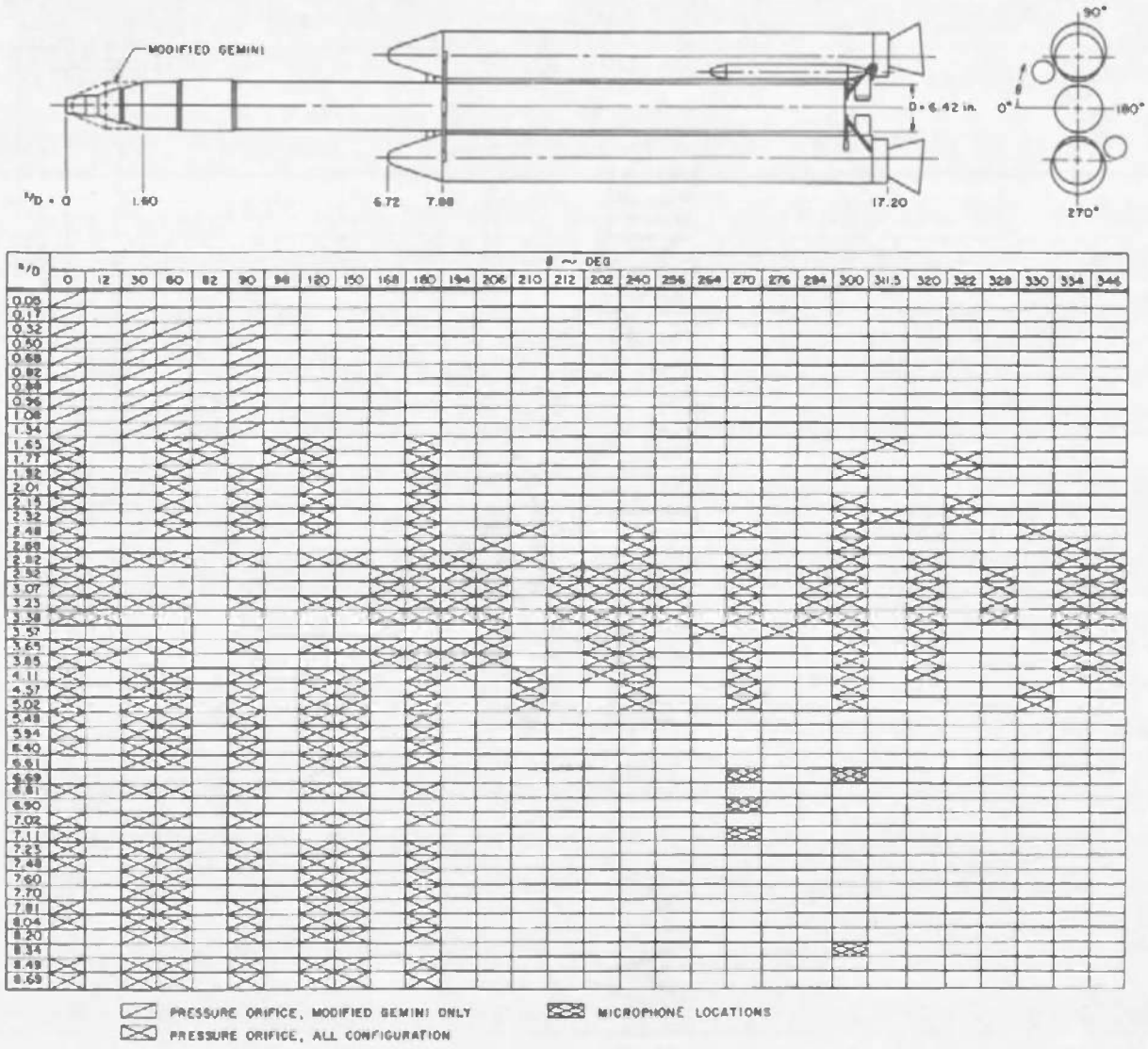

Fig. 6 Sketch of Pressure Model Showing Locations of Pressure Orifices and Microphones

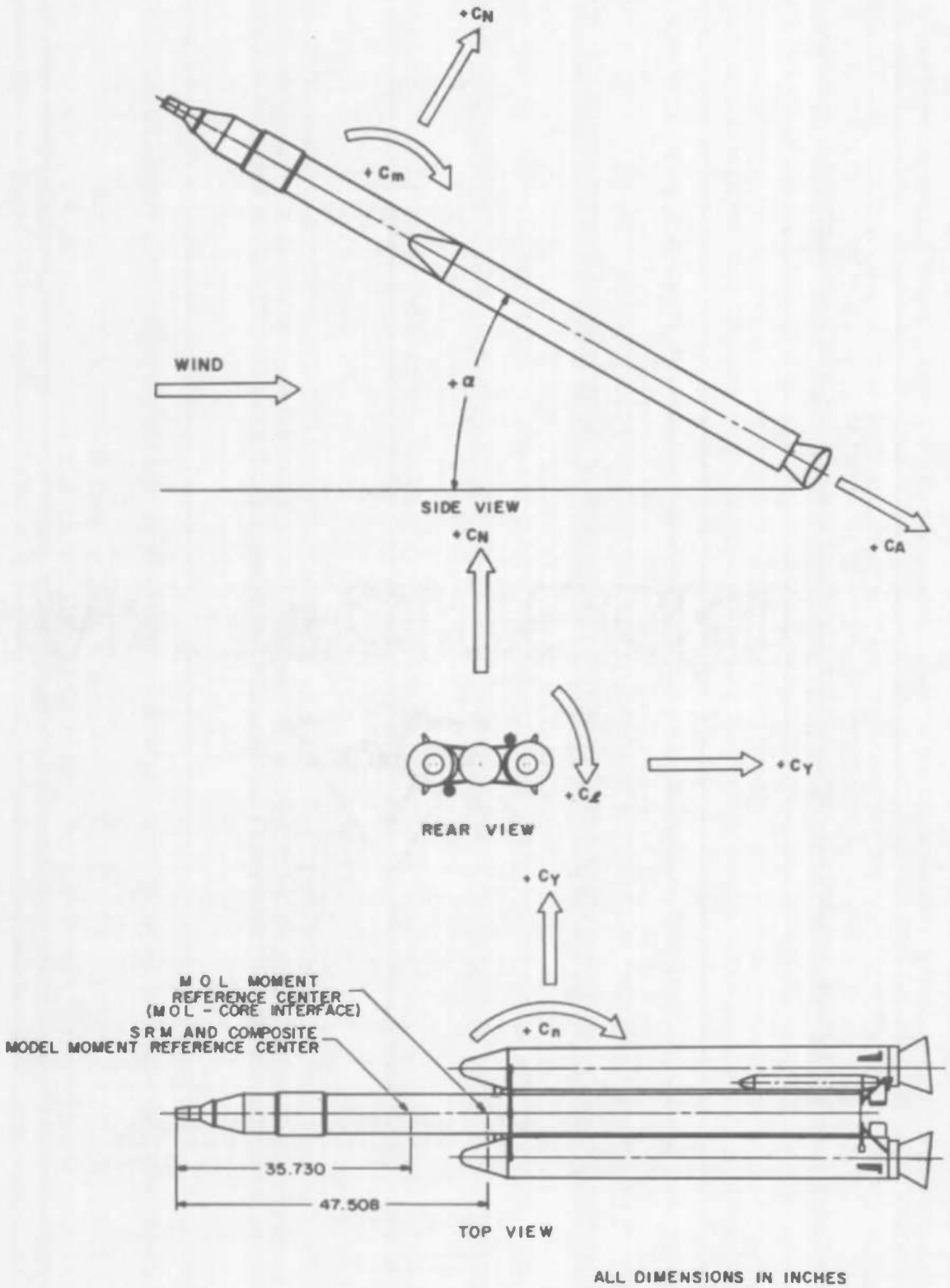

Fig. 7 Orientation of Forces and Moments

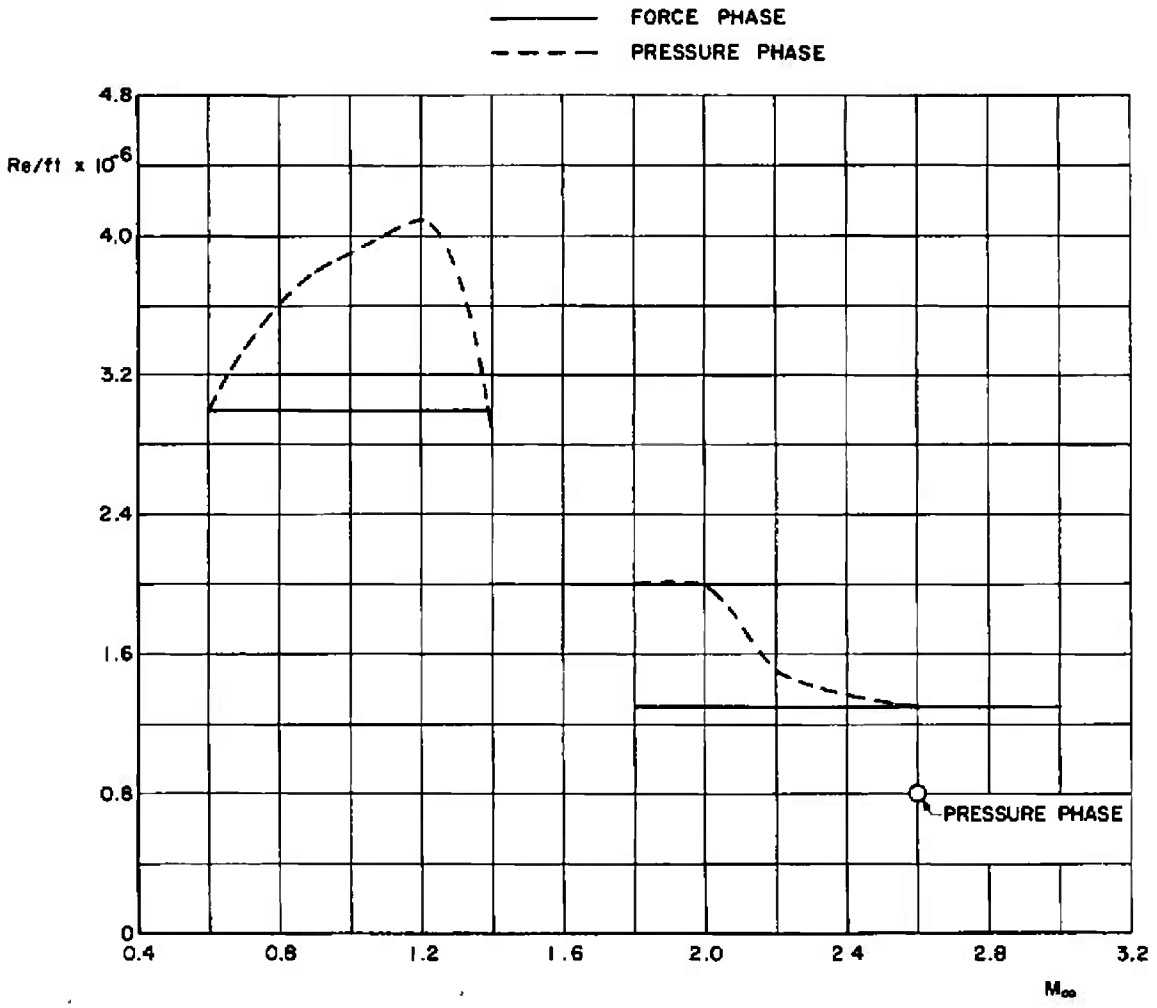

Fig. 8 Variation of Reynolds Number with Mach Number

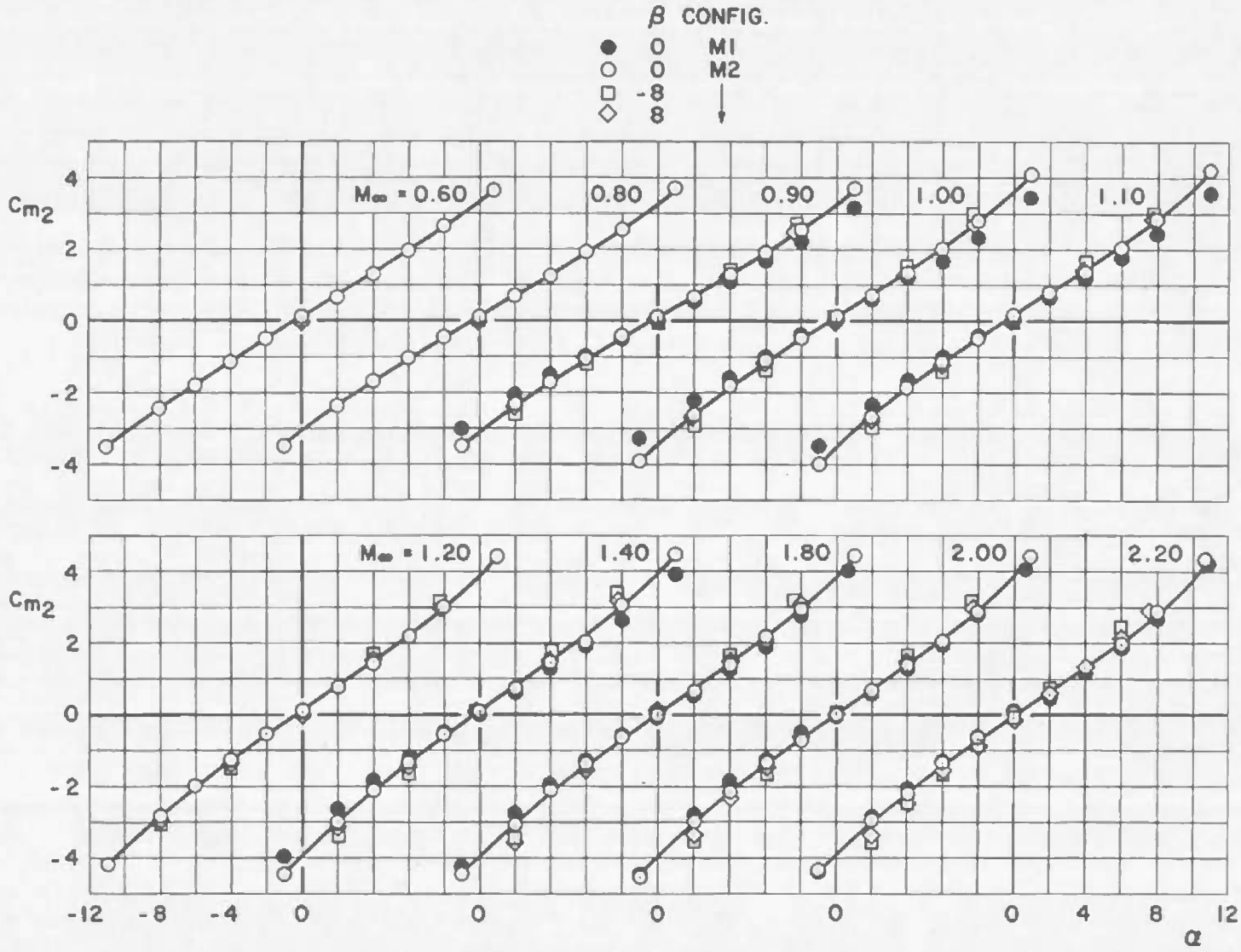

Fig. 9 Variation of MOL-Gemini Pitching-Moment Coefficient with Angle of Attack for Configurations M1 and M2

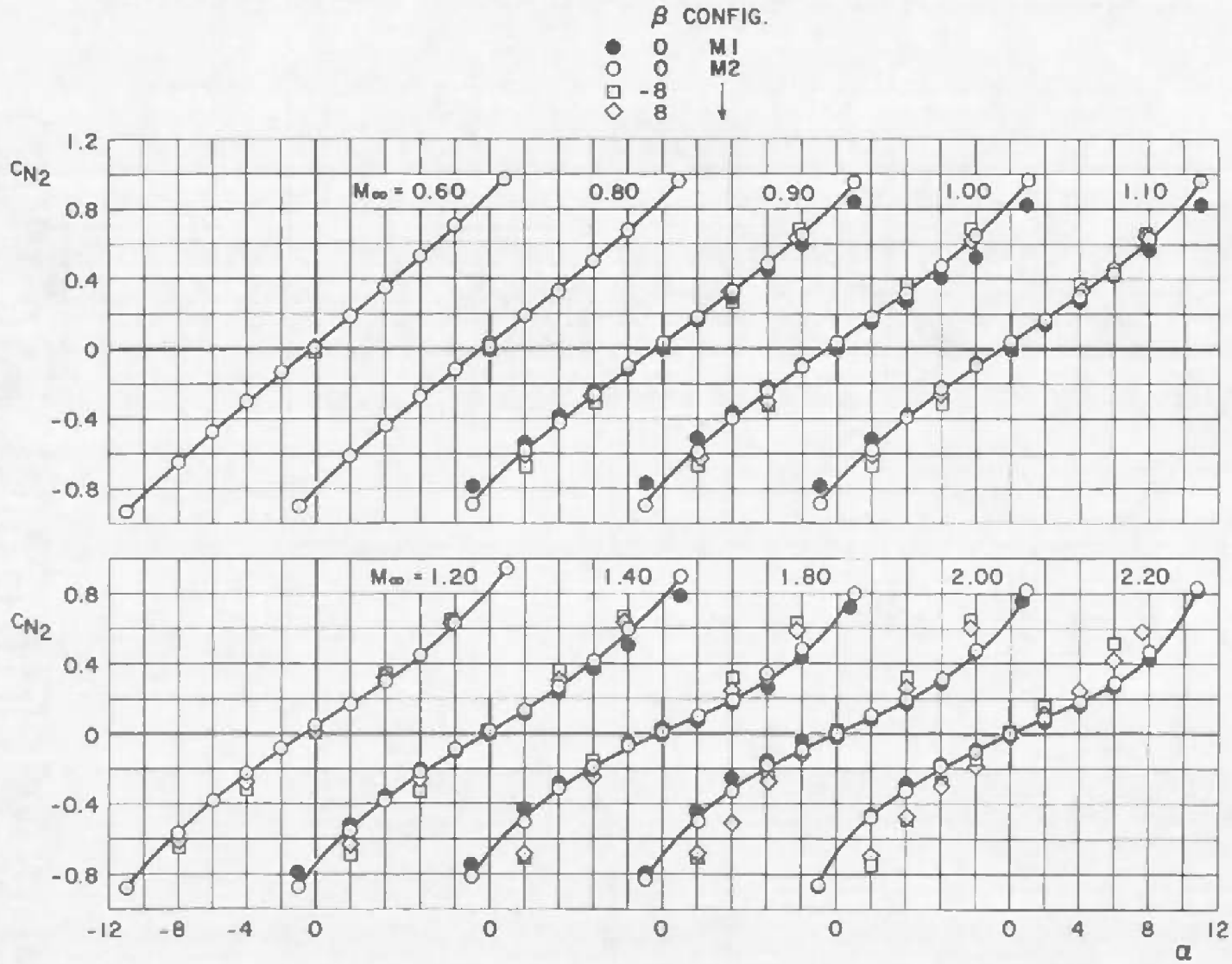

Fig. 10 Variation of MOL-Gemini Normal-Force Coefficient with Angle of Attack for Configurations M1 and M2

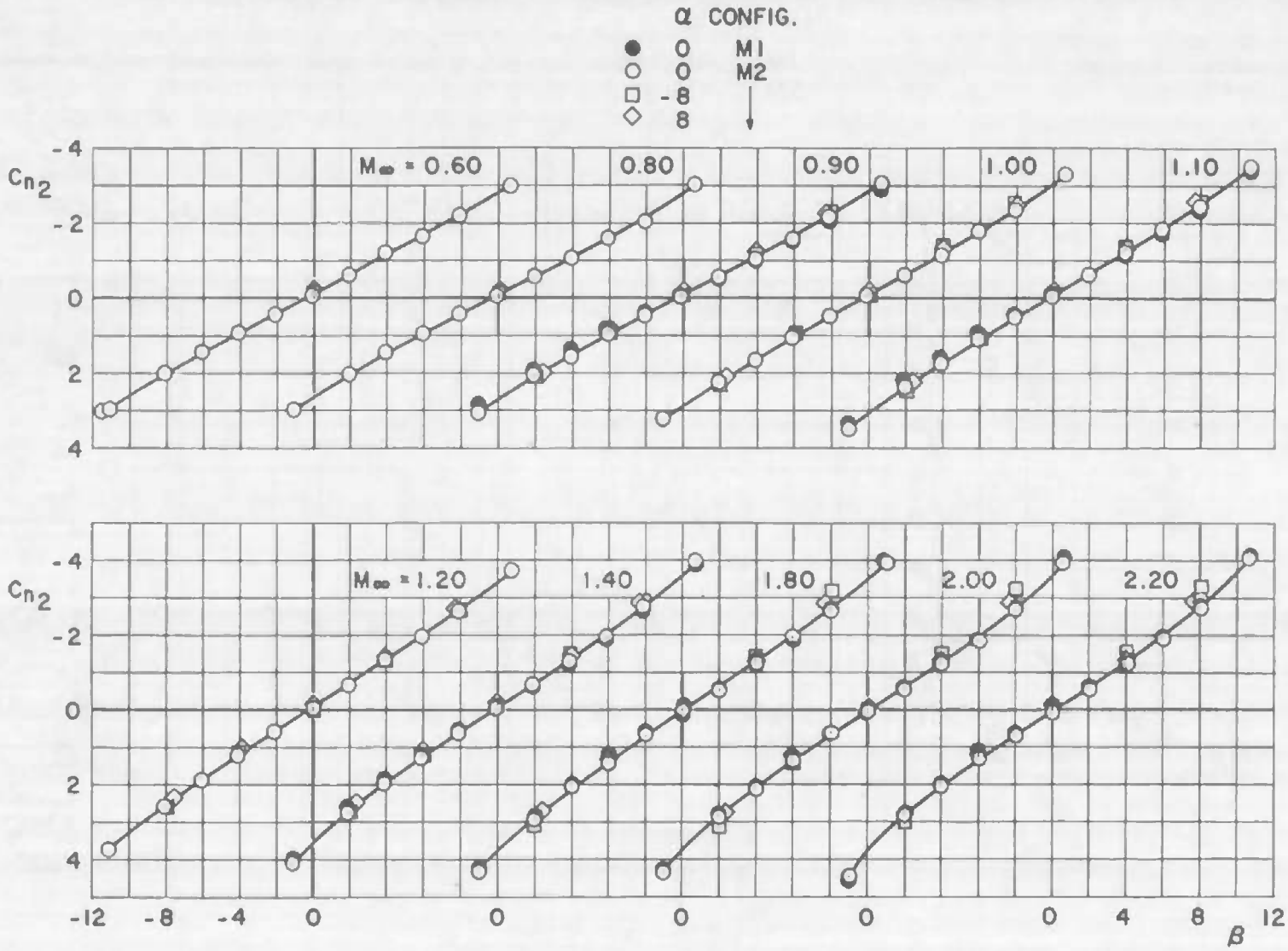

Fig. 11 Variation of MOL-Gemini Yawing-Moment Coefficient with Sideslip Angle for Configurations M1 and M2.

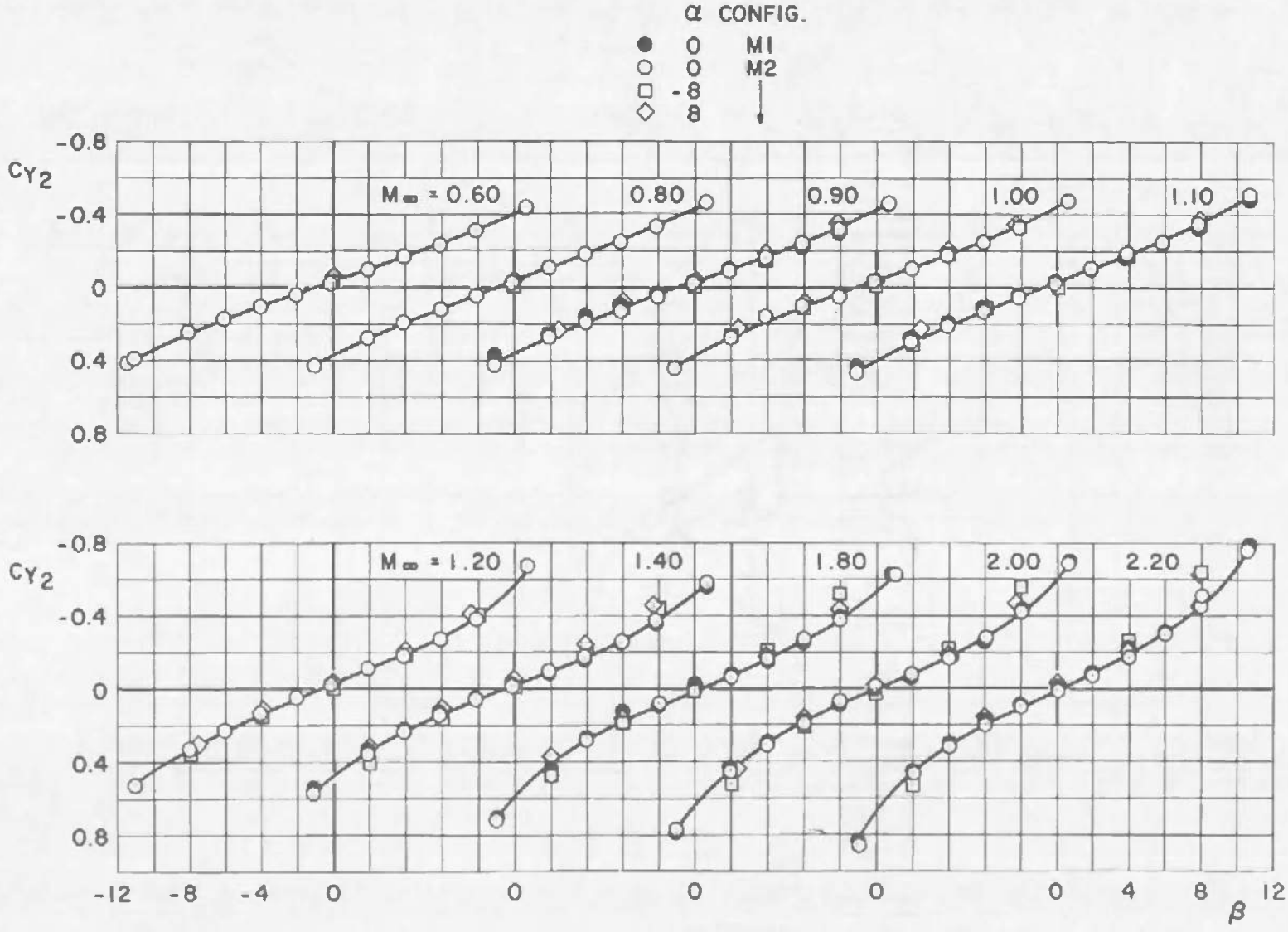

Fig. 12 Variation of MOL-Gemini Side-Force Coefficient with Sideslip Angle for Configurations M1 and M2

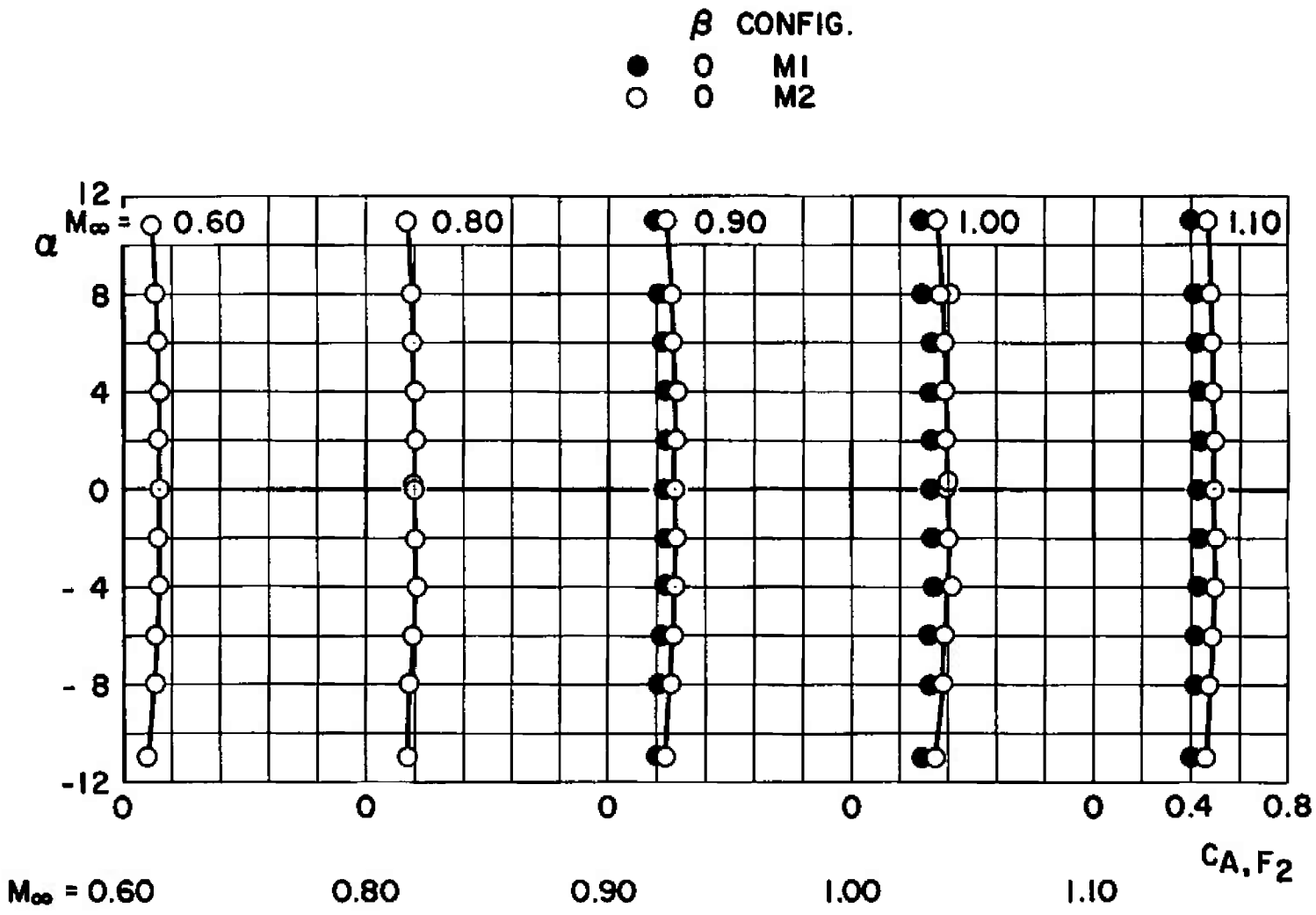

a. Mach Numbers 0.60 through 1.10

Fig. 13 Variation of MOL-Gemini Forebody Axial-Force Coefficient with Angle of Attack for Configurations M1 and M2 at $\beta = 0$

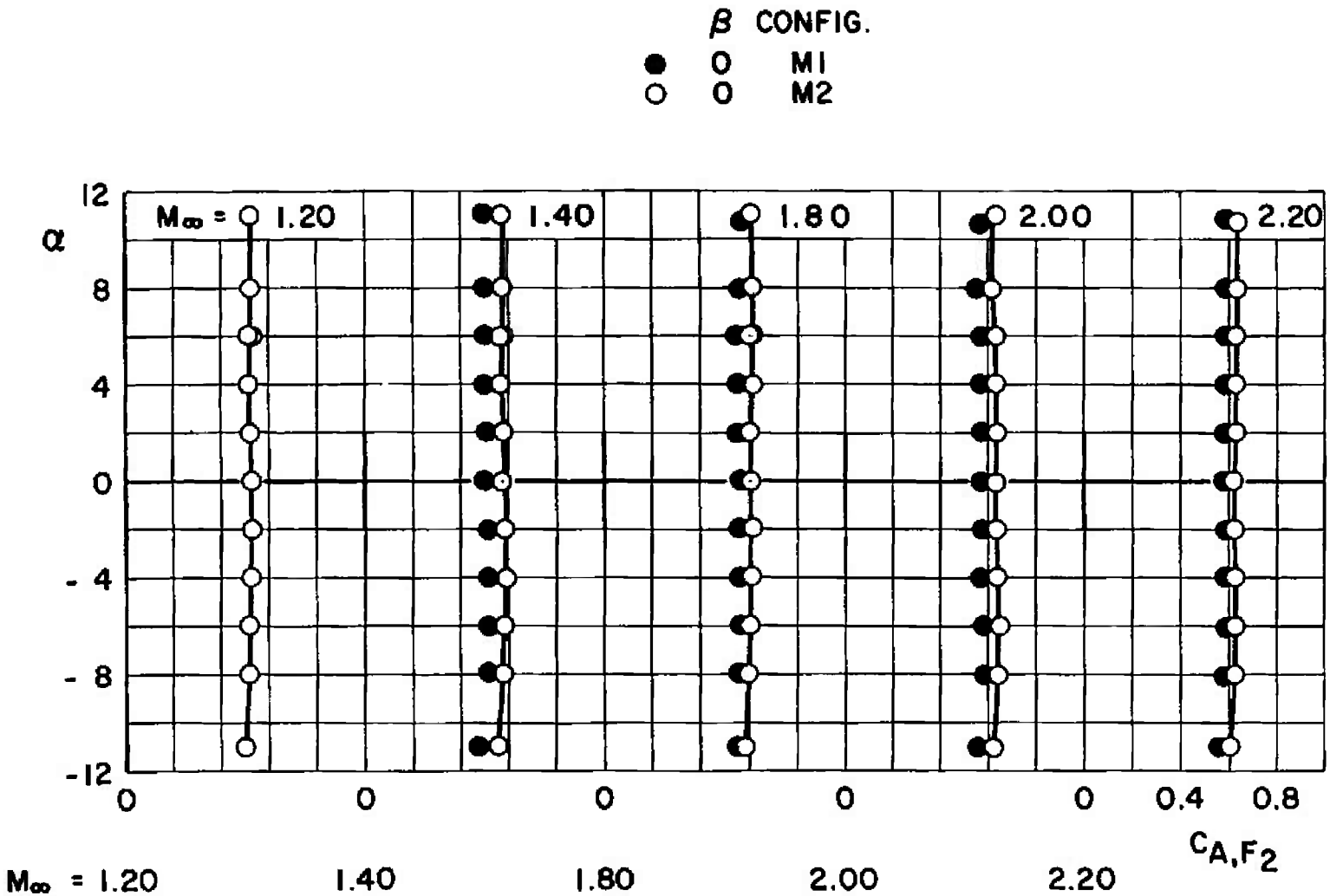

b. Mach Numbers 1.20 through 2.20

Fig. 13 Concluded

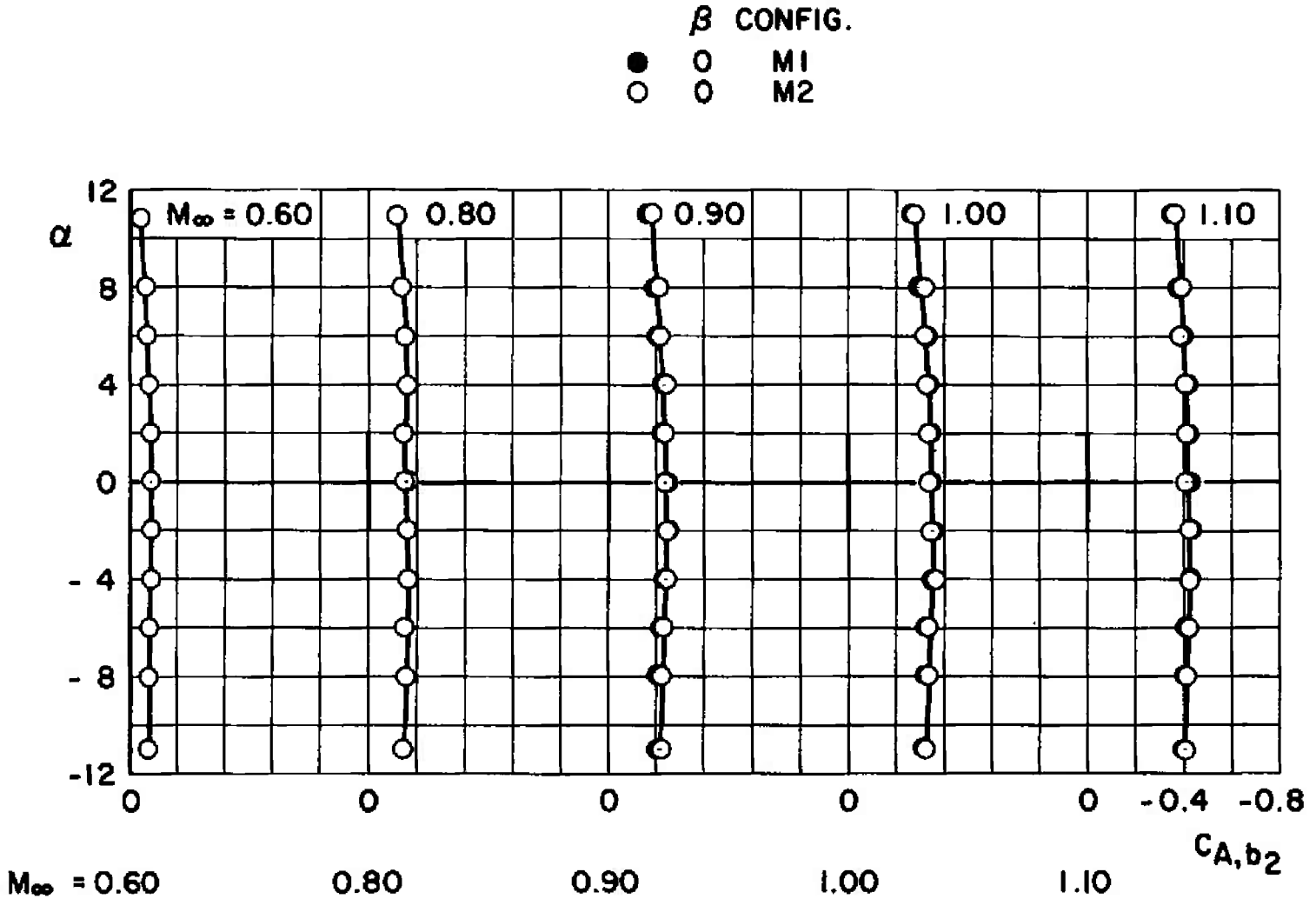

a. Mach Numbers 0.60 through 1.10

Fig. 14 Variation of MOL-Gemini Base Axial-Force Coefficient with Angle of Attack for Configurations M1 and M2 at $\beta = 0$

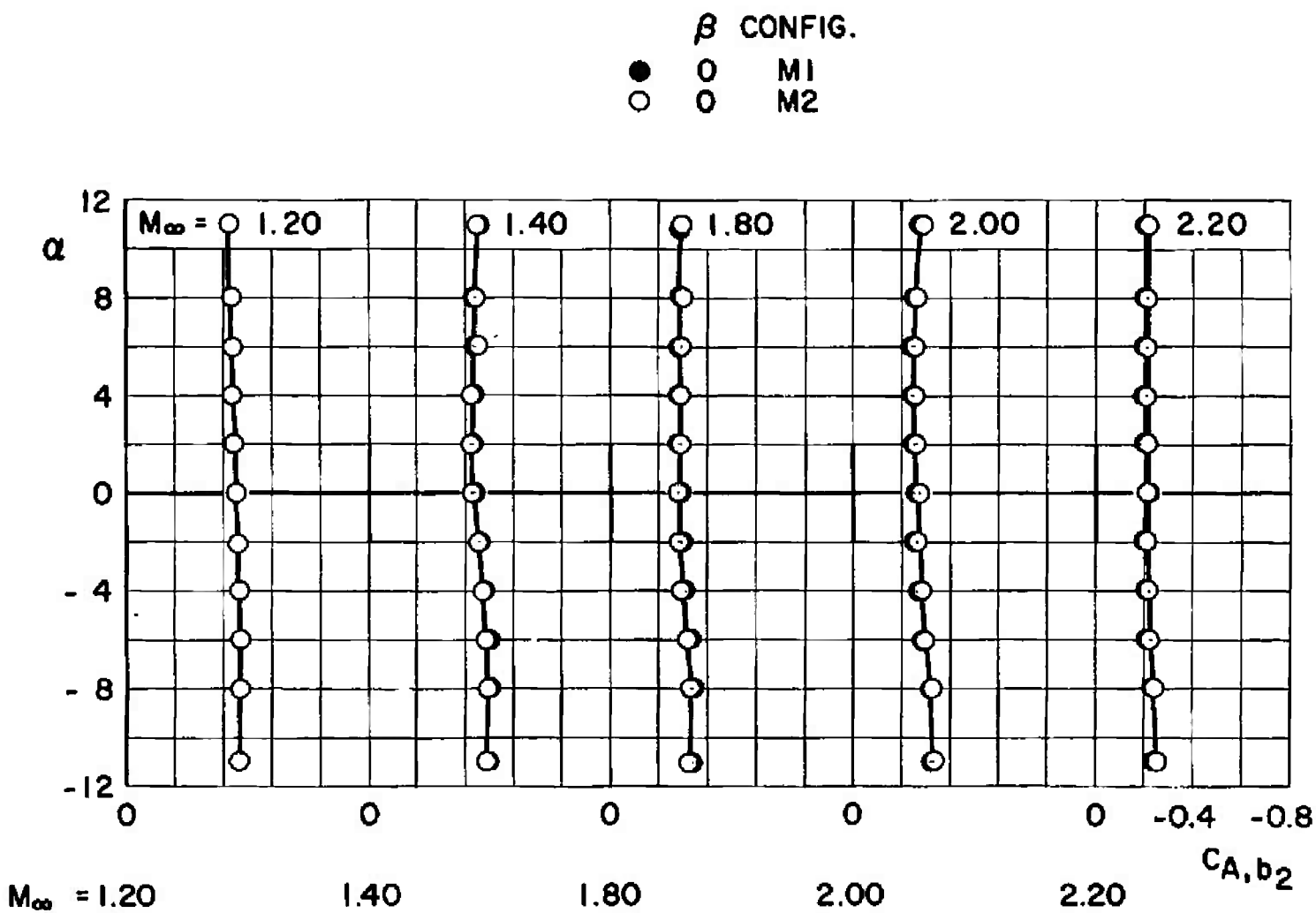

b. Mach Numbers 1.20 through 2.20

Fig. 14 Concluded

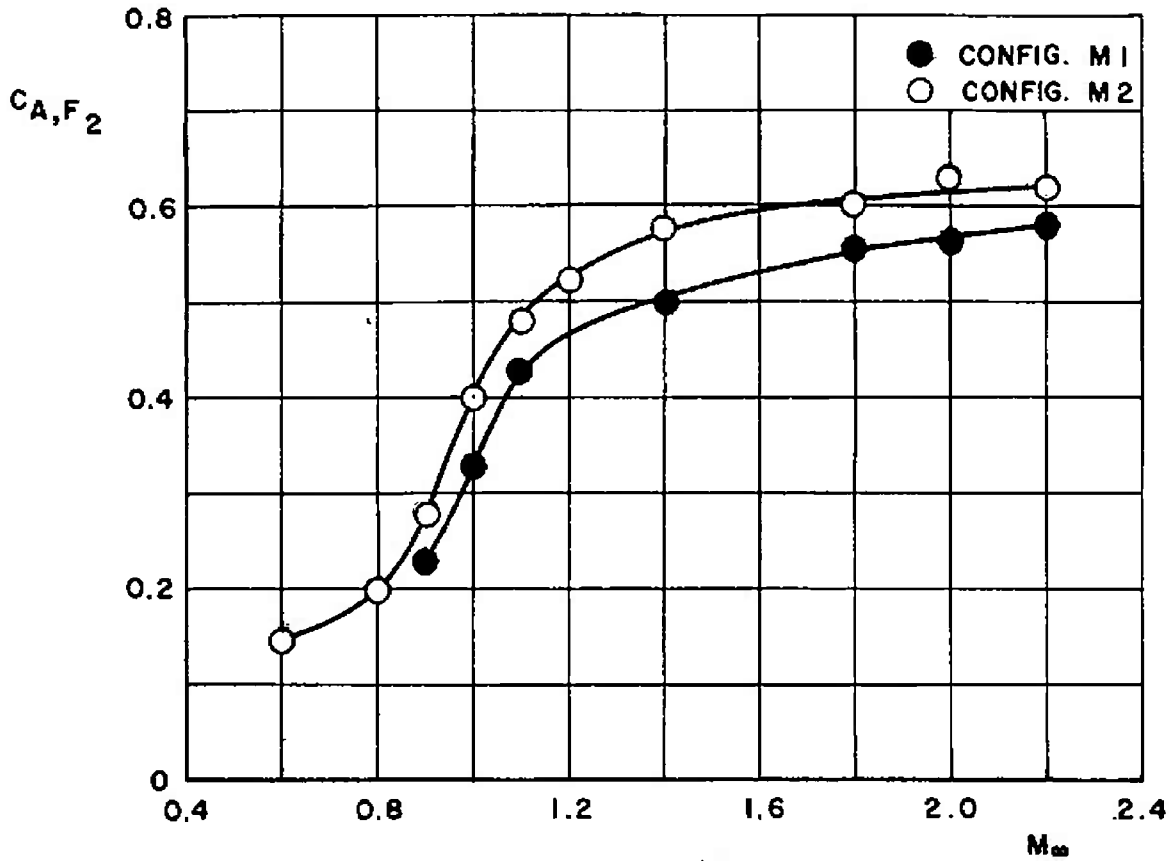

Fig. 15 Variation of MOL-Gemini Forebody Axial-Force Coefficient with Mach Number for Configurations M1 and M2 at α, β = 0

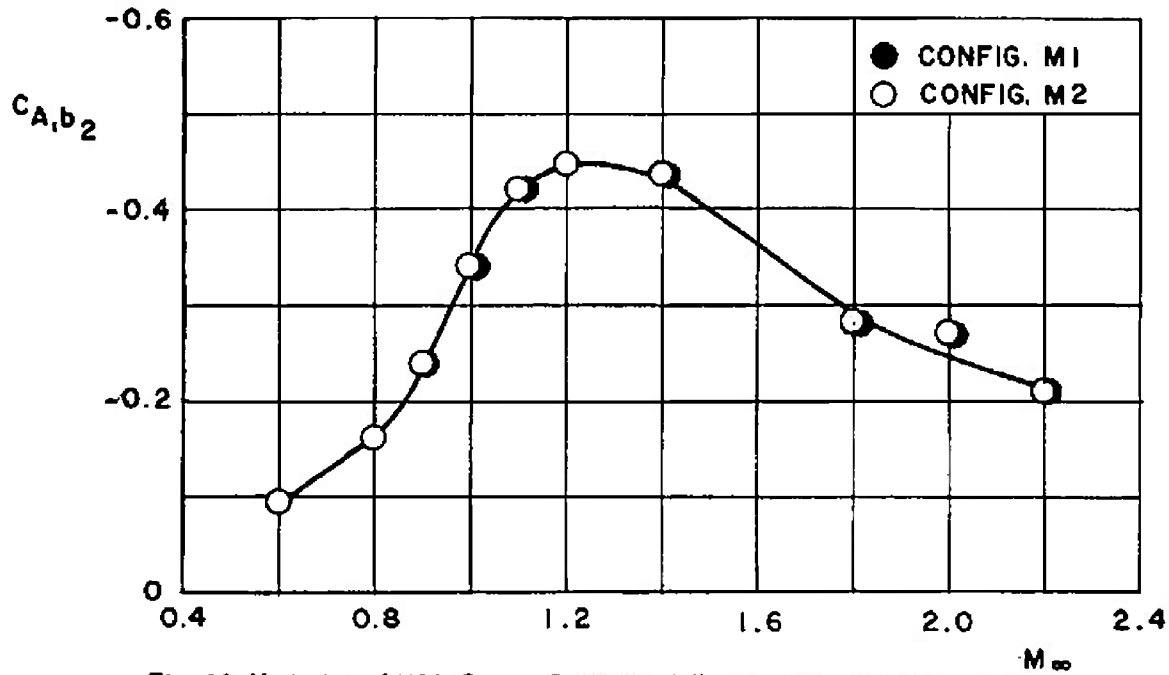

Fig. 16 Variation of MOL-Gemini Base Axial-Force Coefficient with Mach Number for Configurations M1 and M2 at α, β = 0

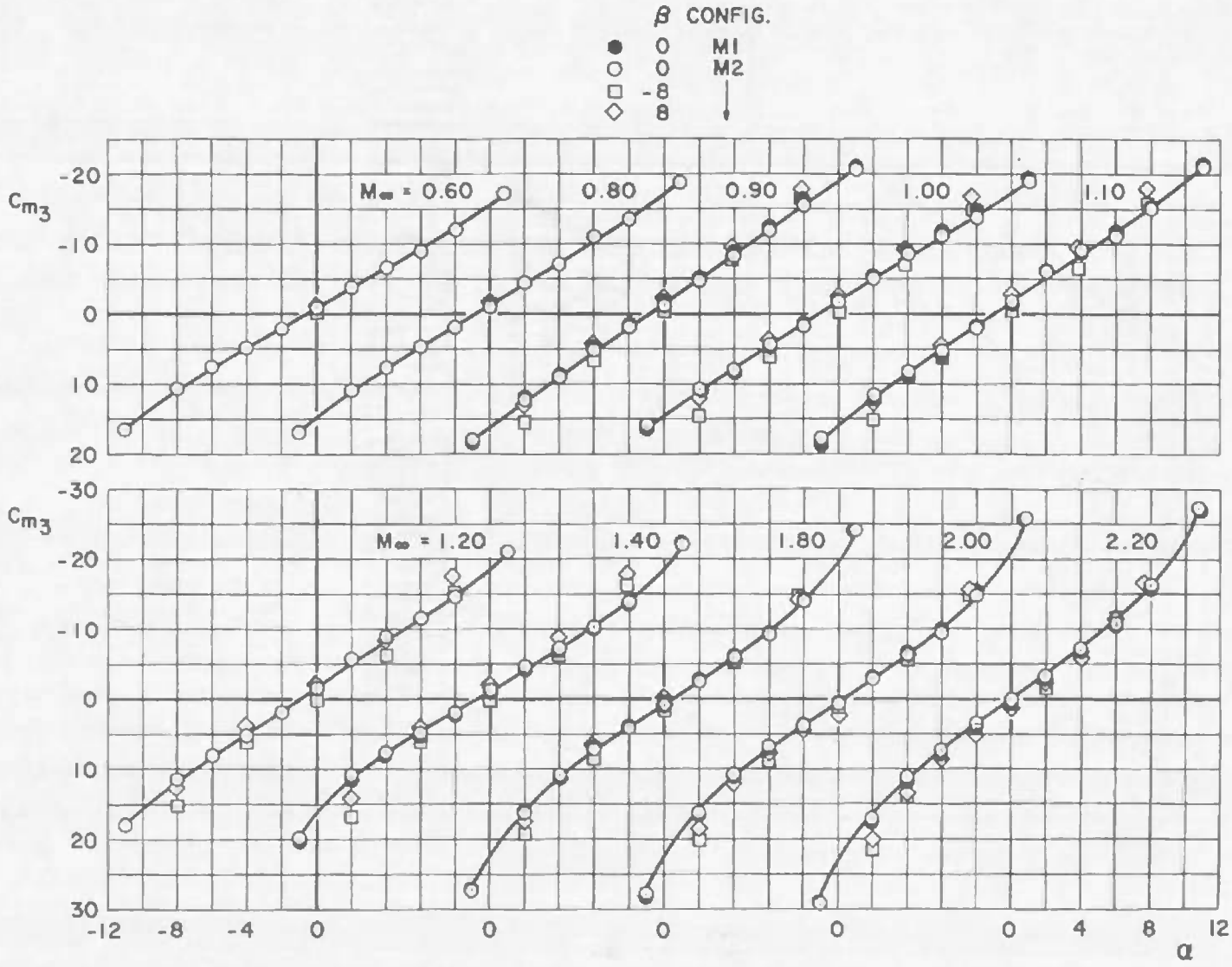

Fig. 17 Variation of Composite Model Pitching-Moment Coefficient with Angle of Attack for Configurations M1 and M2

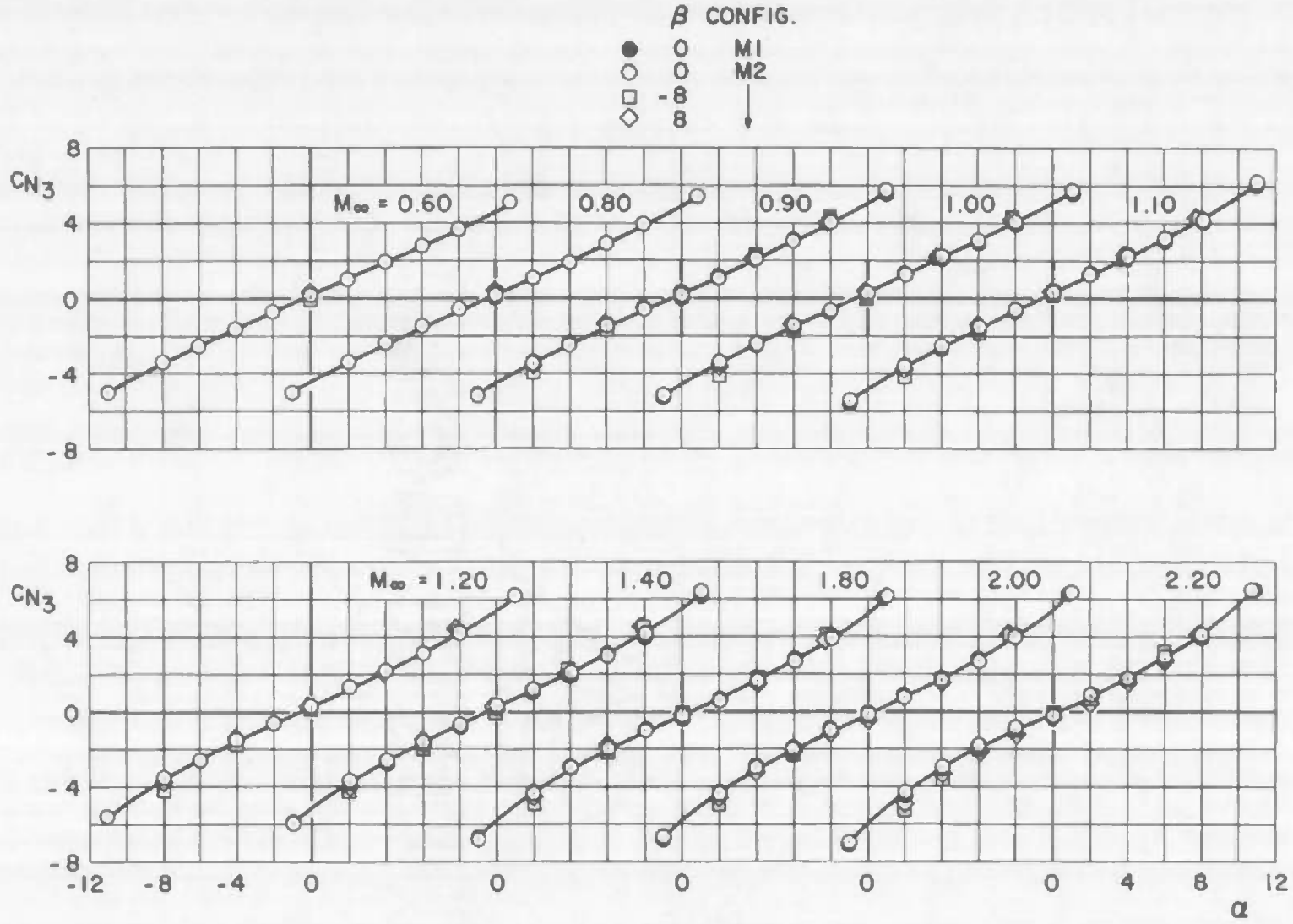

Fig. 18 Variation of Composite Model Normal-Force Coefficient with Angle of Attack for Configurations M1 and M2

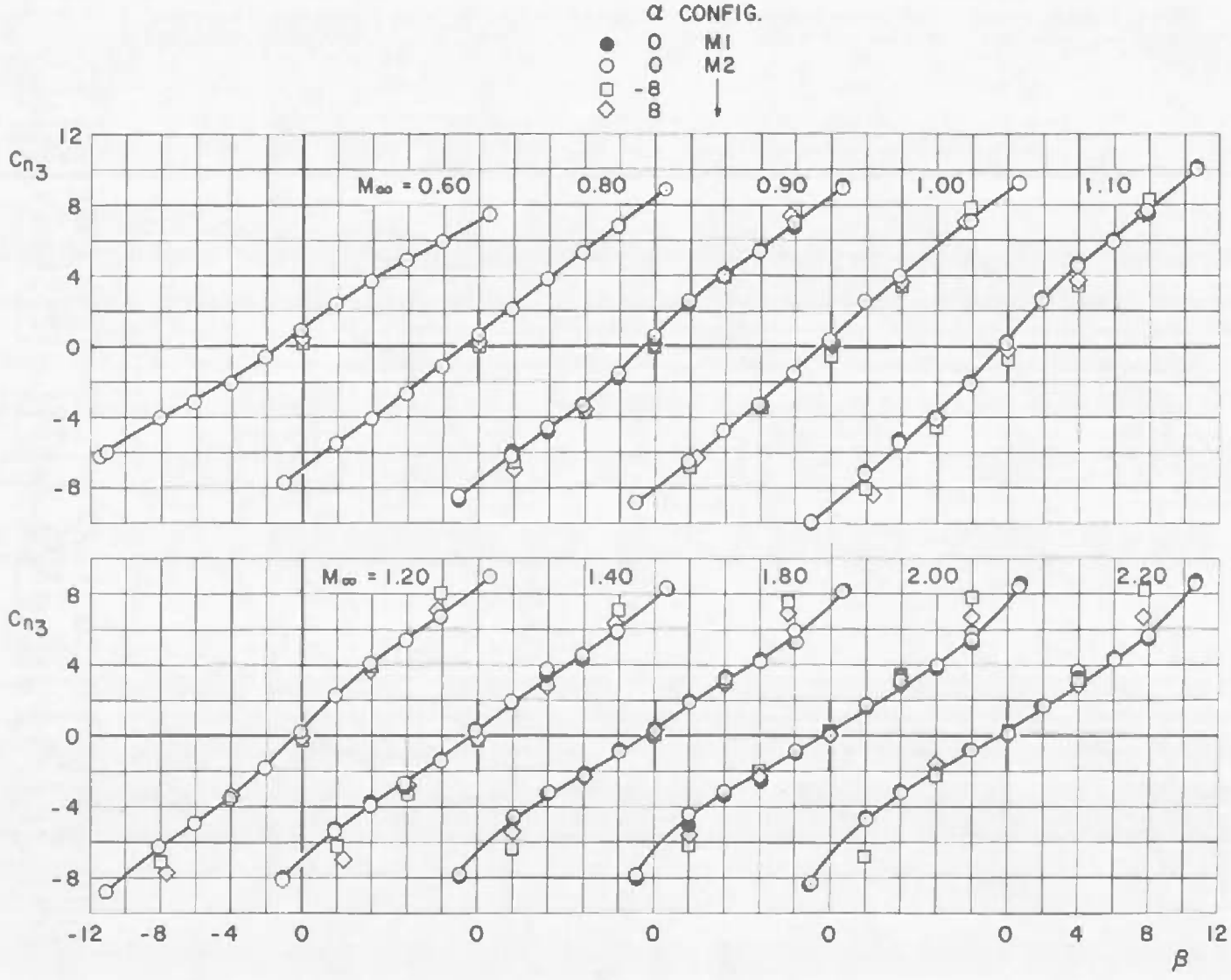

Fig. 19 Variation of Composite Model Yawing-Moment Coefficient with Sideslip Angle for Configurations M1 and M2

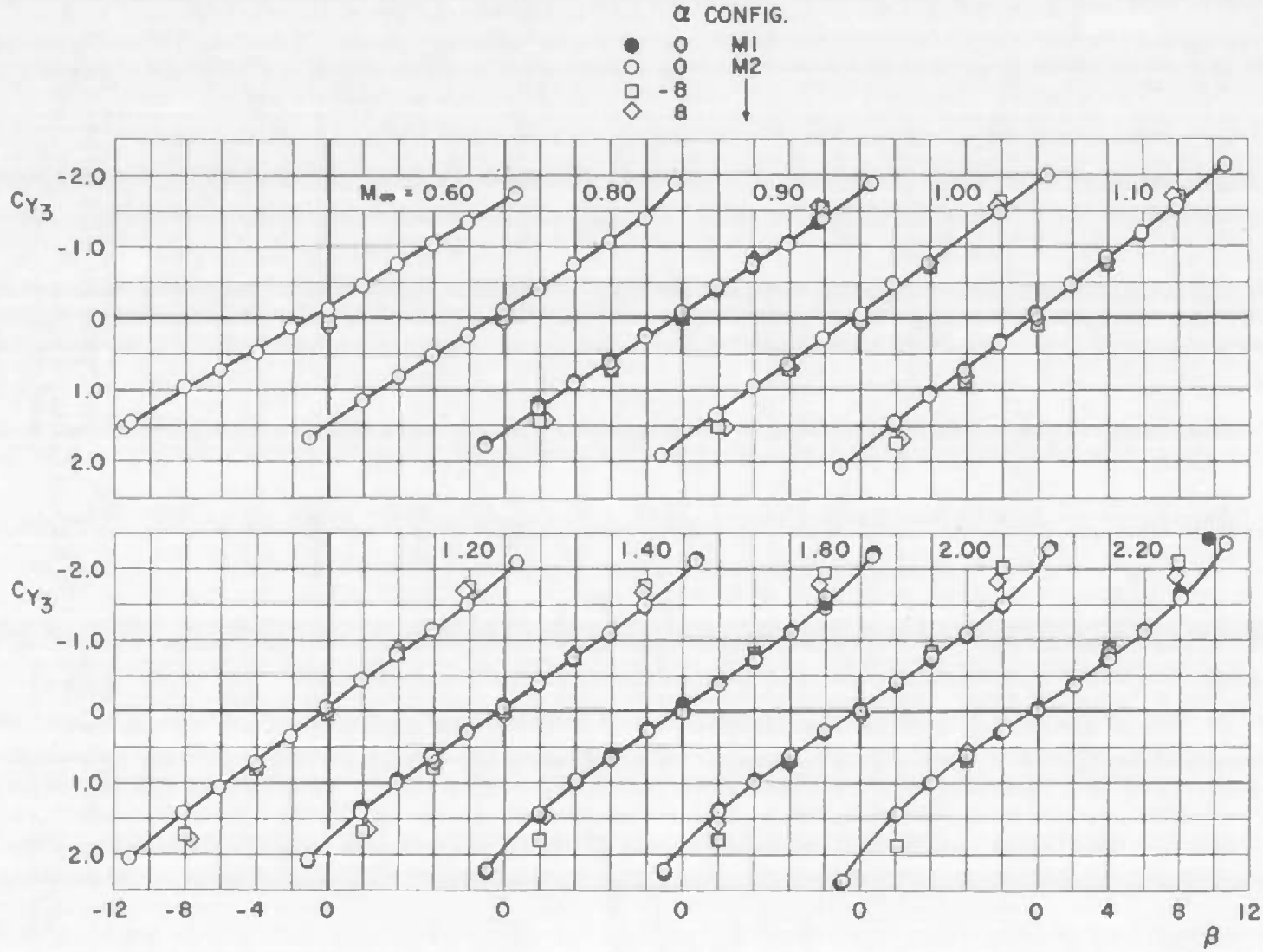

Fig. 20 Variation of Composite Model Side-Force Coefficient with Sideslip Angle for Configurations M1 and M2

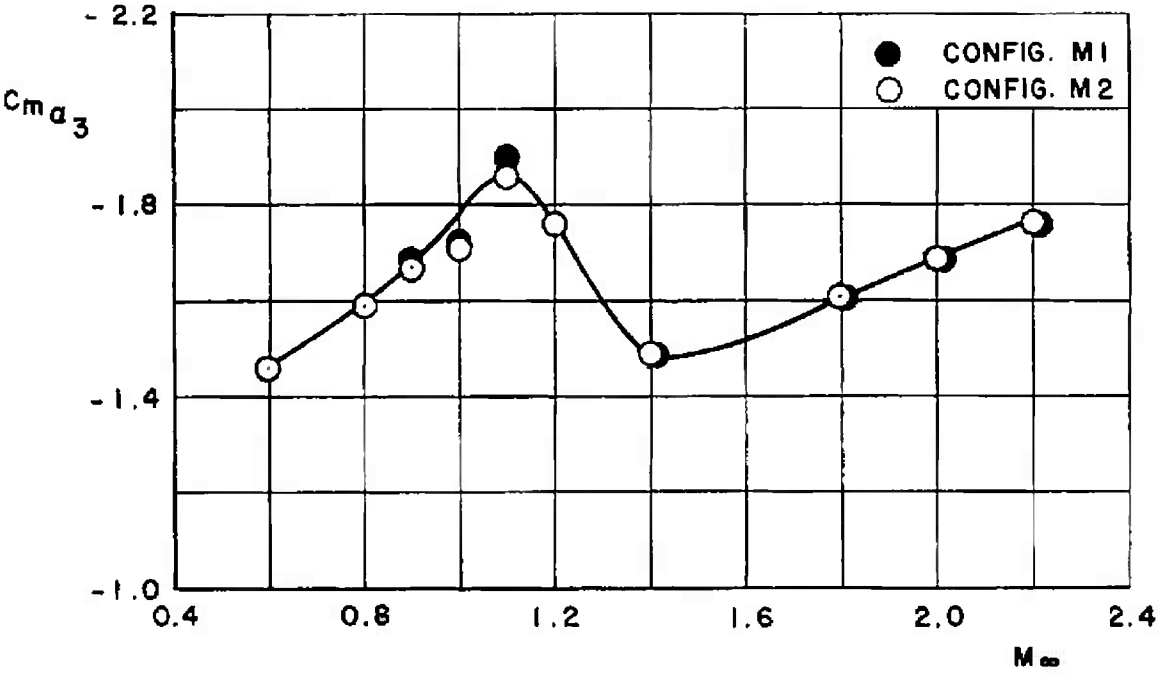

Fig. 21 Variation of Composite Model Pitching-Moment Curve Slope with Mach Number for Configurations M1 and M2

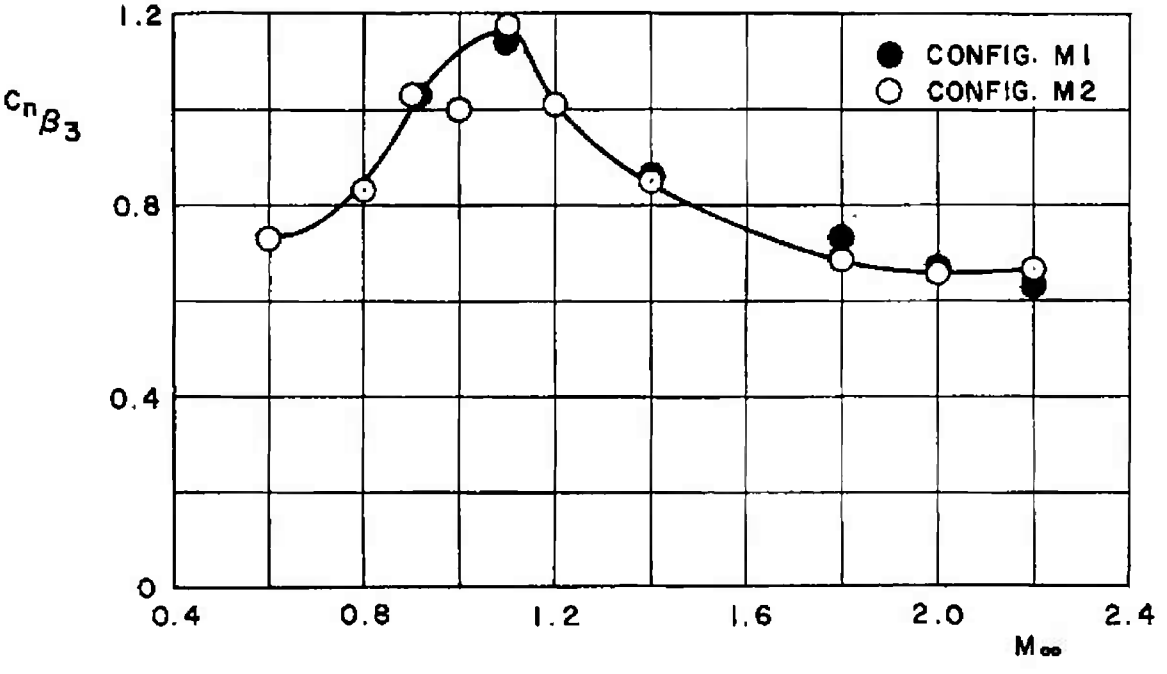

Fig. 22 Variation of Composite Model Yawing-Moment Curve Slope with Mach Number for Configurations M1 and M2

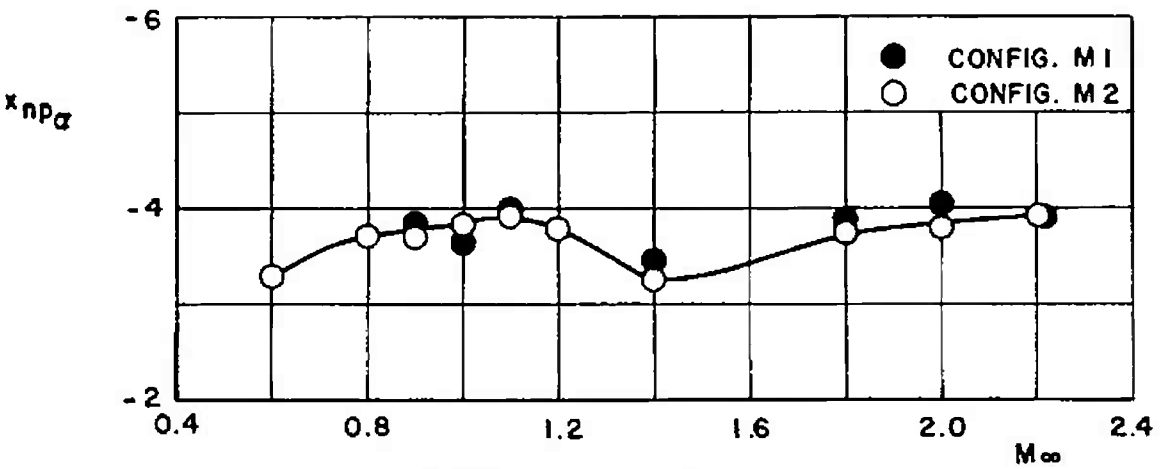

a. Longitudinal Neutral Point

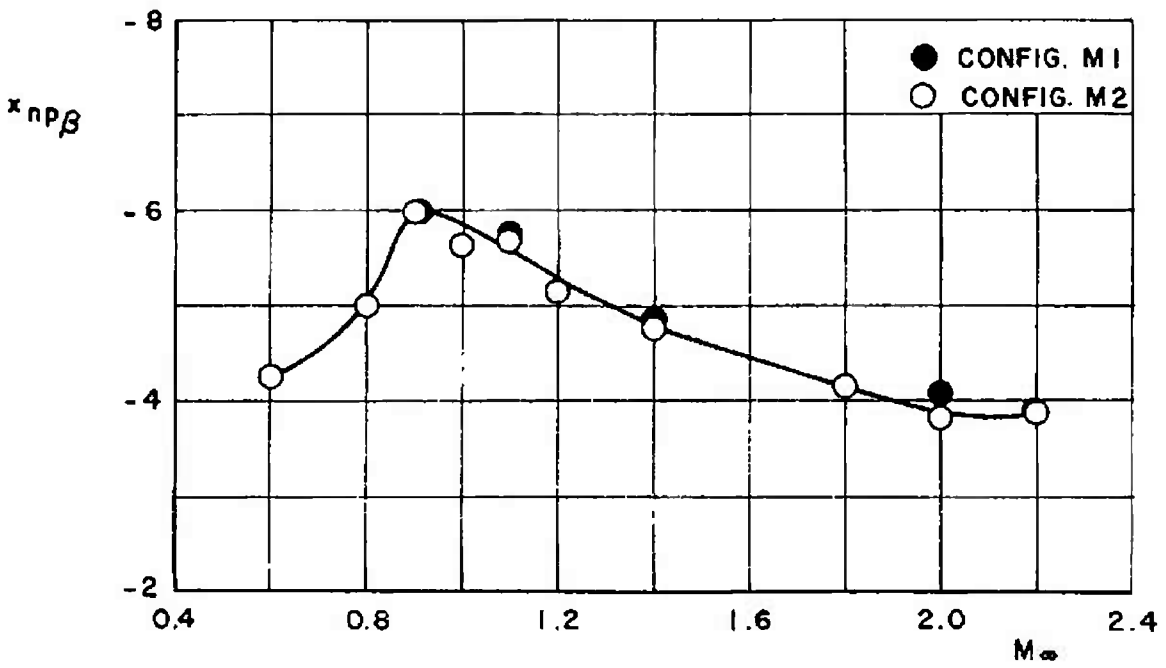

b. Lateral Neutral Point

Fig. 23 Variation of Composite Neutral-Point Location with Mach Number for Configurations M1 and M2

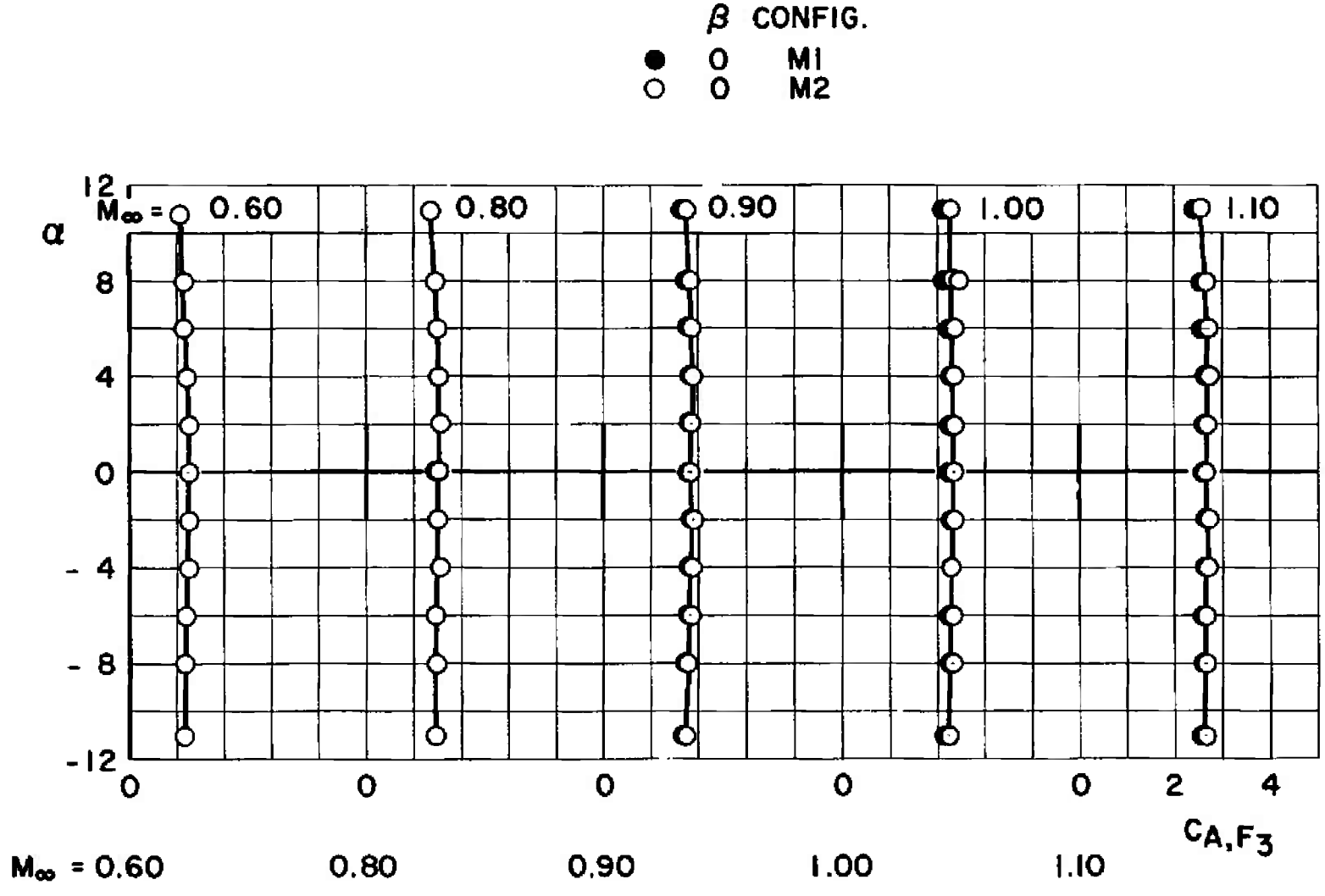

a. Mach Numbers 0.60 through 1.10

Fig. 24 Variation of Composite Model Forebody Axial-Force Coefficient with Angle of Attack for Configurations M1 and M2 at $\beta = 0$

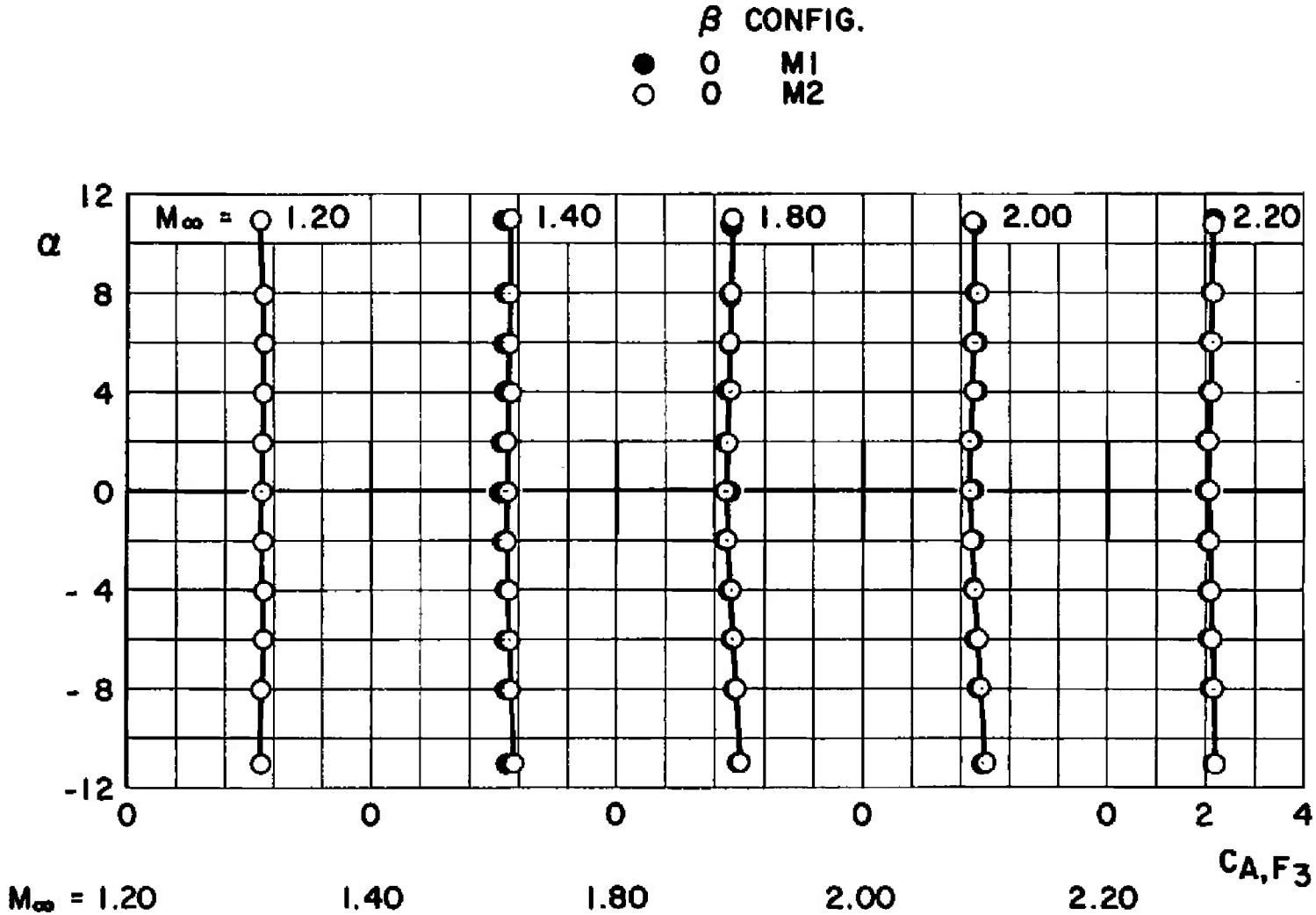

b. Mach Numbers 1.20 through 2.20

Fig. 24 Concluded

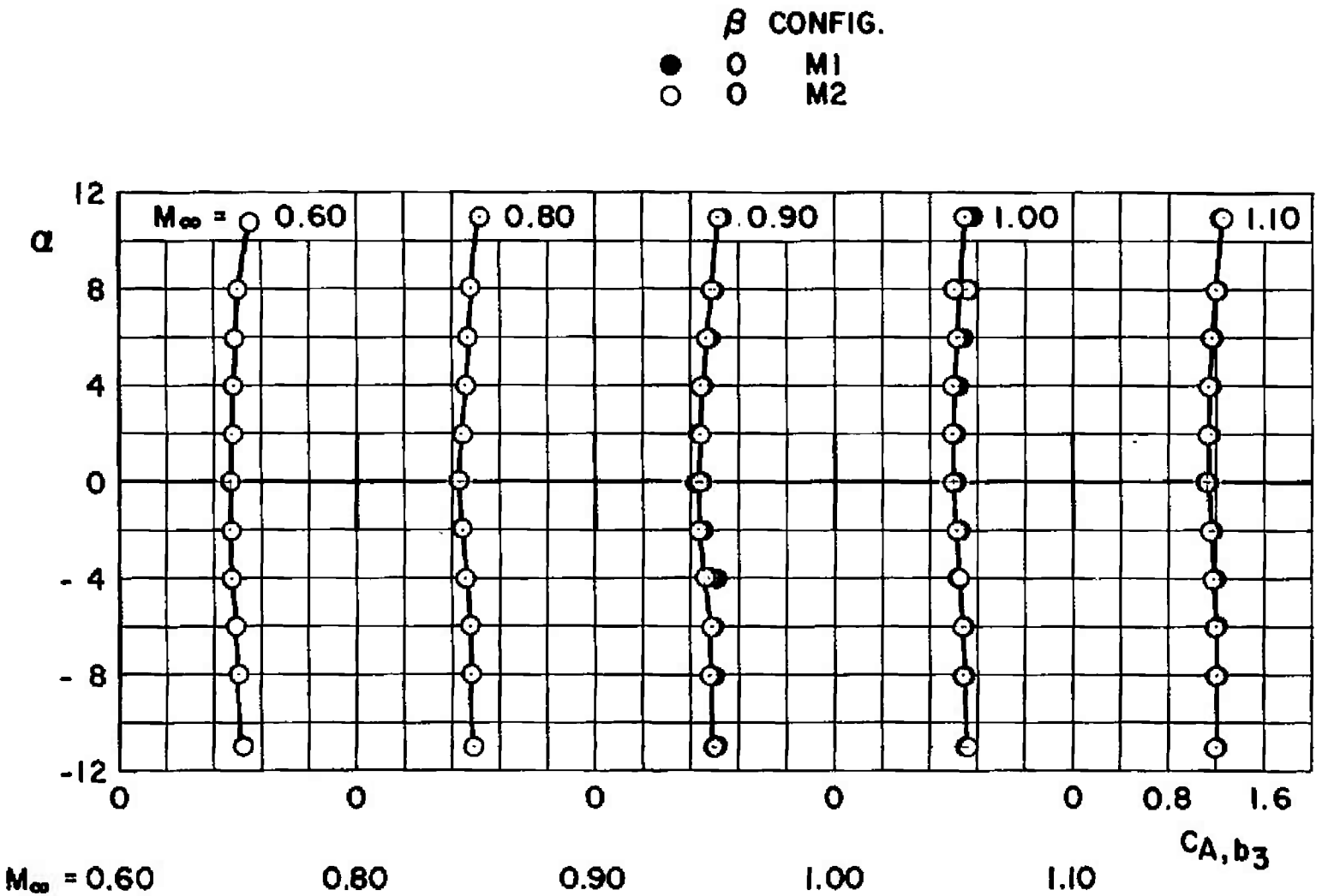

a. Mach Numbers 0.60 through 1.10

Fig. 25 Variation of Composite Model Base Axial-Force Coefficient with Angle of Attack for Configurations M1 and M2 at $\beta = 0$

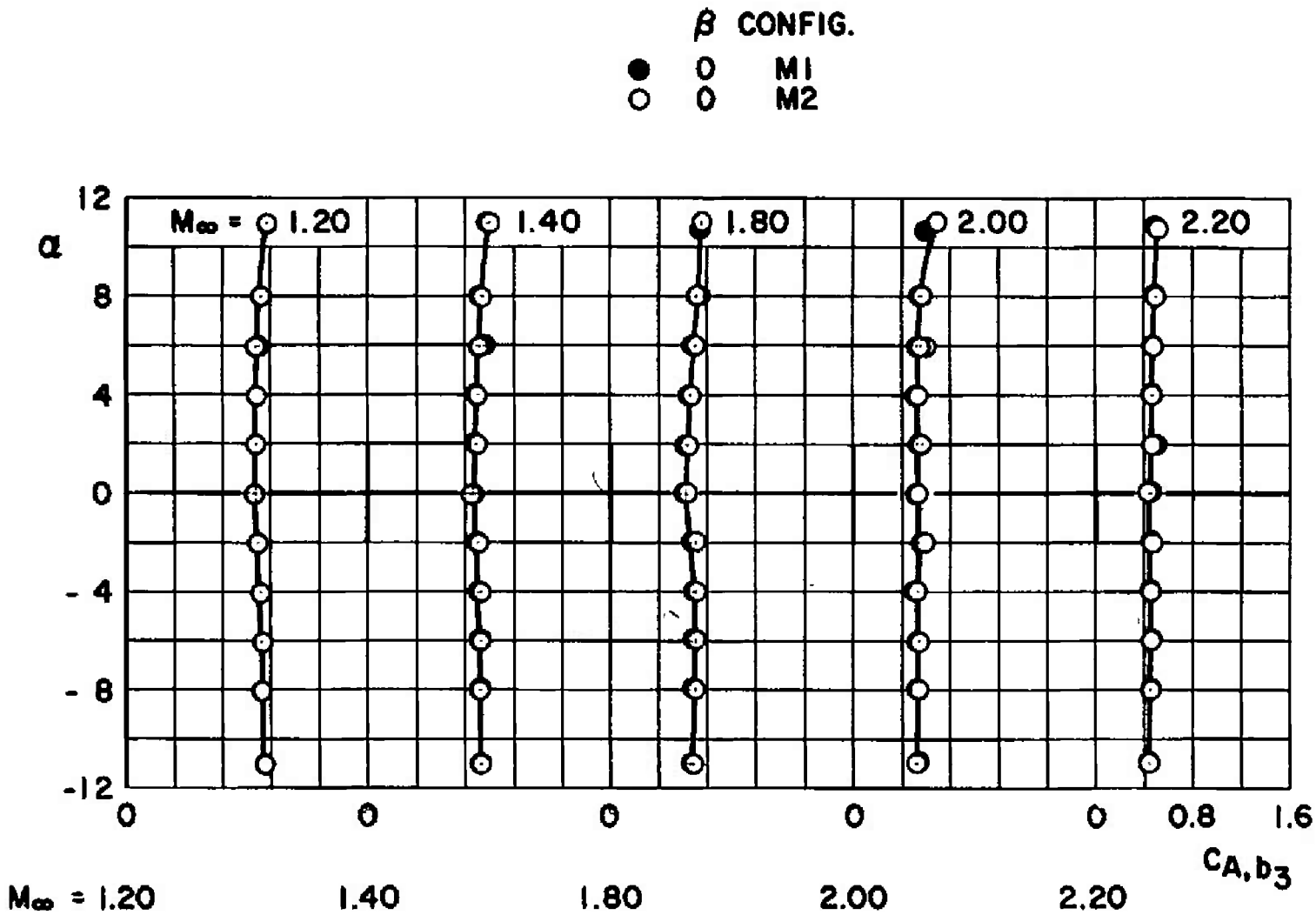

b. Mach Numbers 1.20 through 2.20

Fig. 25 Concluded

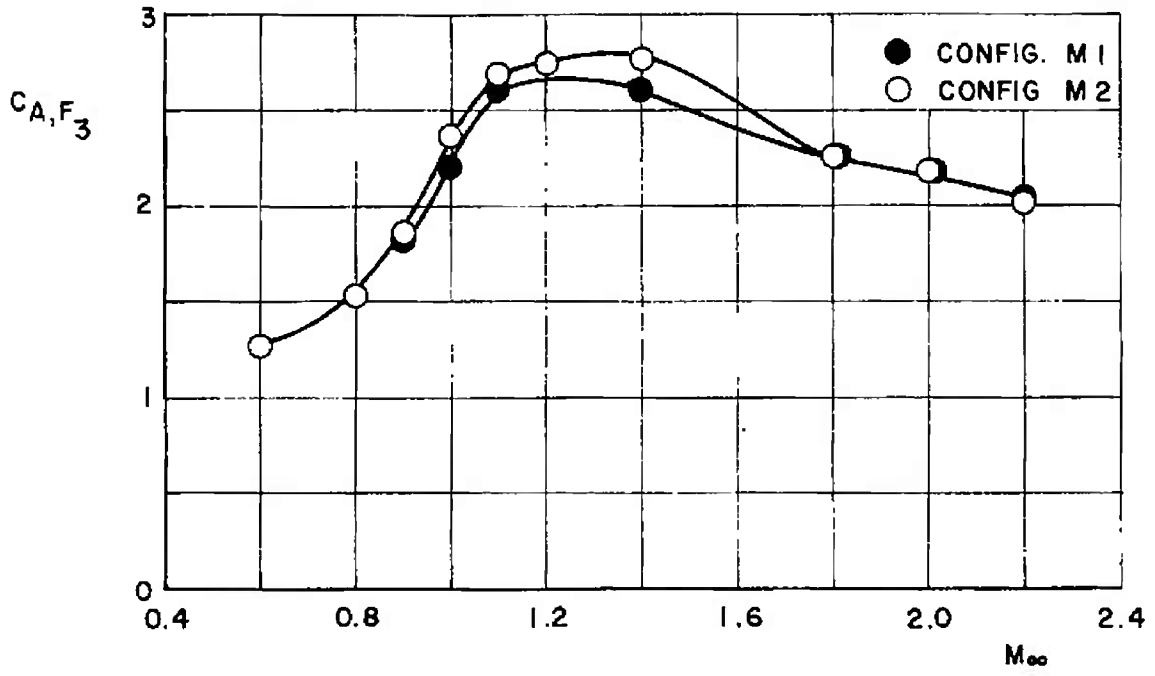

Fig. 26 Variation of Composite Model Forebody Axial-Force Coefficient with Mach Number for Configurations M1 and M2 at $\alpha, \beta = 0$

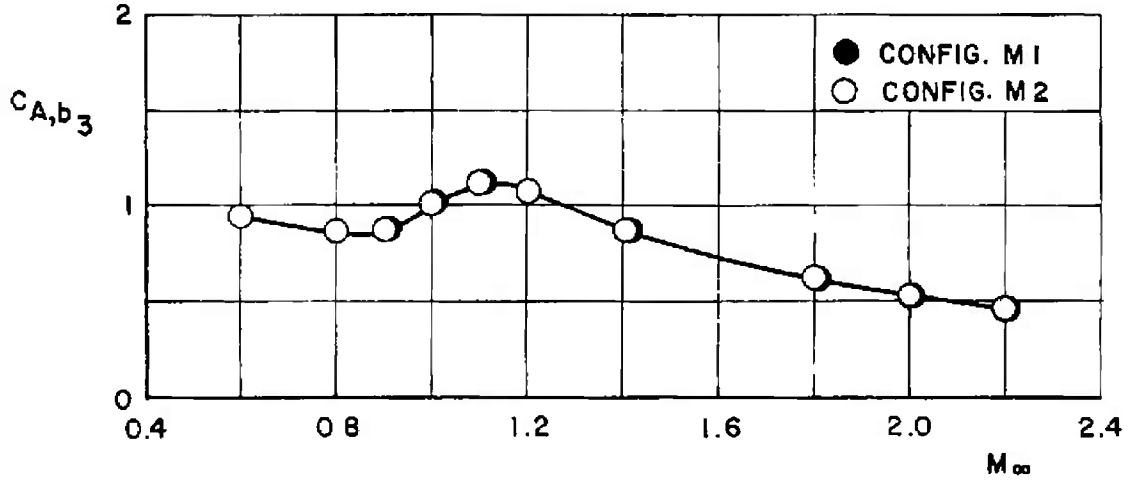

Fig. 27 Variation of Composite Model Base Axial-Force Coefficient with Mach Number for Configurations M1 and M2 at $\alpha, \beta = 0$

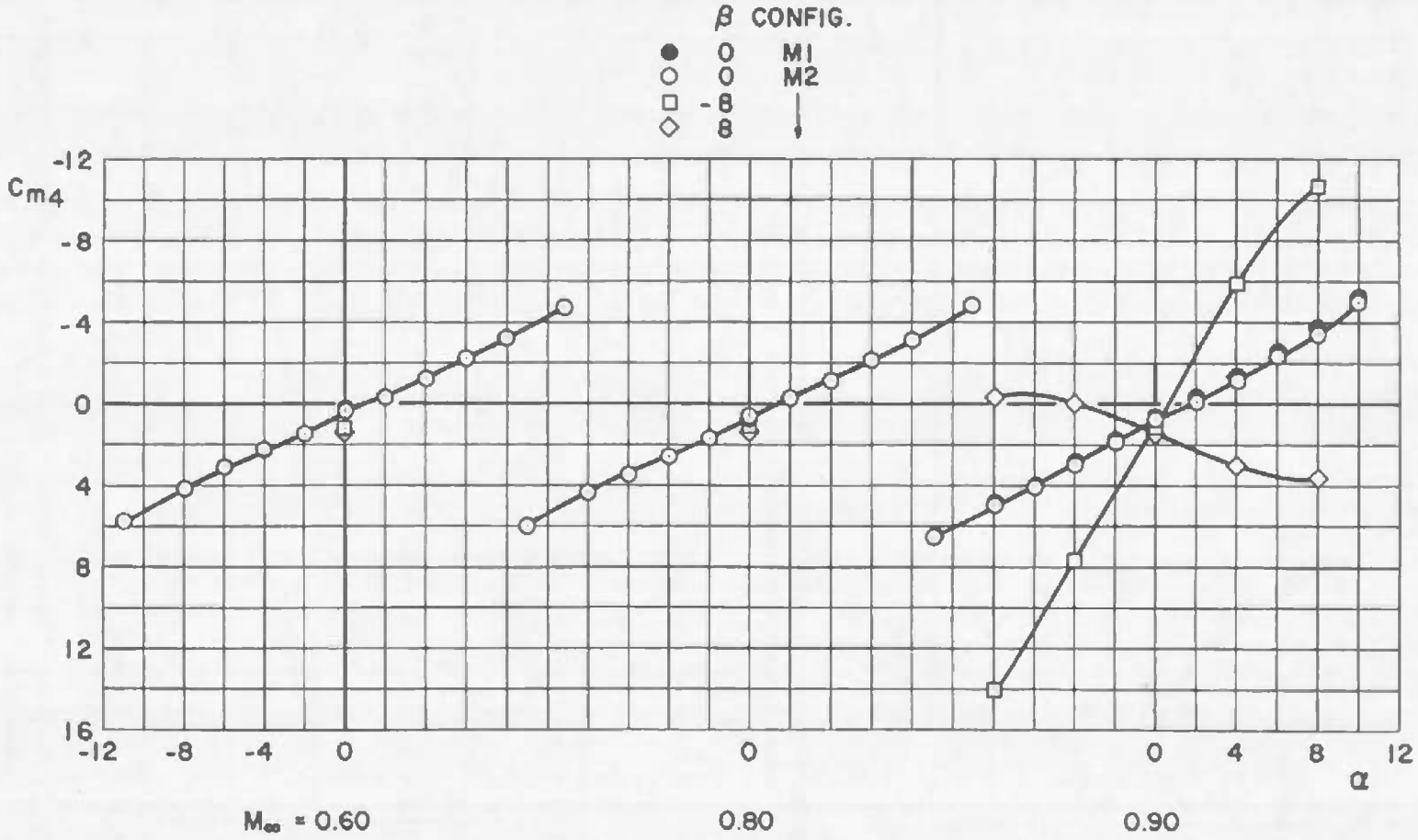

a. Mach Numbers 0.60, 0.80, and 0.90

Fig. 28 Variation of SRM Pitching-Moment Coefficient with Angle of Attack for Configurations M1 and M2

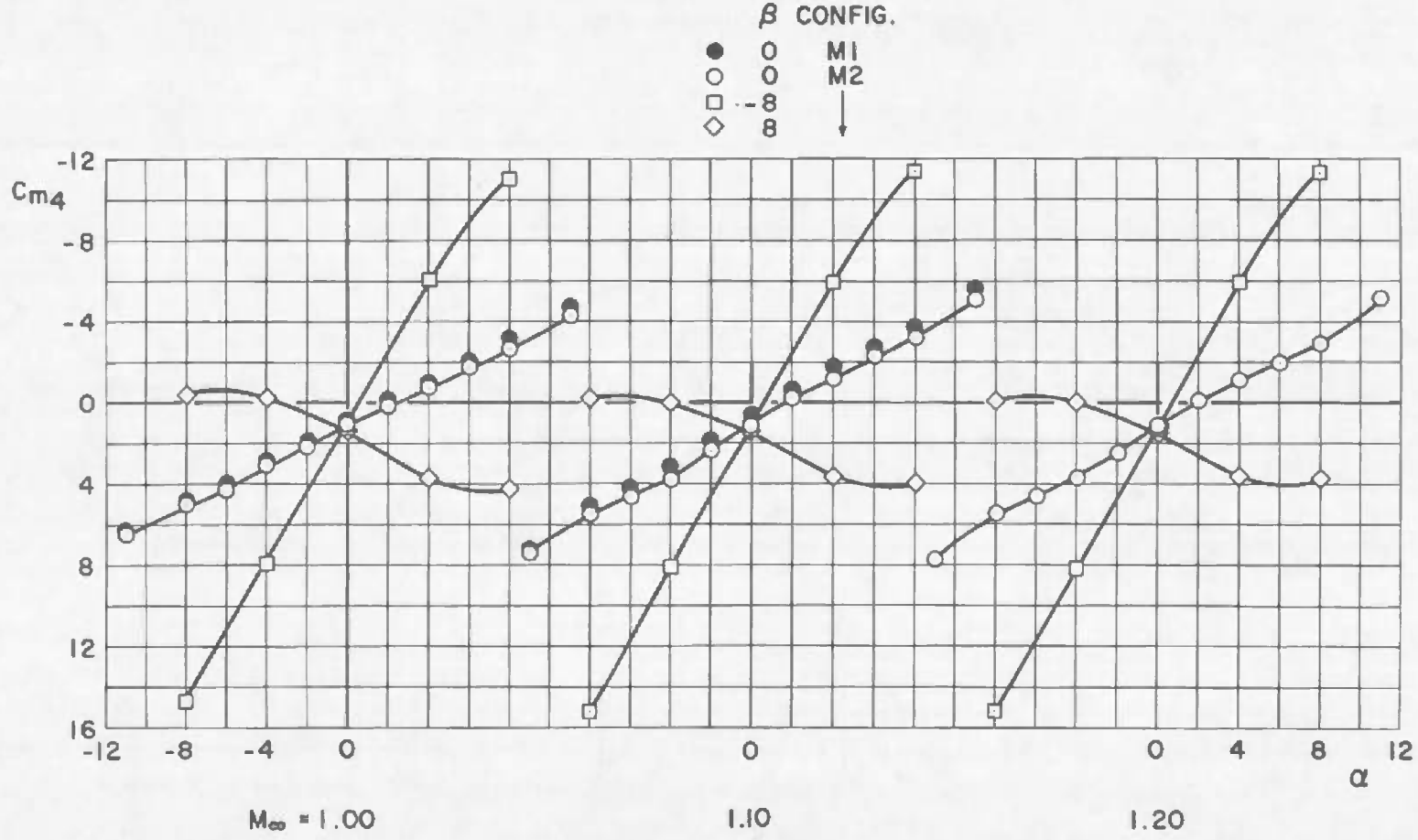

b. Mach Numbers 1.00, 1.10, and 1.20

Fig. 28 Continued

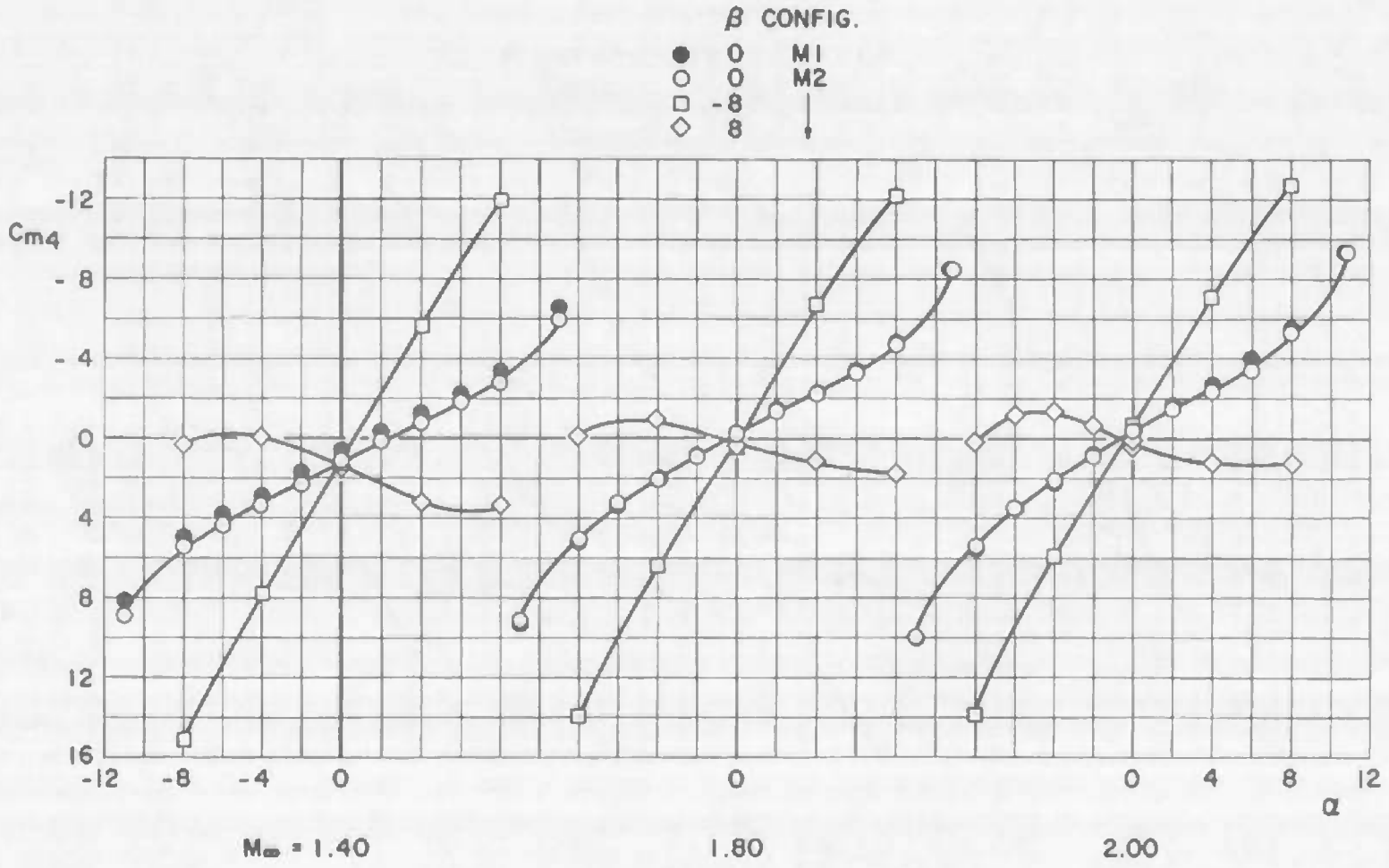

c. Mach Numbers 1.40, 1.80, and 2.00

Fig. 28 Continued

d. Mach Number 2.20

Fig. 28 Concluded

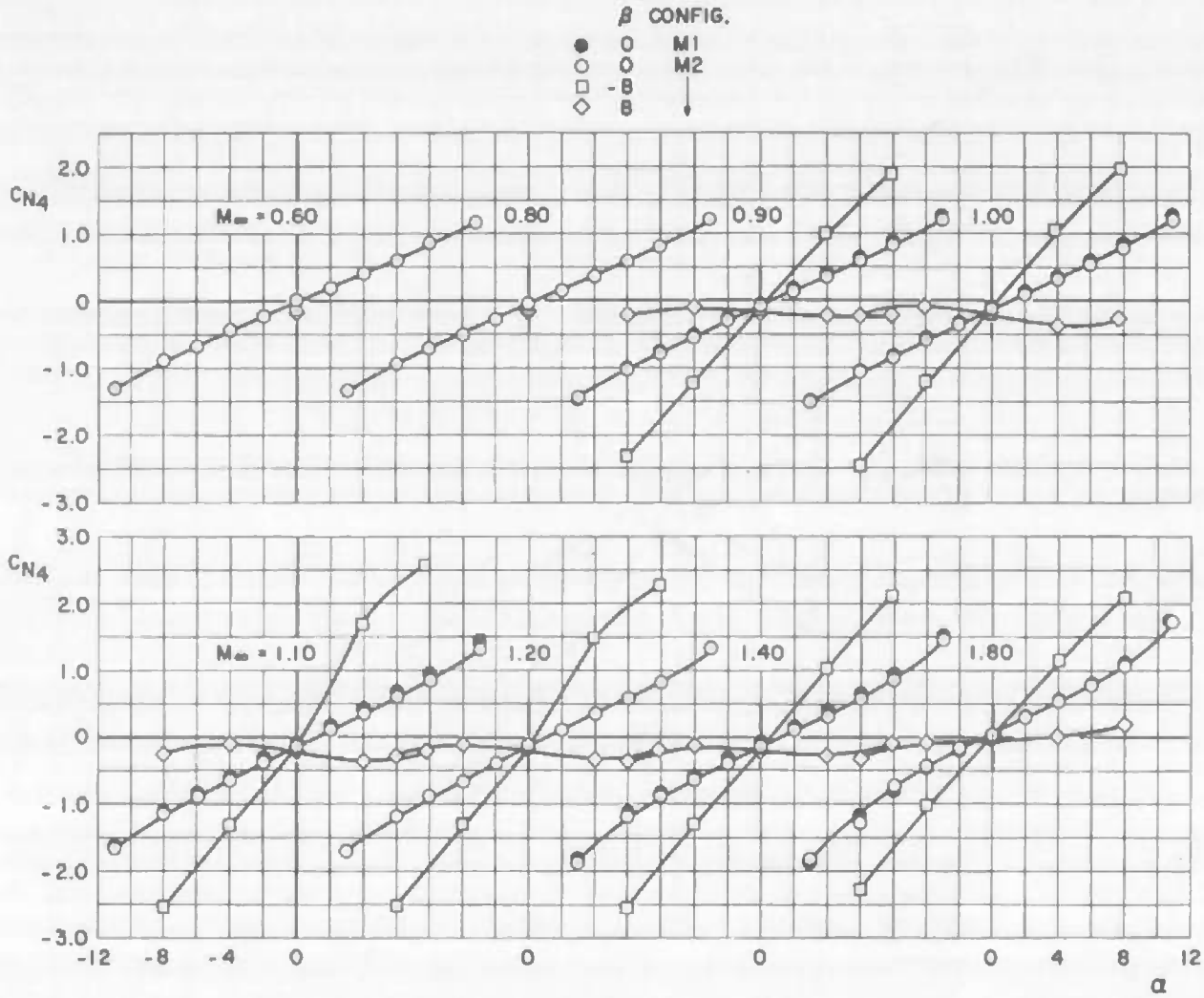

a. Mach Numbers 0.60 through 1.80

Fig. 29 Variation of SRM Normal-Force Coefficient with Angle of Attack for Configurations M1 and M2

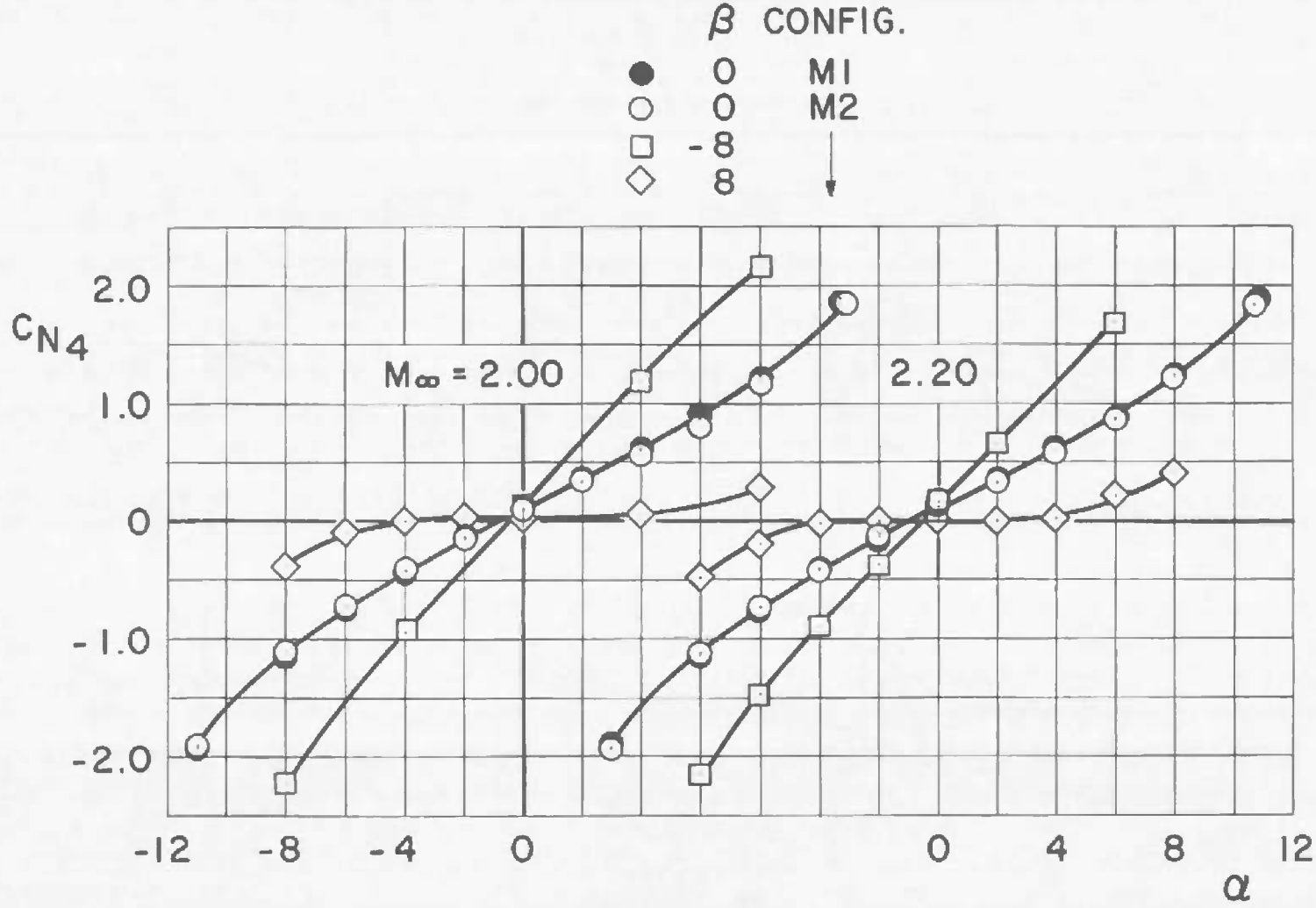

b. Mach Numbers 2.00 and 2.20

Fig. 29 Concluded

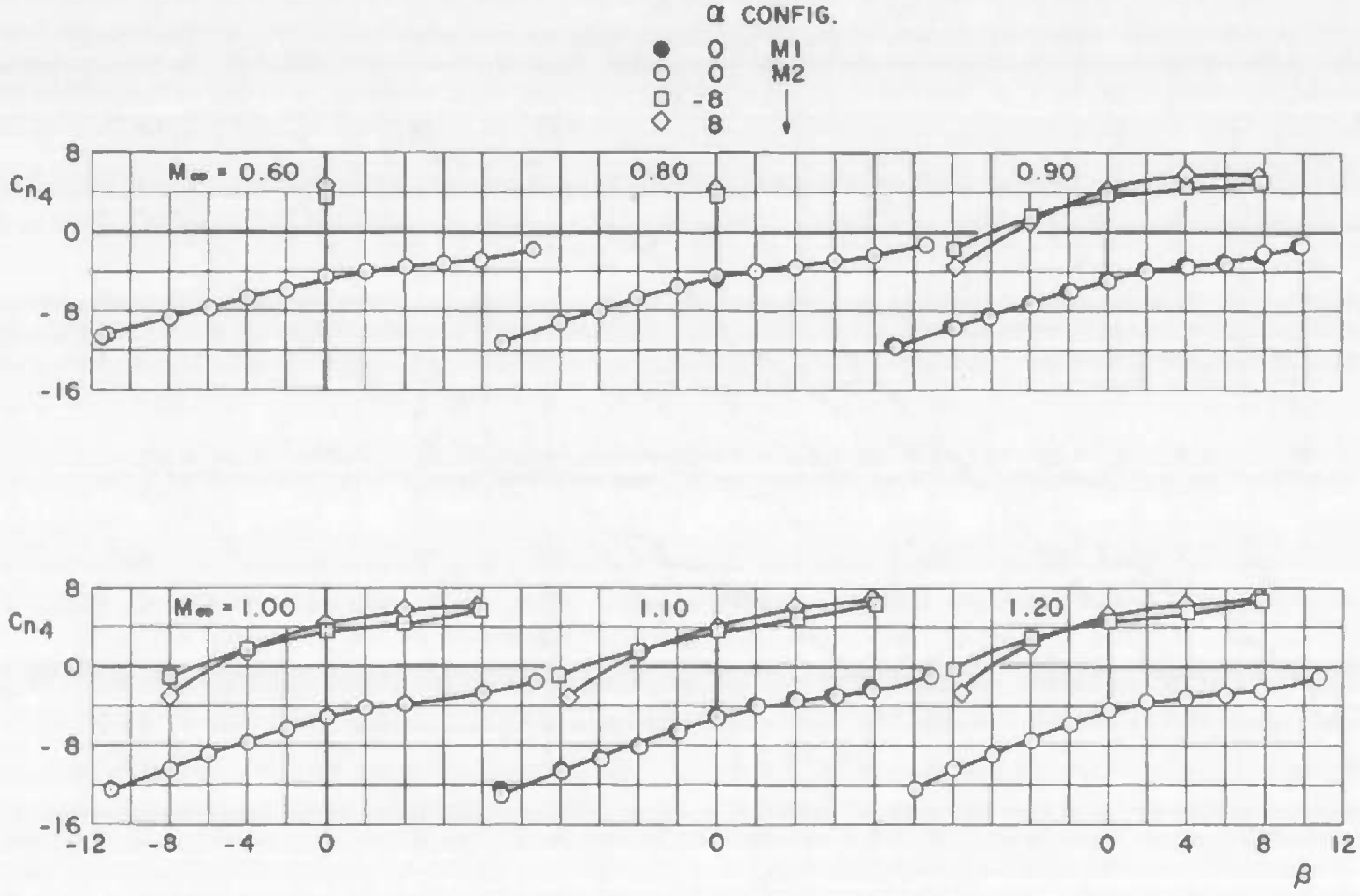

a. Mach Numbers 0.60 through 1.20

Fig. 30 Variation of SRM Yawing-Moment Coefficient with Sideslip Angle for Configurations M1 and M2

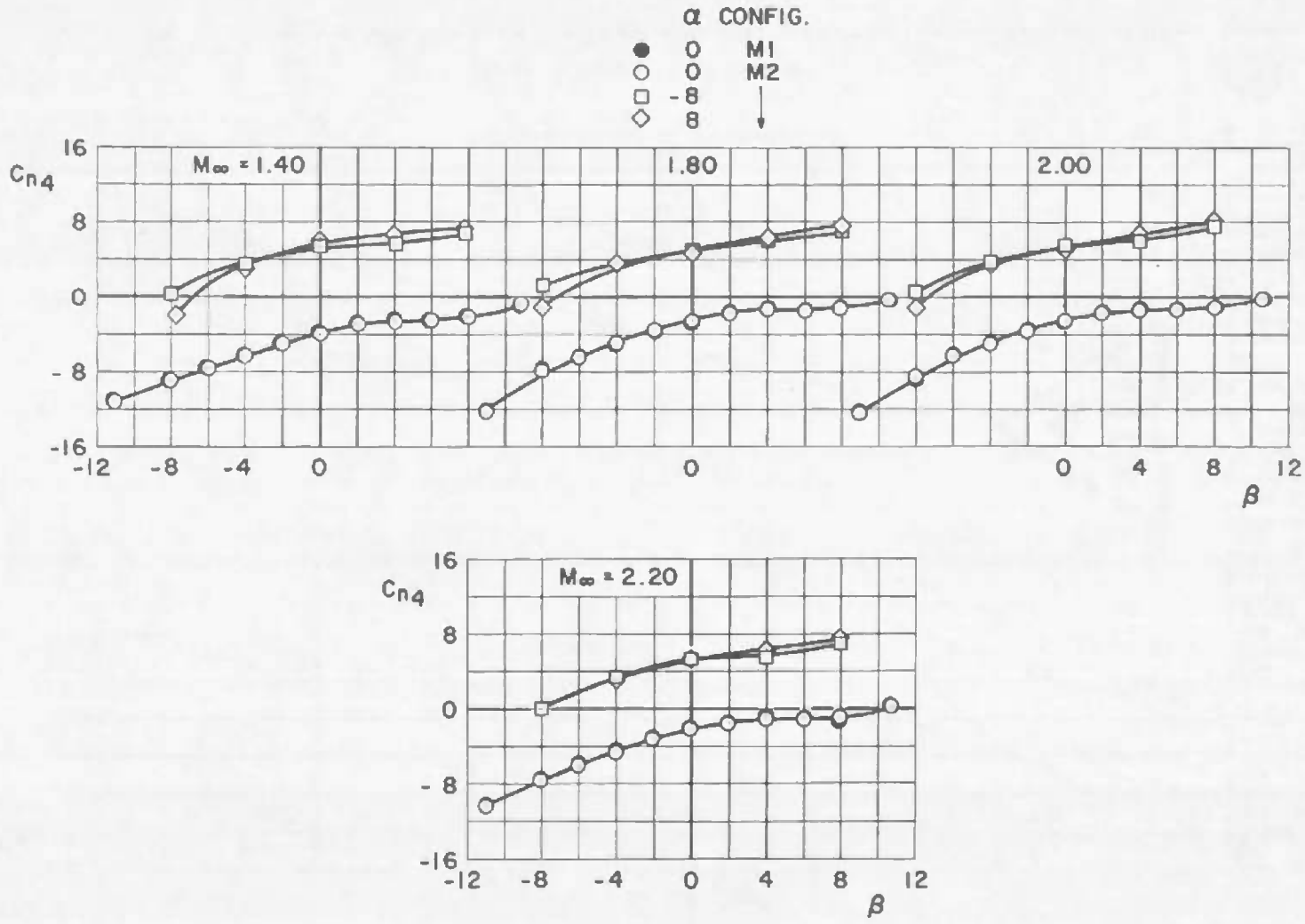

b. Mach Numbers 1.40 through 2.20

Fig. 30 Concluded

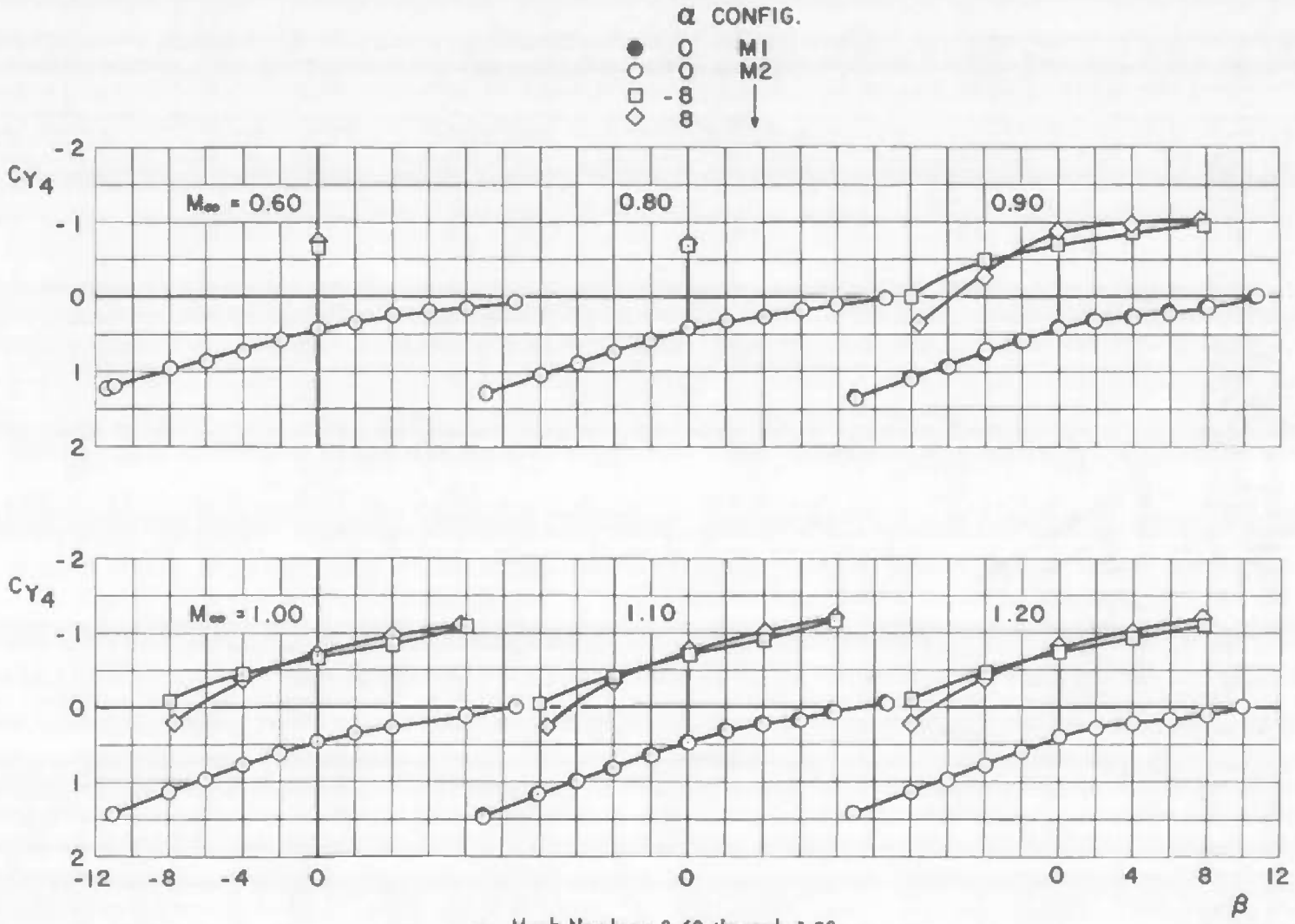

a. Mach Numbers 0.60 through 1.20

Fig. 31 Variation of SRM Side-Force Coefficient with Sideslip Angle for Configurations M1 and M2

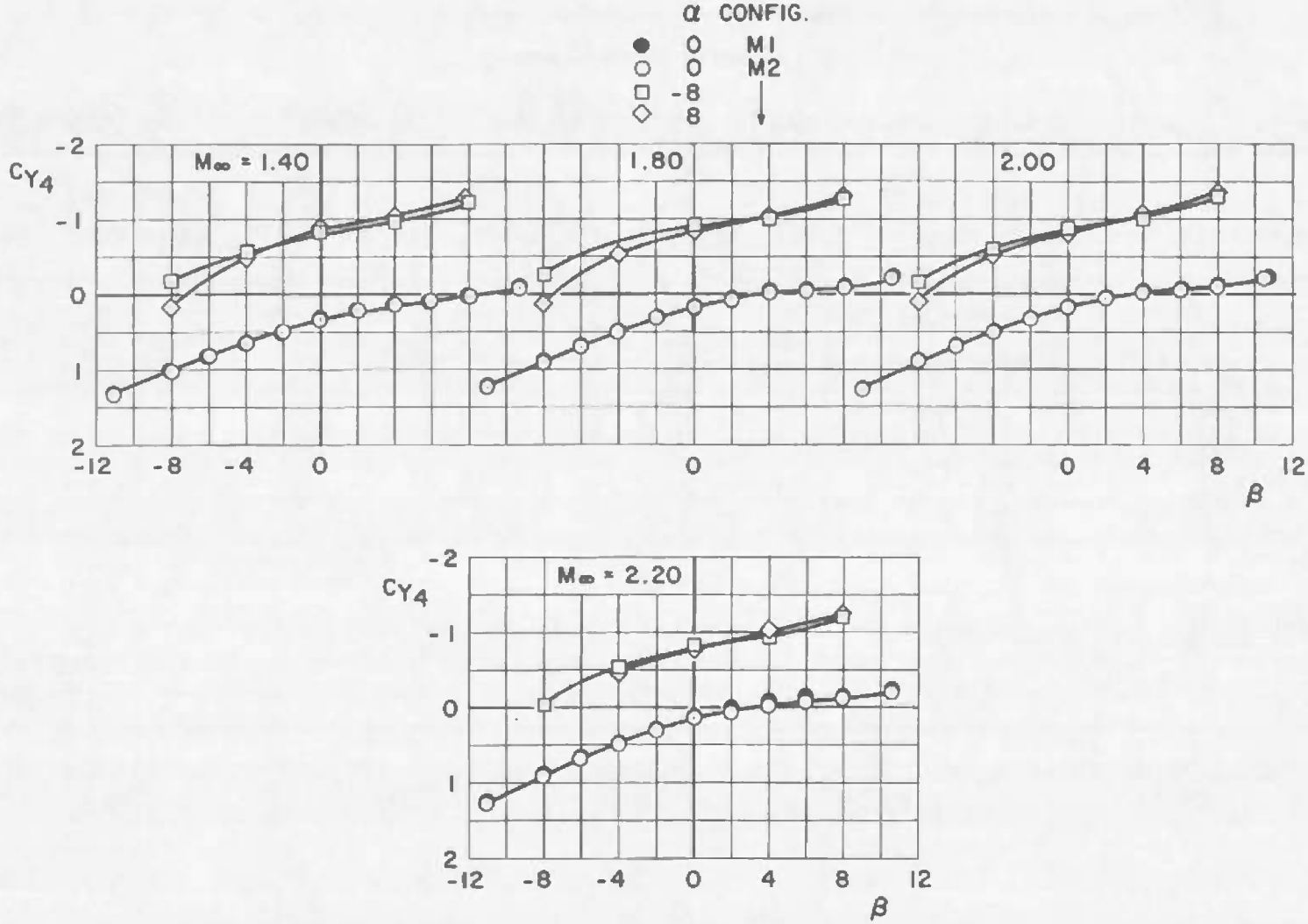

b. Mach Numbers 1.40 through 2.20

Fig. 31 Concluded

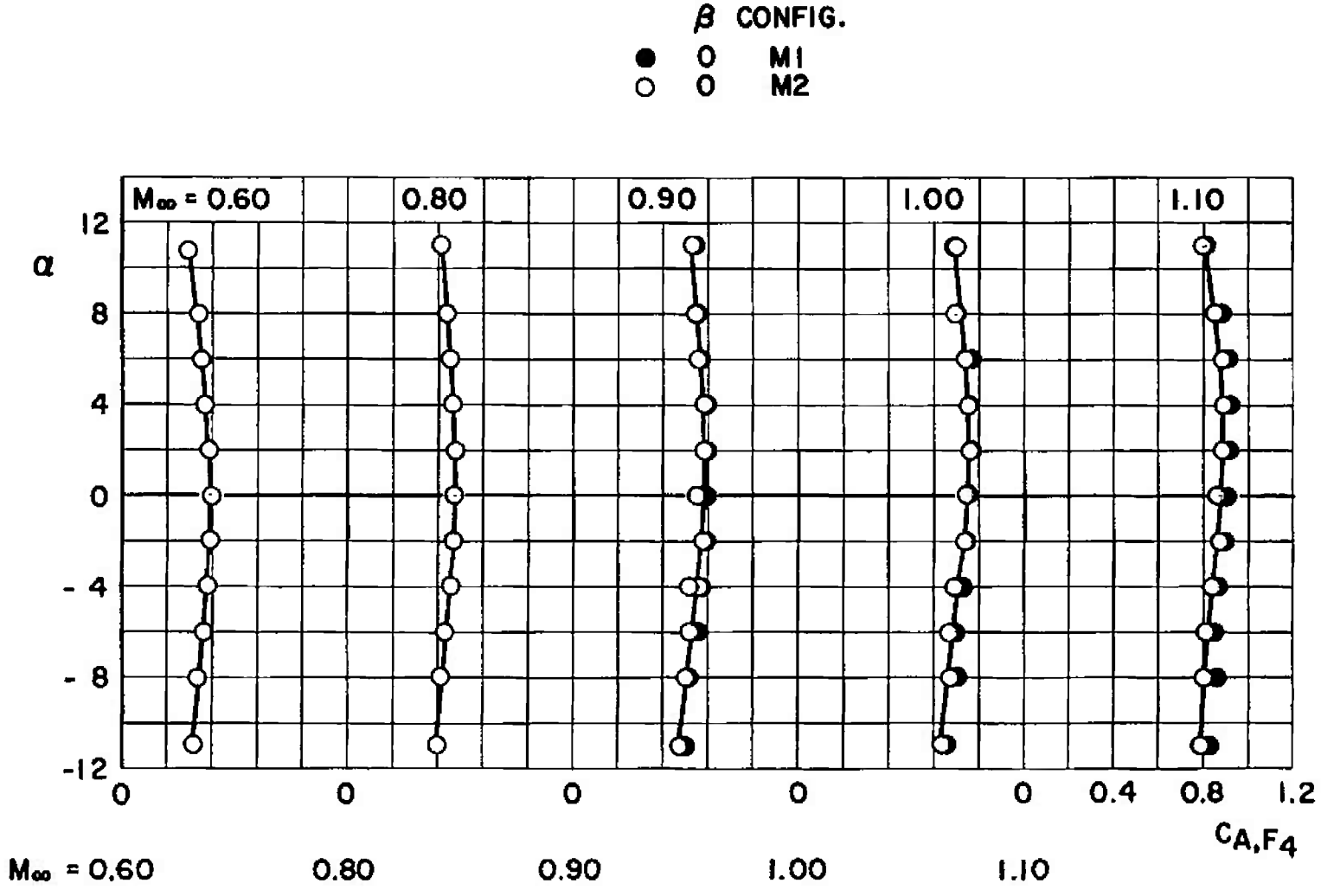

a. Mach Numbers 0.60 through 1.10

Fig. 32 Variation of SRM Forebody Axial-Force Coefficient with Angle of Attack for Configurations M1 and M2 at $\beta = 0$

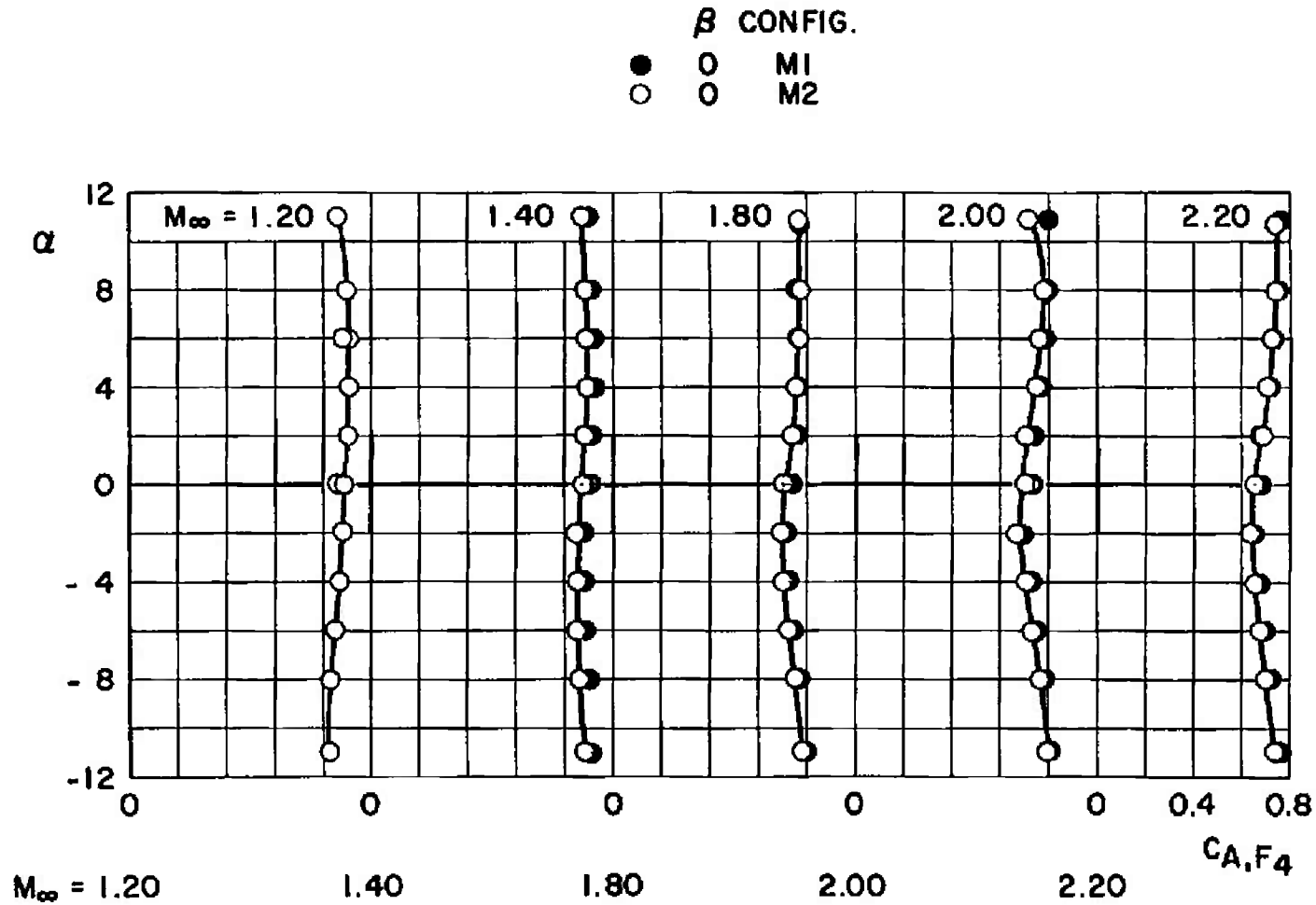

b. Mach Numbers 1.20 through 2.20

Fig. 32 Concluded

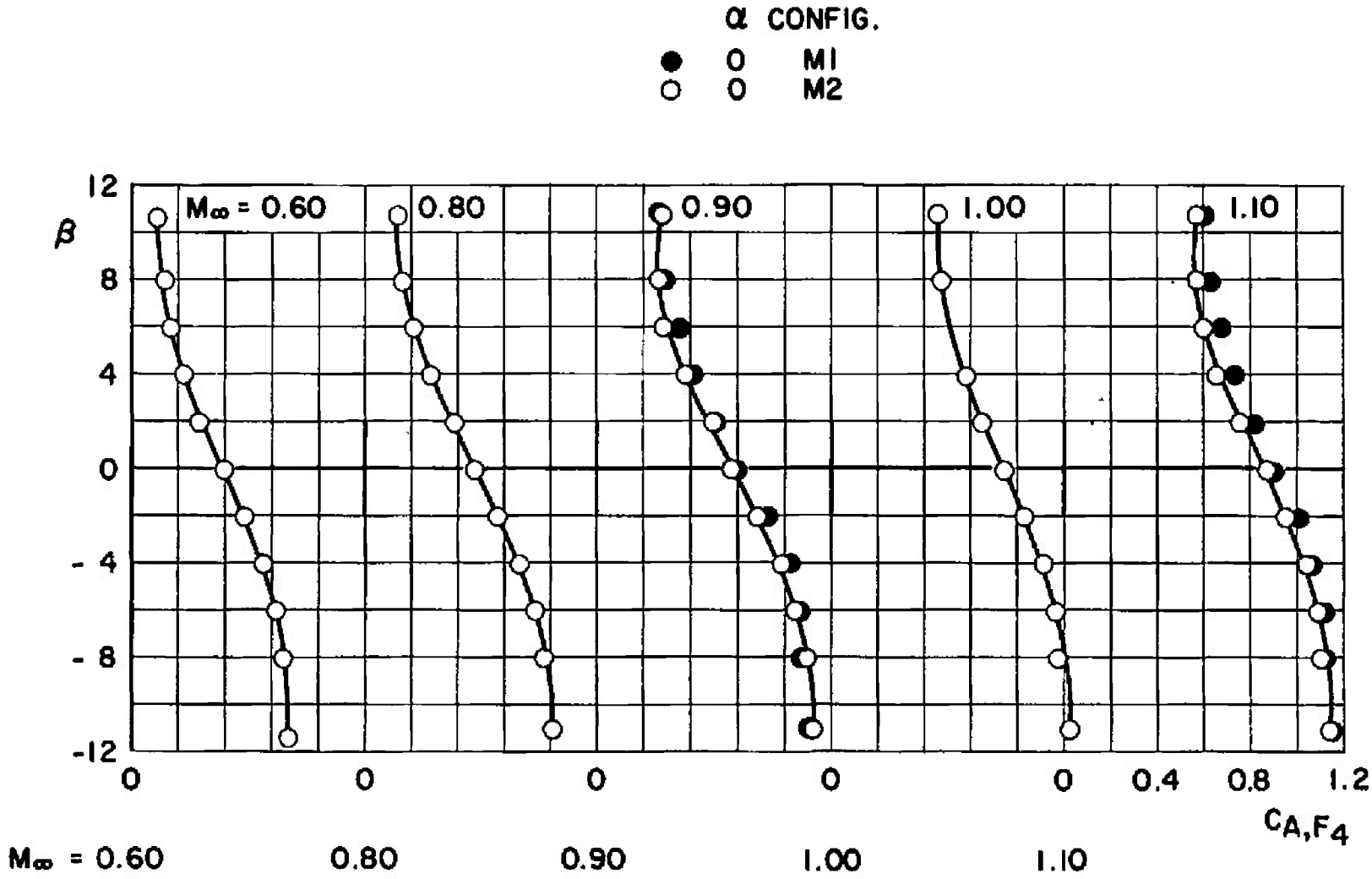

a. Mach Numbers 0.60 through 1.10

Fig. 33 Variation of SRM Forebody Axial-Force Coefficient with Sideslip Angle for Configurations M1 and M2 at $\alpha = 0$

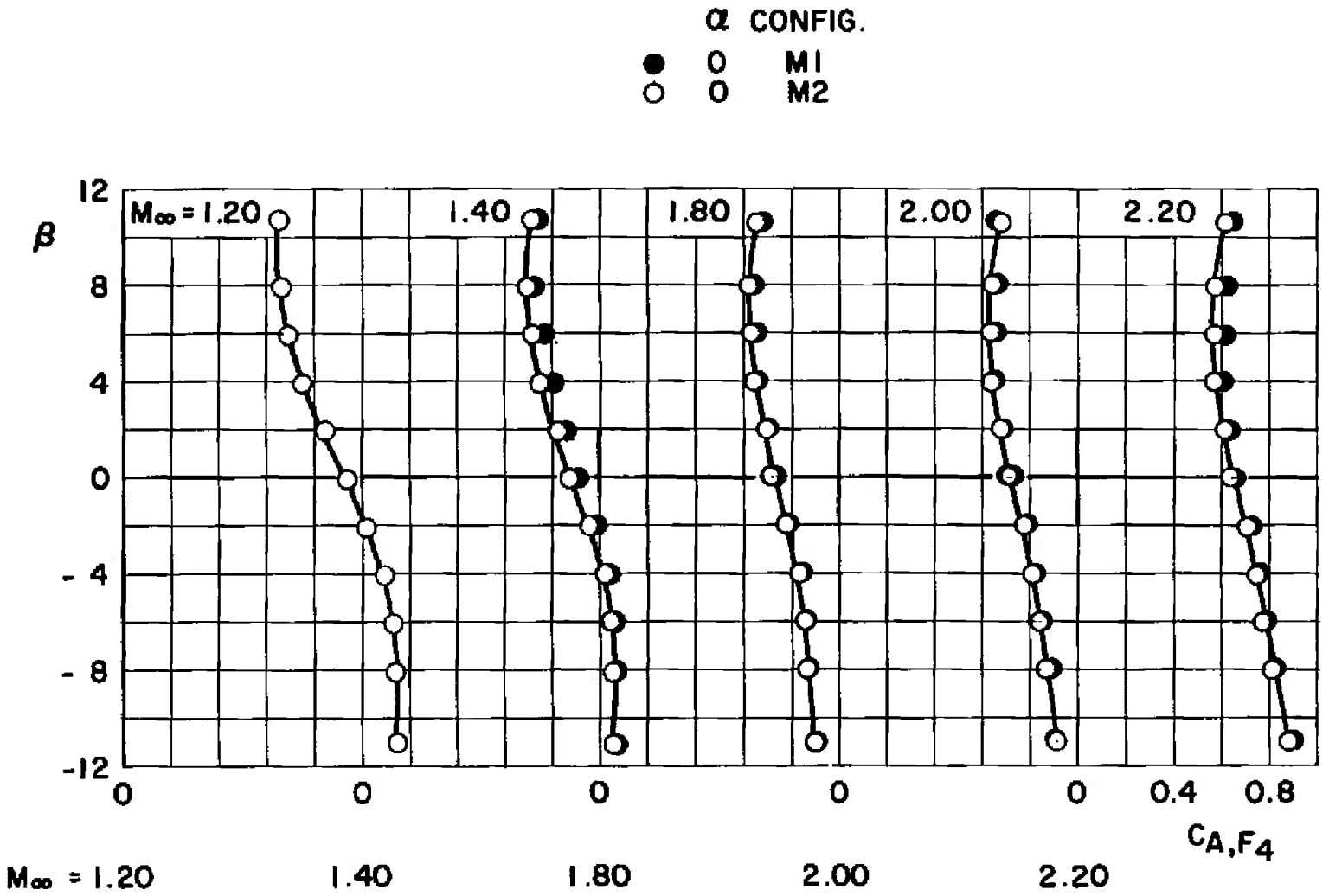

b. Mach Numbers 1.20 through 2.20

Fig. 33 Concluded

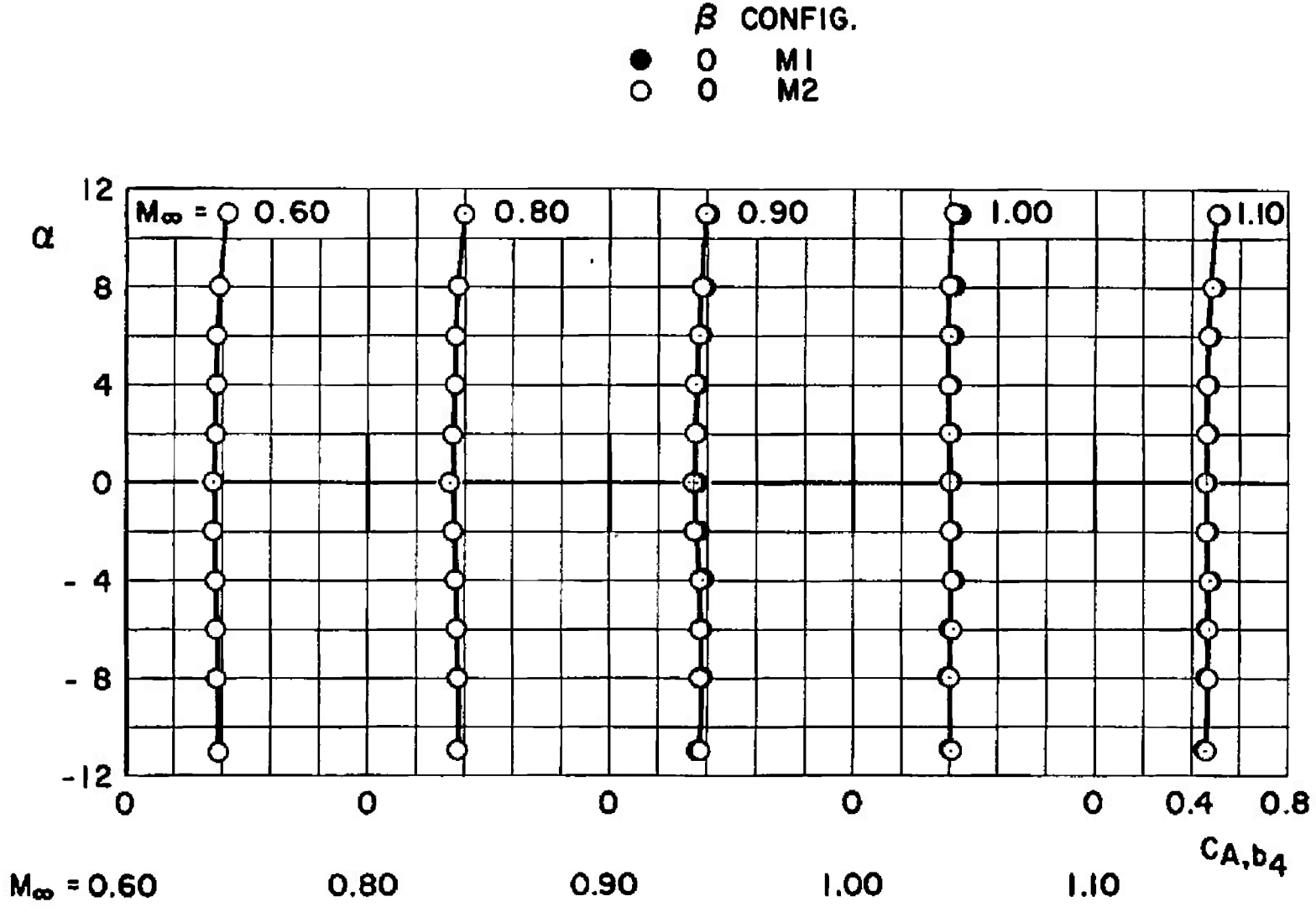

a. Mach Numbers 0.60 through 1.10

Fig. 34 Variation of SRM Base Axial-Force Coefficient with Angle of Attack for Configurations M1 and M2 at $\beta = 0$

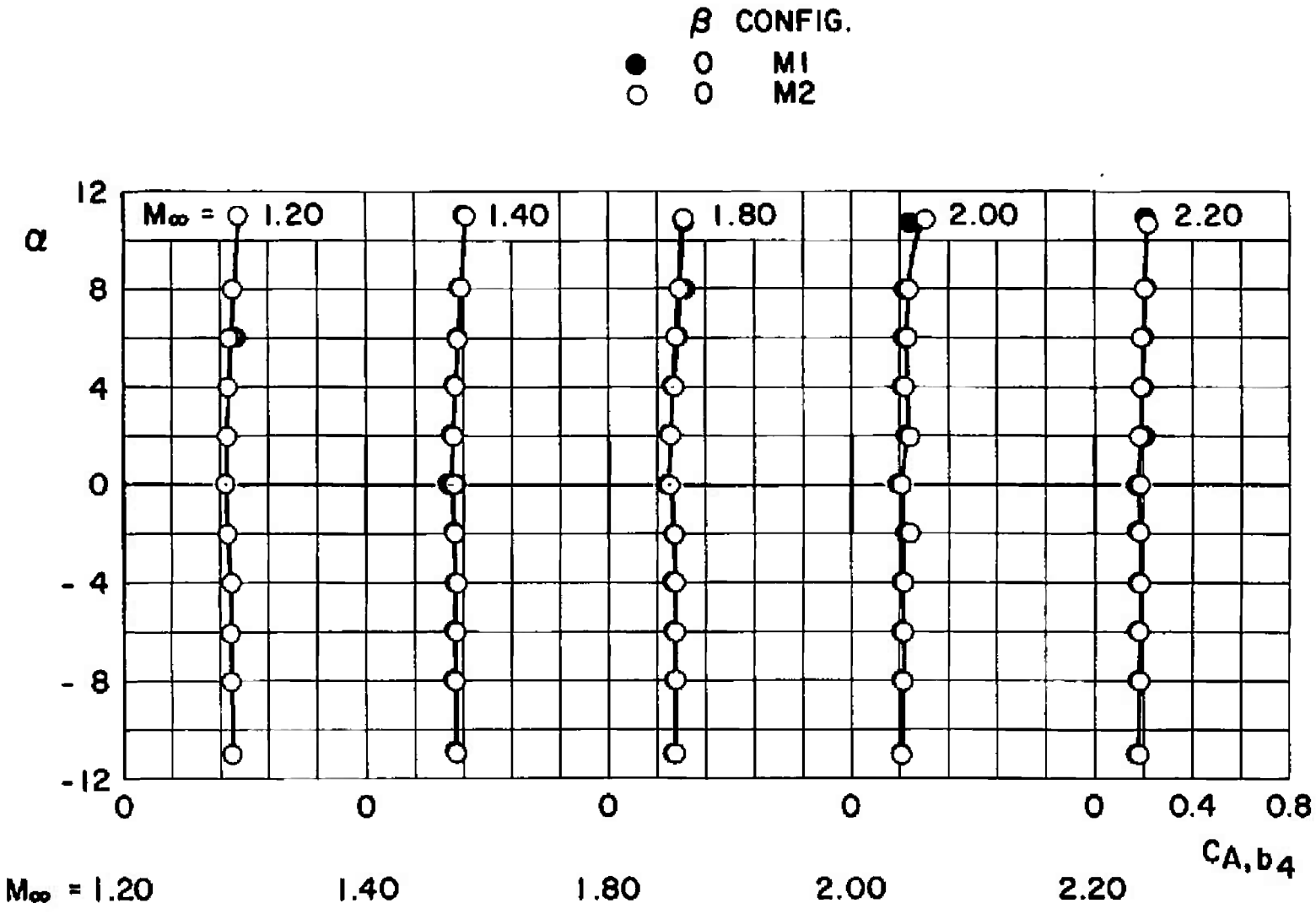

b. Mach Numbers 1.20 through 2.20

Fig. 34 Concluded

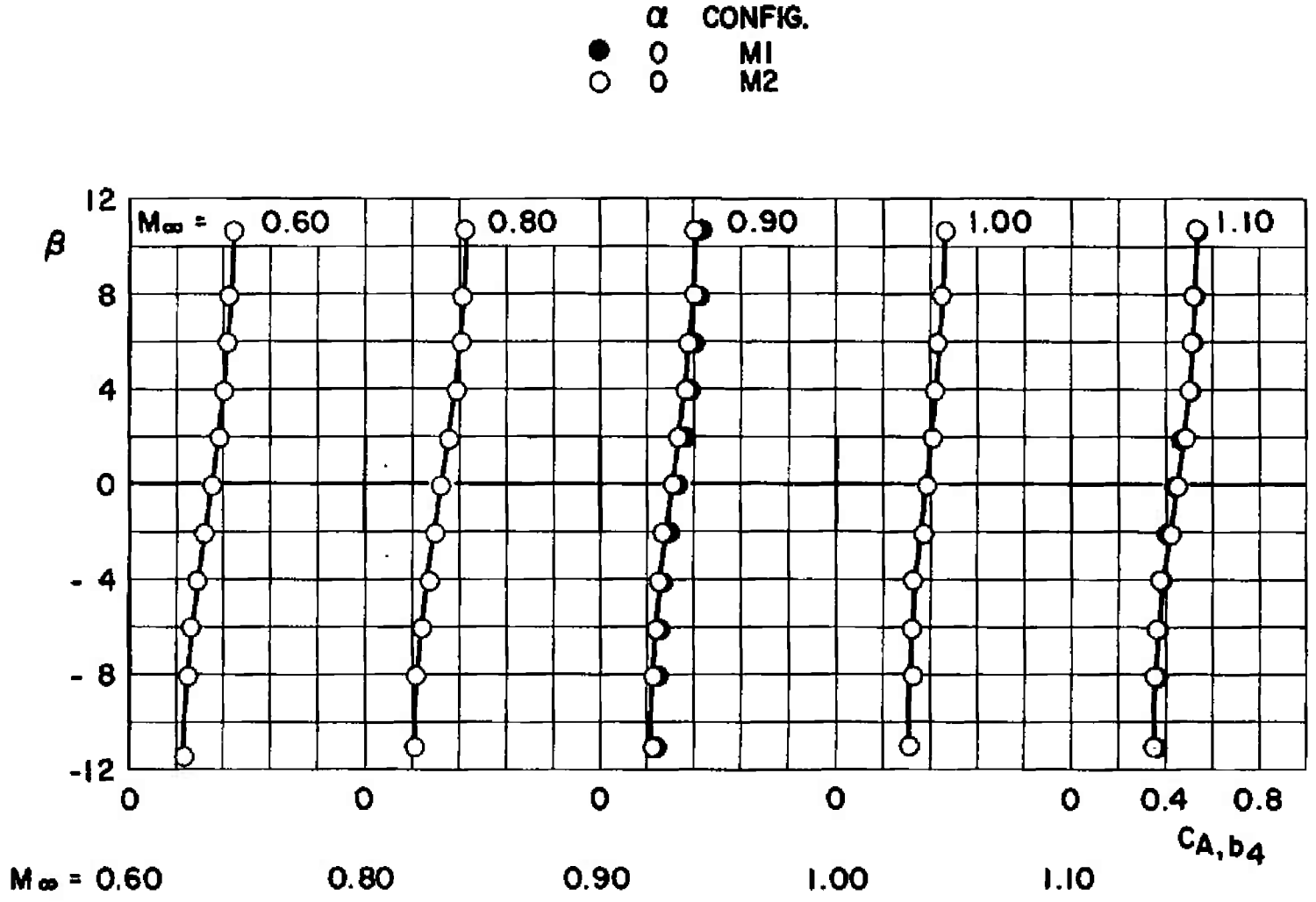

a. Mach Numbers 0.60 through 1.10

Fig. 35 Variation of SRM Base Axial-Force Coefficient with Sideslip Angle for Configurations M1 and M2 at $\alpha = 0$

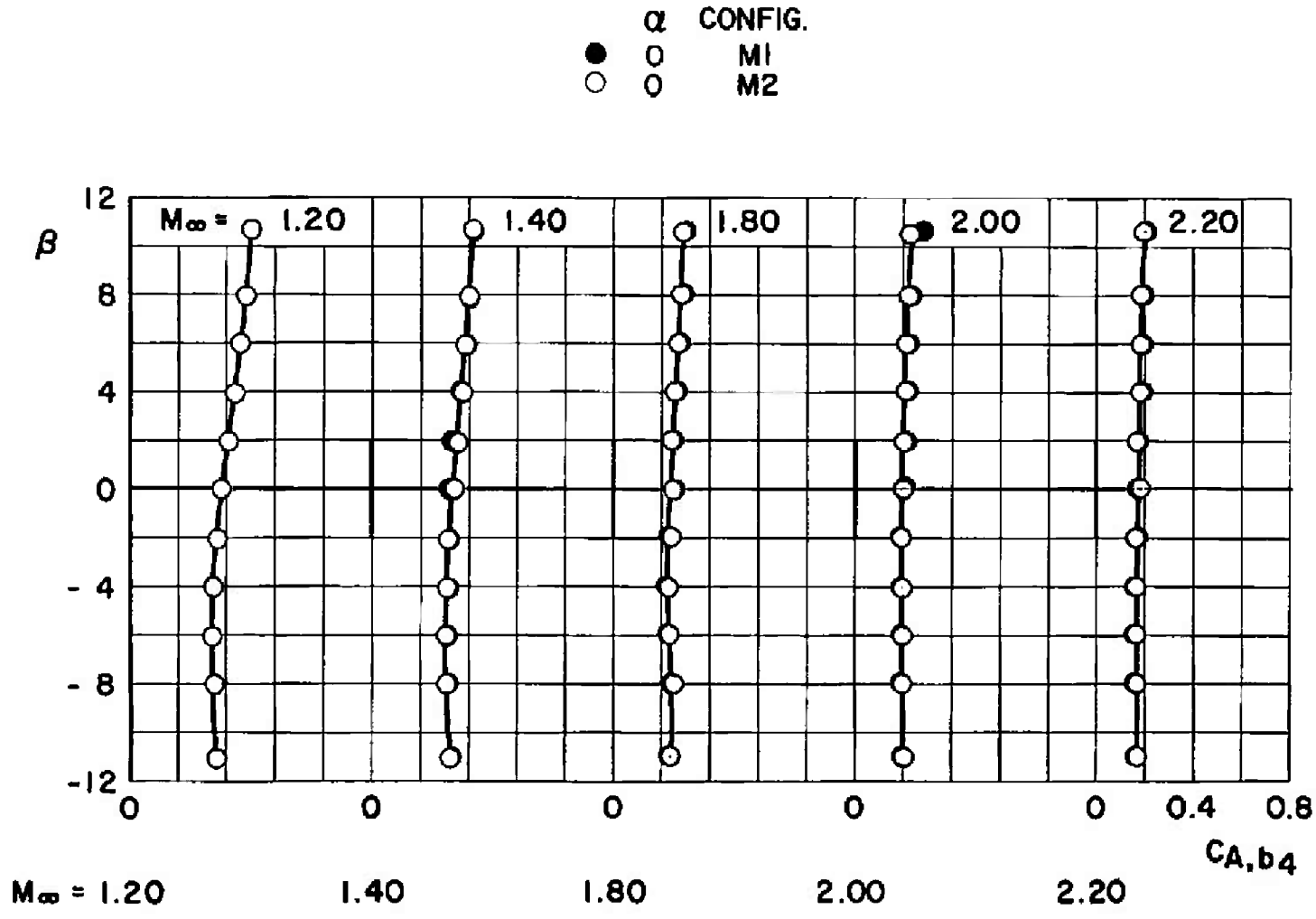

b. Mach Numbers 1.20 through 2.20

Fig. 35 Concluded

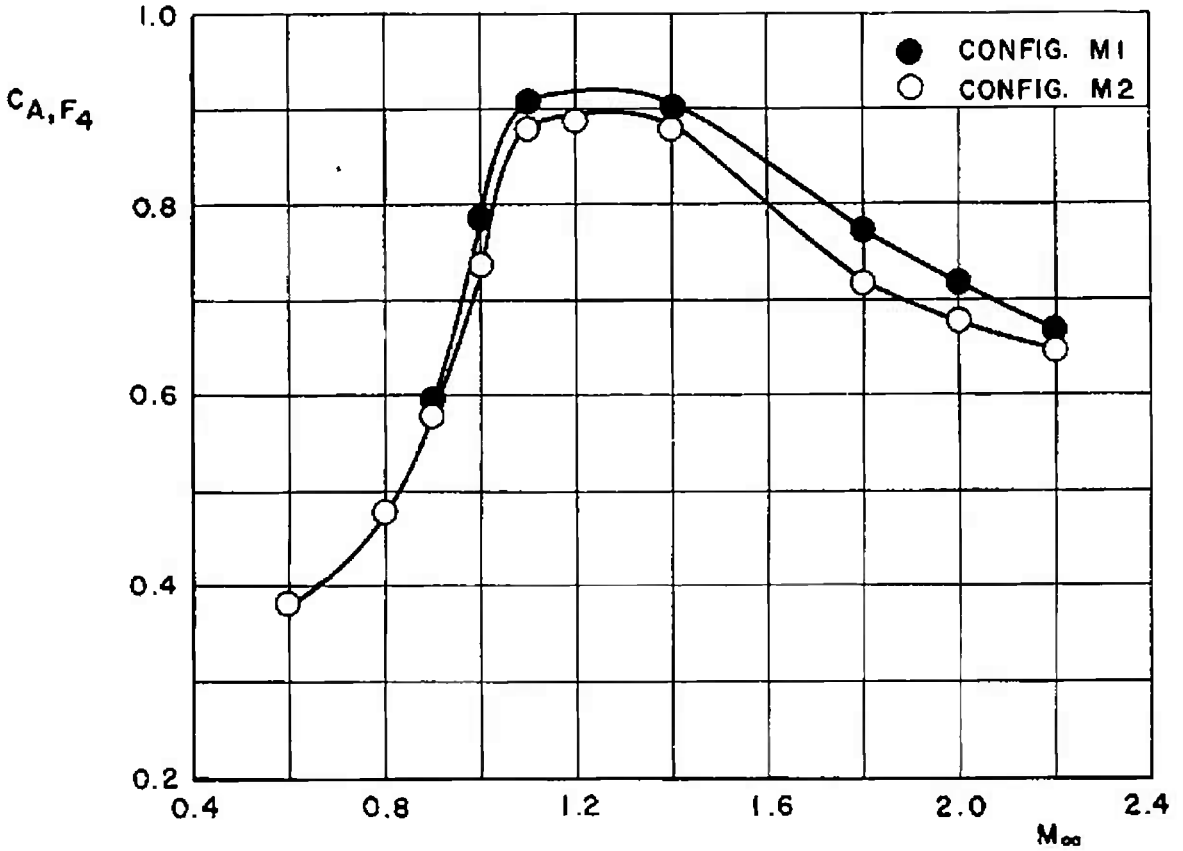

Fig. 36 Variation of SRM Forebody Axial-Force Coefficient with Mach Number for Configurations M1 and M2 at $\alpha, \beta = 0$

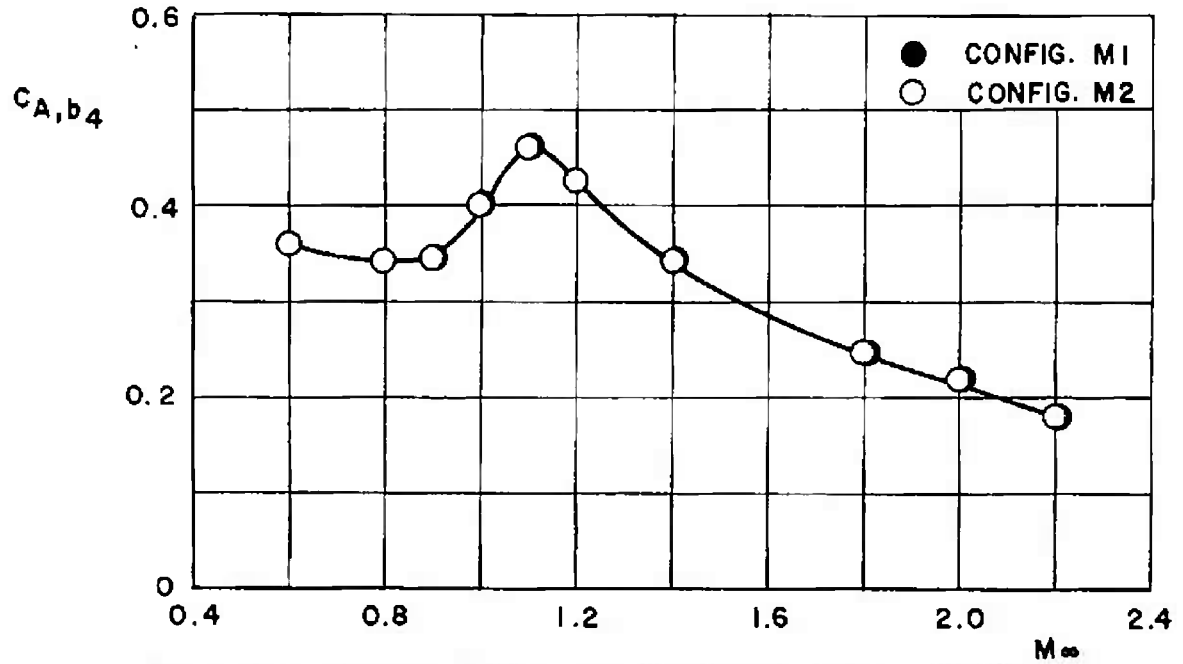

Fig. 37 Variation of SRM Base Axial-Force Coefficient with Mach Number for Configurations M1 and M2 at $\alpha, \beta = 0$

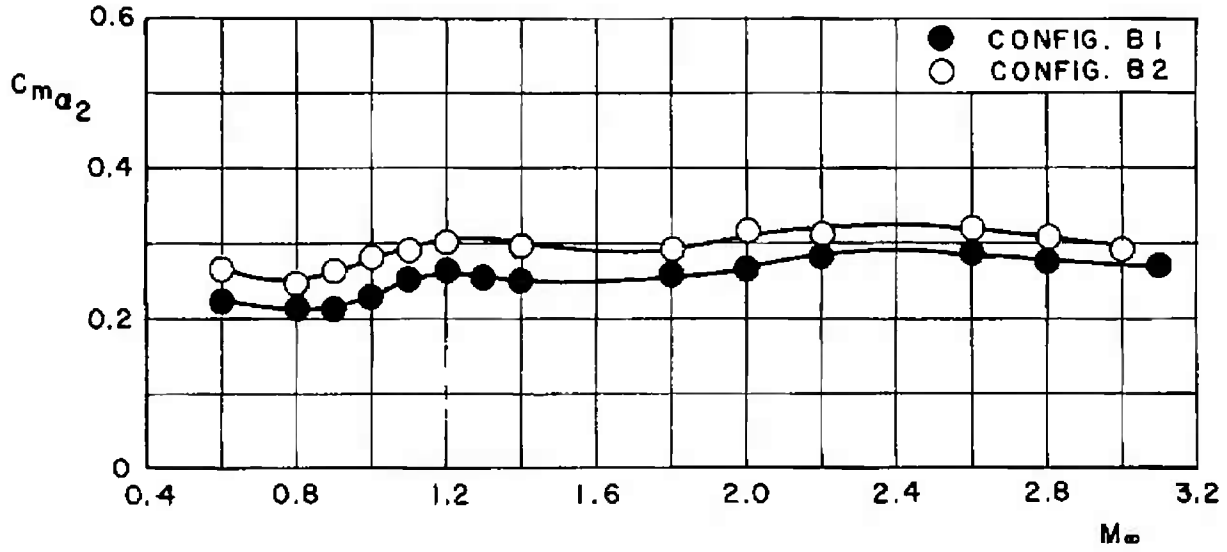

Fig. 38 Variation of MOL-Gemini Pitching-Moment Curve Slope with Mach Number for Configurations B1 and B2

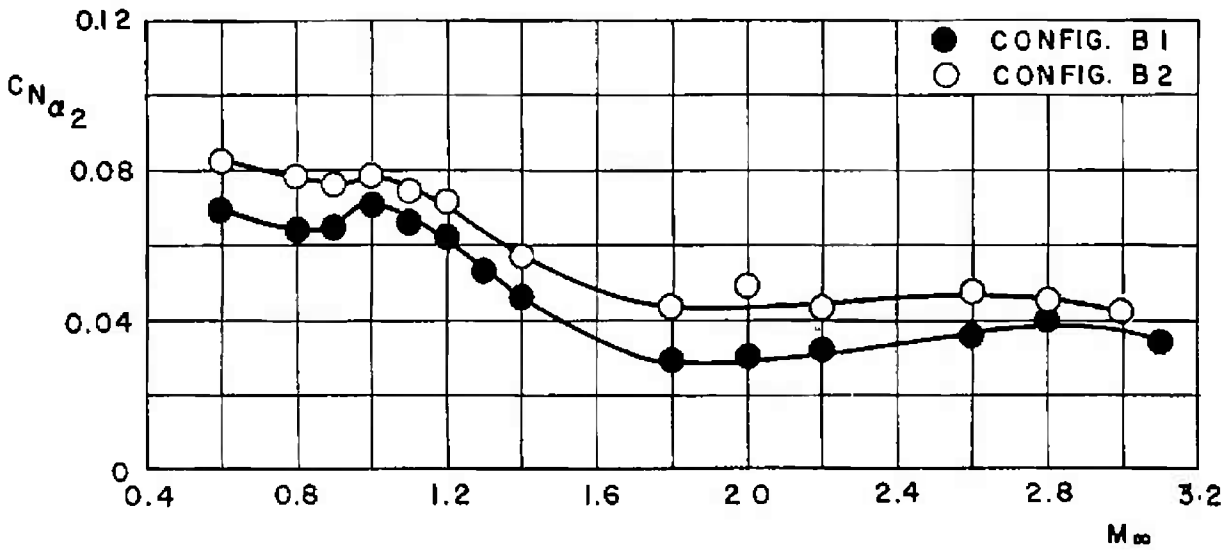

Fig. 39 Variation of MOL-Gemini Normal-Force Curve Slope with Mach Number for Configurations B1 and B2

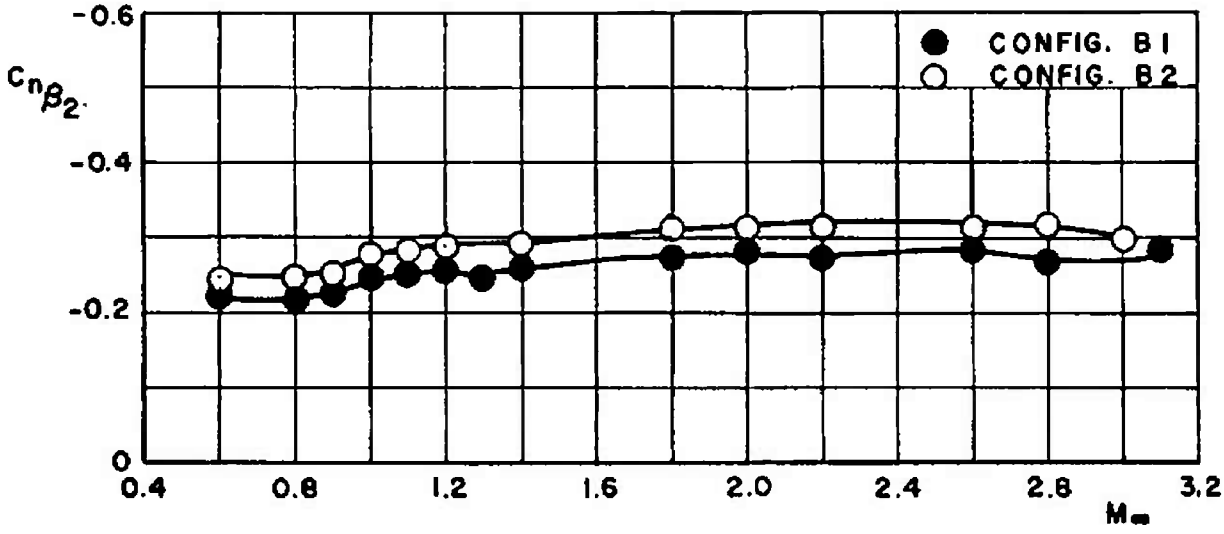

Fig. 40 Variation of MOL-Gemini Yawing-Moment Curve Slope with Mach Number for Configurations B1 and B2

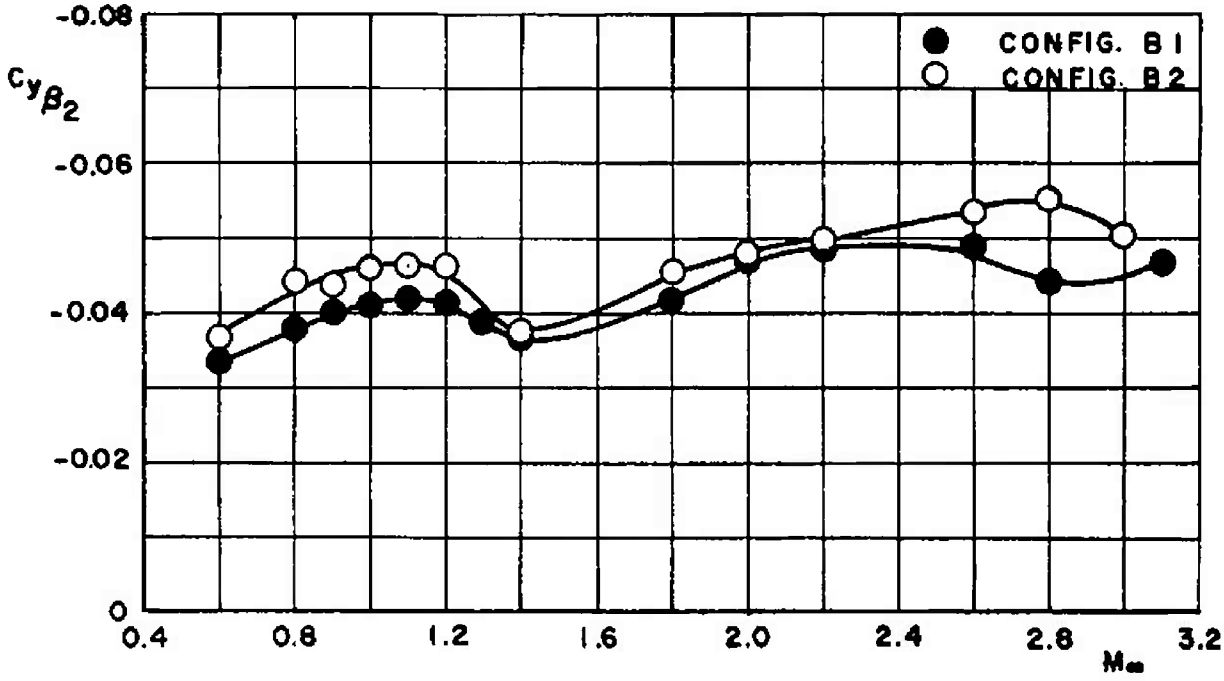

Fig. 41 Variation of MOL-Gemini Side-Force Curve Slope with Mach Number for Configurations B1 and B2

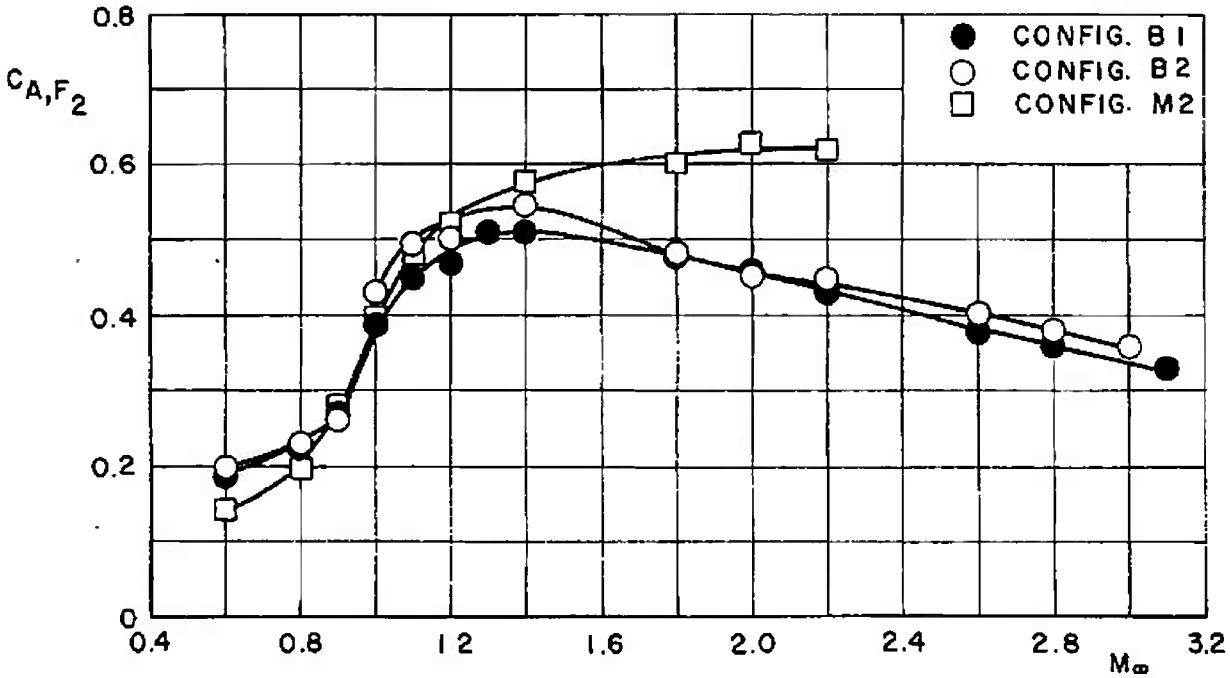

Fig. 42 Variation of MOL-Gemini Forebody Axial-Force Coefficient with Mach Number for Configurations B1, B2, and M2 at α, β = 0

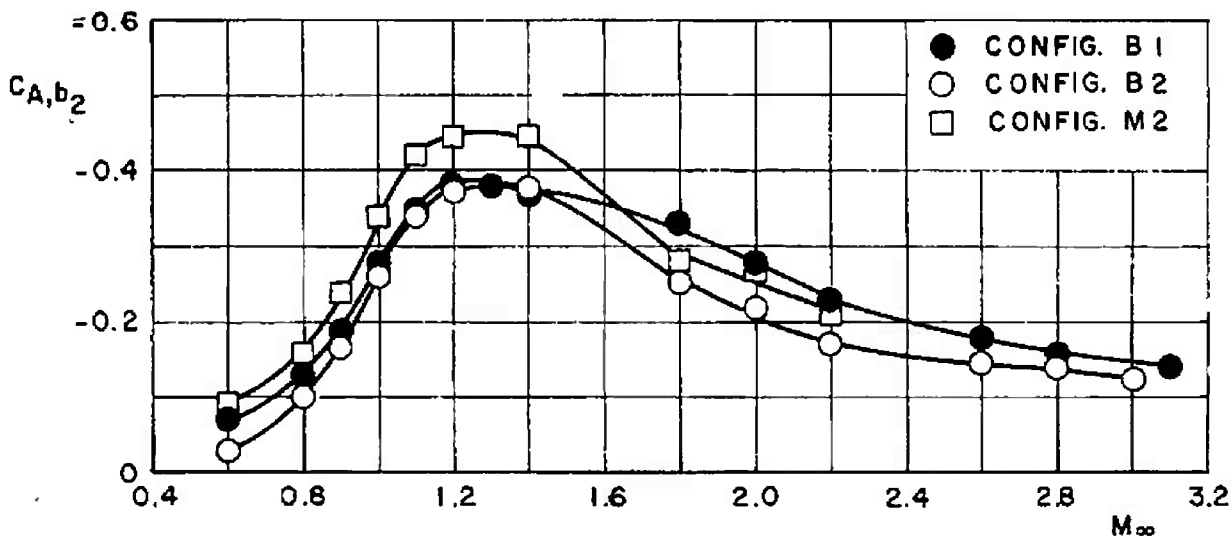

Fig. 43 Variation of MOL-Gemini Base Axial-Force Coefficient with Mach Number for Configurations B1, B2, and M2 at α, β = 0

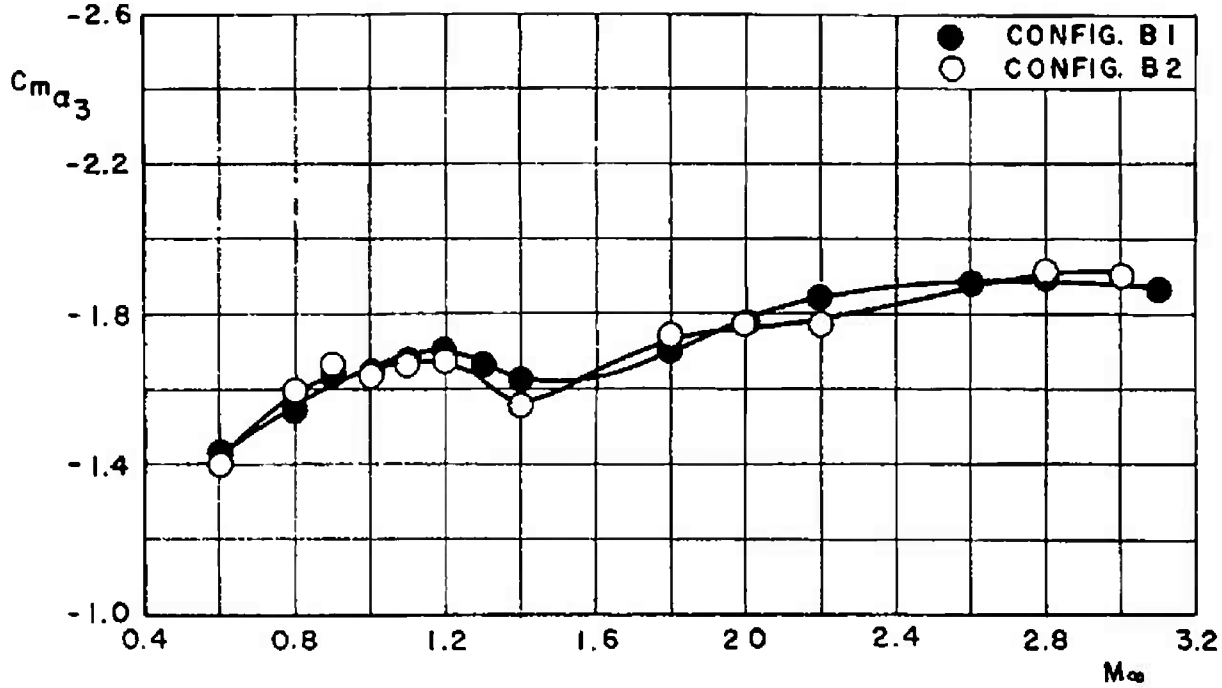

Fig. 44 Variation of Composite Model Pitching-Moment Curve Slope with Mach Number for Configurations B1 and B2

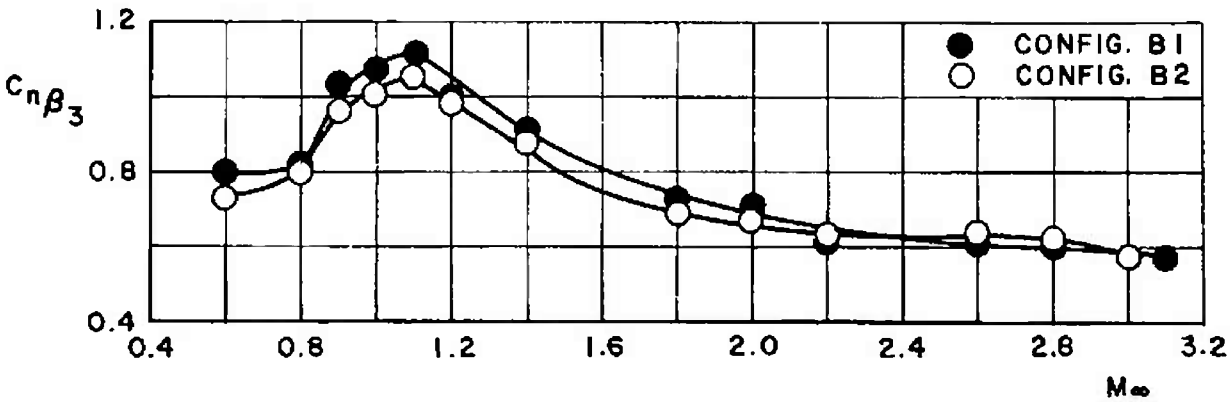

Fig. 45 Variation of Composite Model Yawing-Moment Curve Slope with Mach Number for Configurations B1 and B2

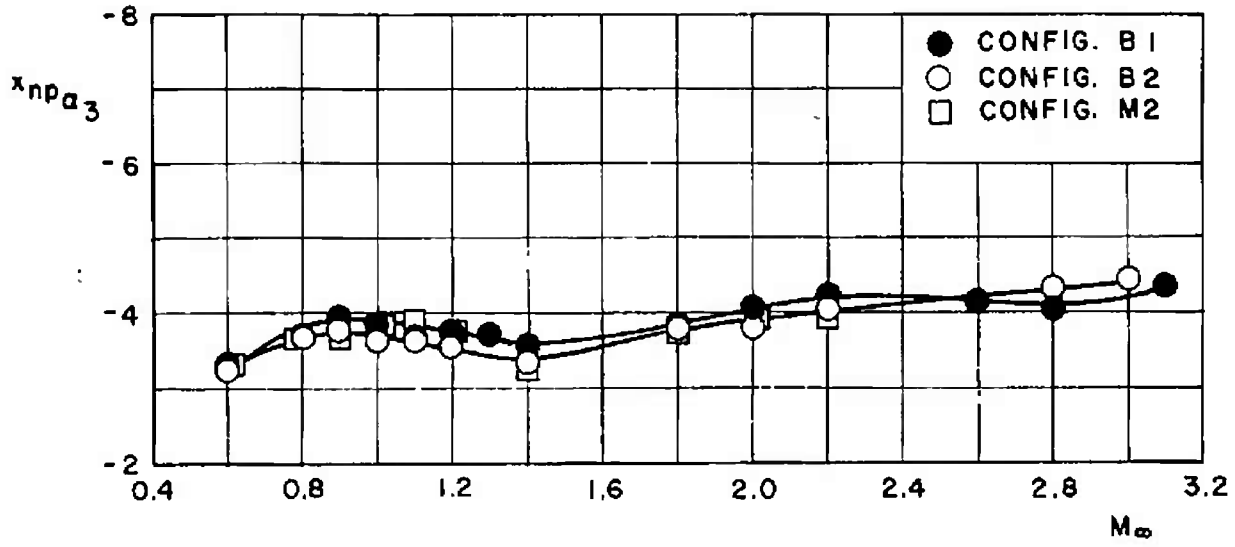

a. Longitudinal Neutral Point

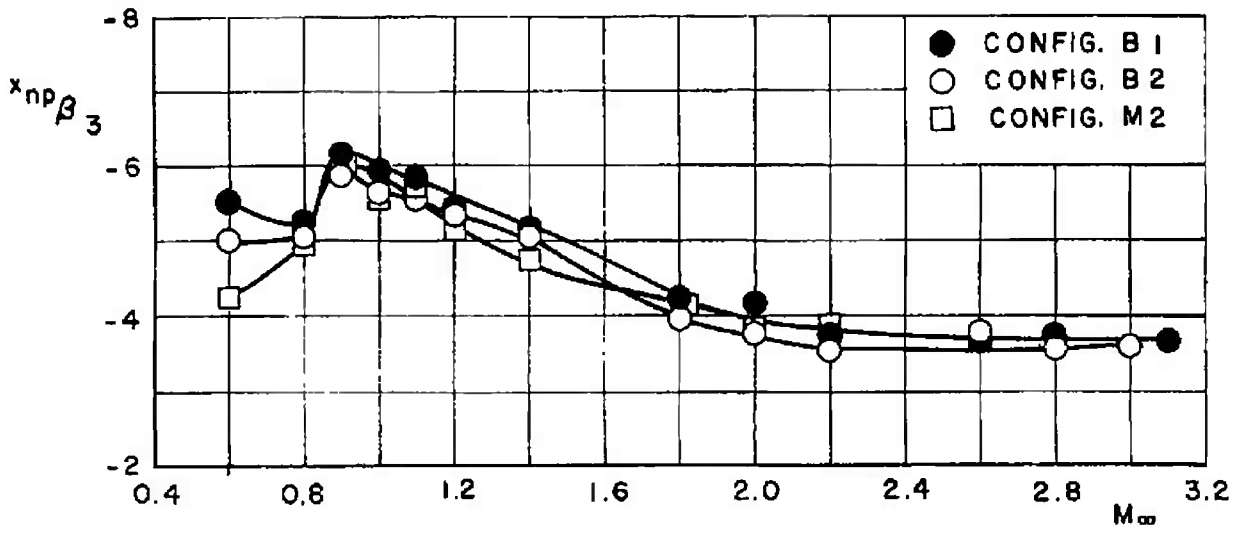

b. Lateral Neutral Point

Fig. 46 Variation of Composite Model Neutral-Point Location with Mach Number for Configurations B1, B2, and M2

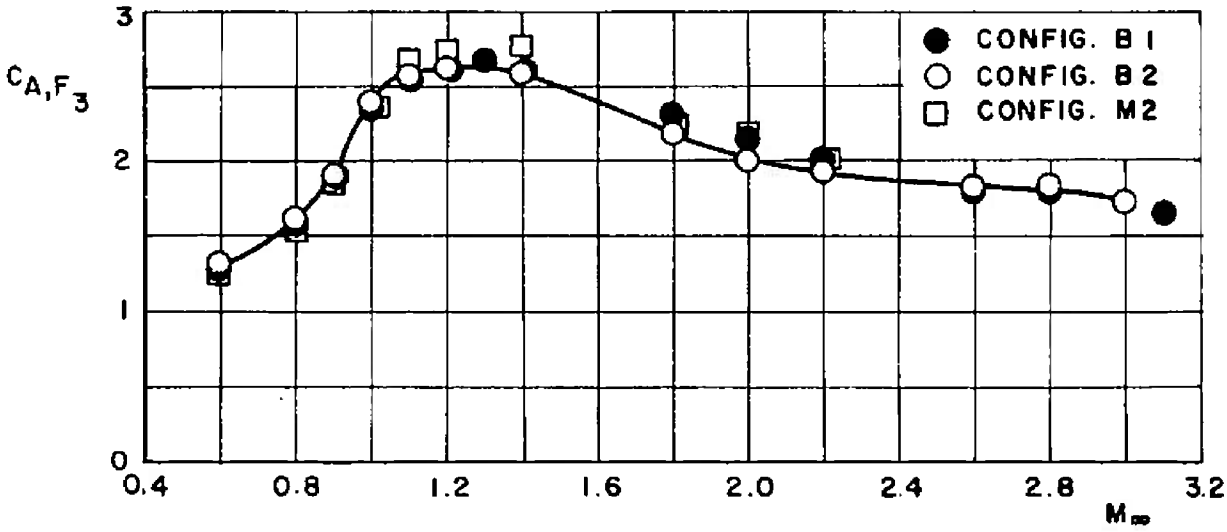

Fig. 47 Variation of Composite Model Forebody Axial-Force Coefficient with Mach Number for Configurations B1, B2, and M2 at α, β = 0

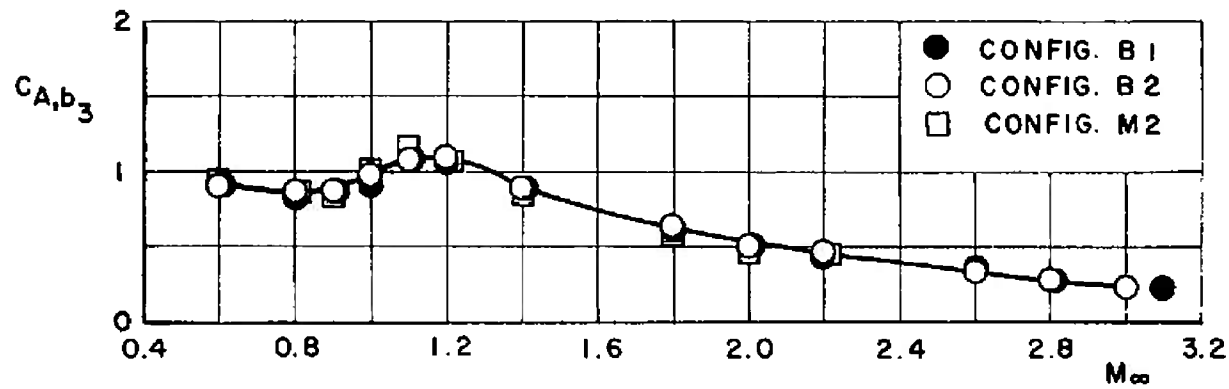

Fig. 48 Variation of Composite Model Base Axial-Force Coefficient with Mach Number for Configurations B1, B2, and M2 at α, β = 0

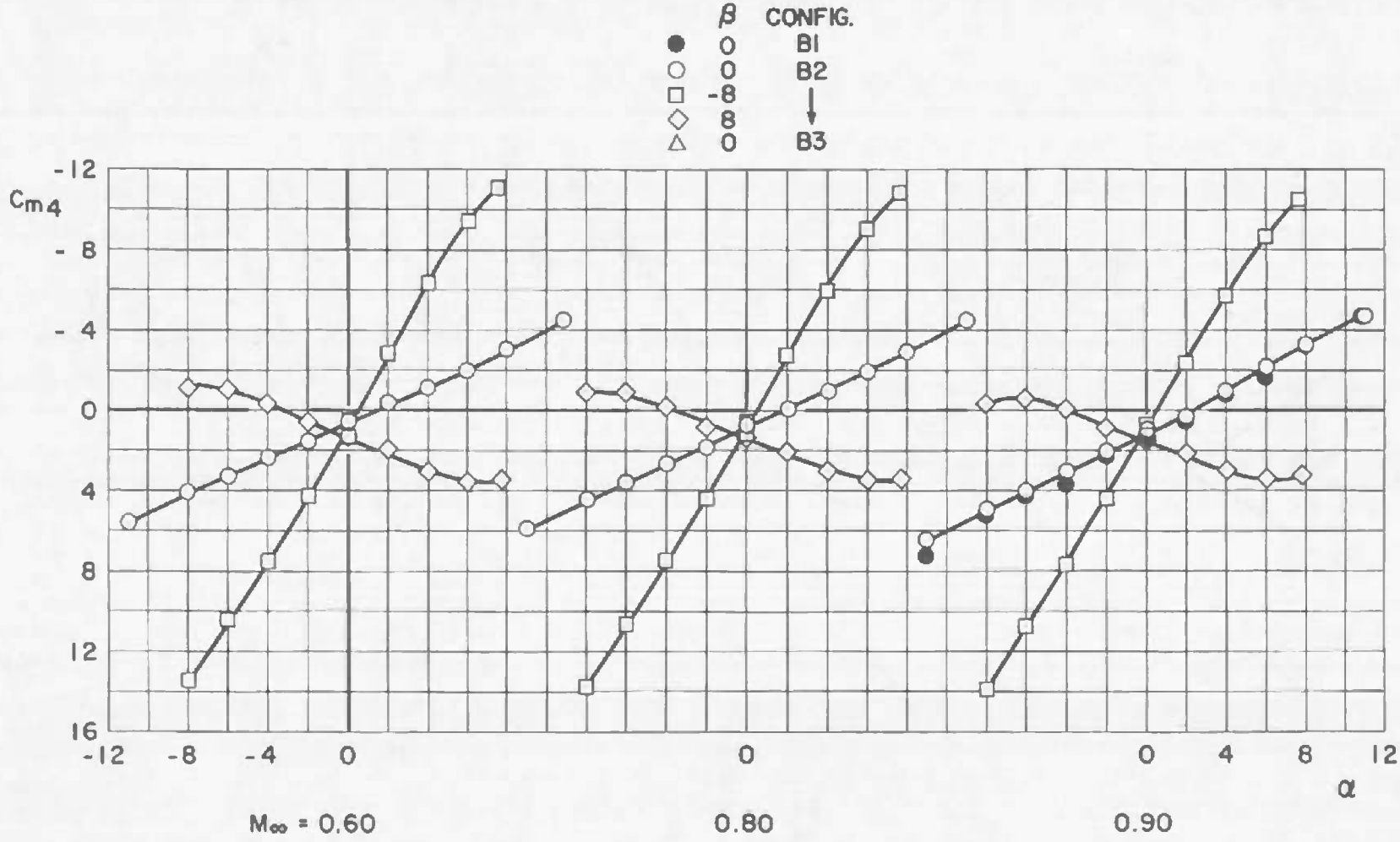

a. Mach Numbers 0.60, 0.80, and 0.90

Fig. 49 Variation of SRM Pitching-Moment Coefficient with Angle of Attack for Configurations B1, B2, and B3

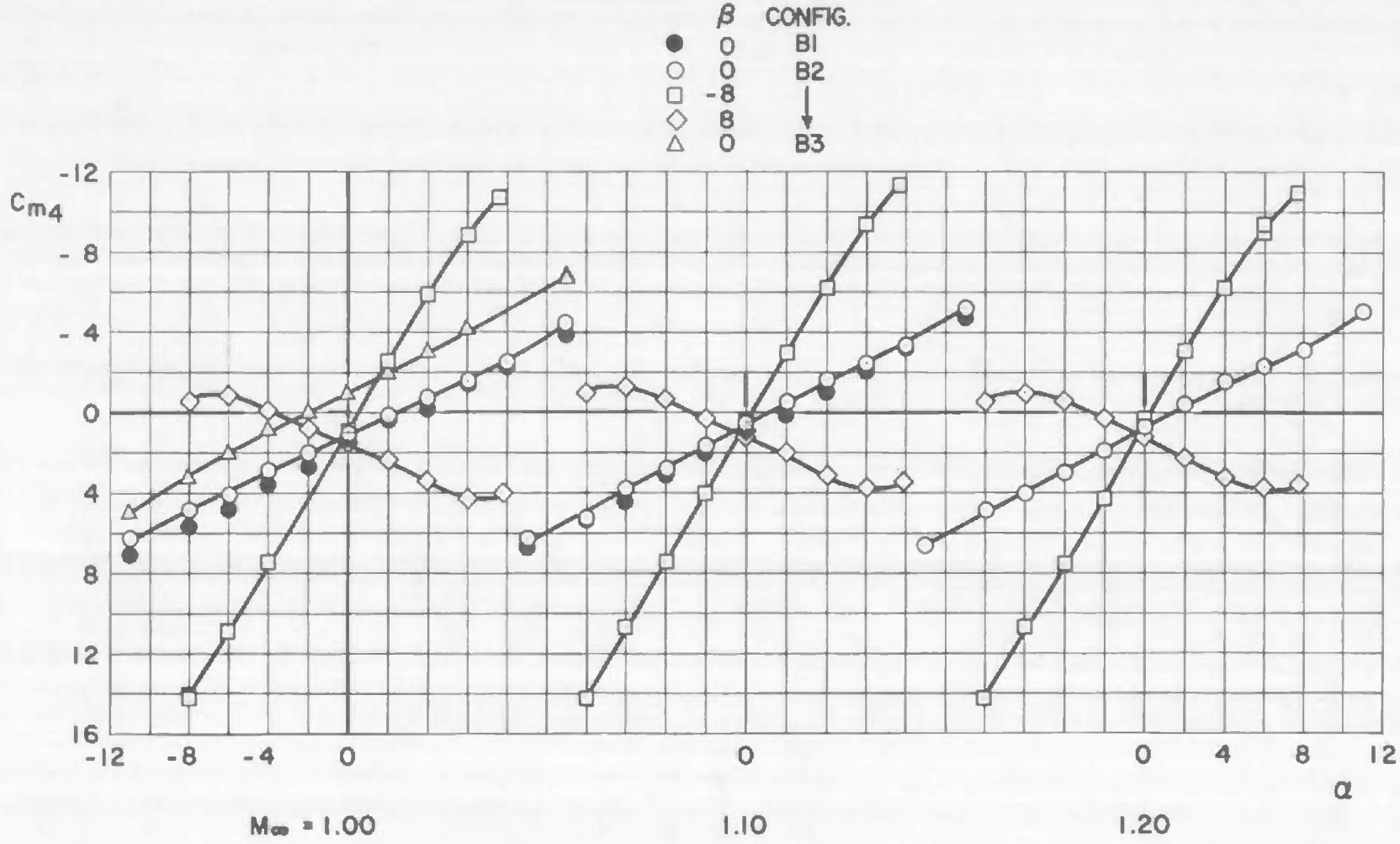

b. Mach Numbers 1.00, 1.10, and 1.20

Fig. 49 Continued

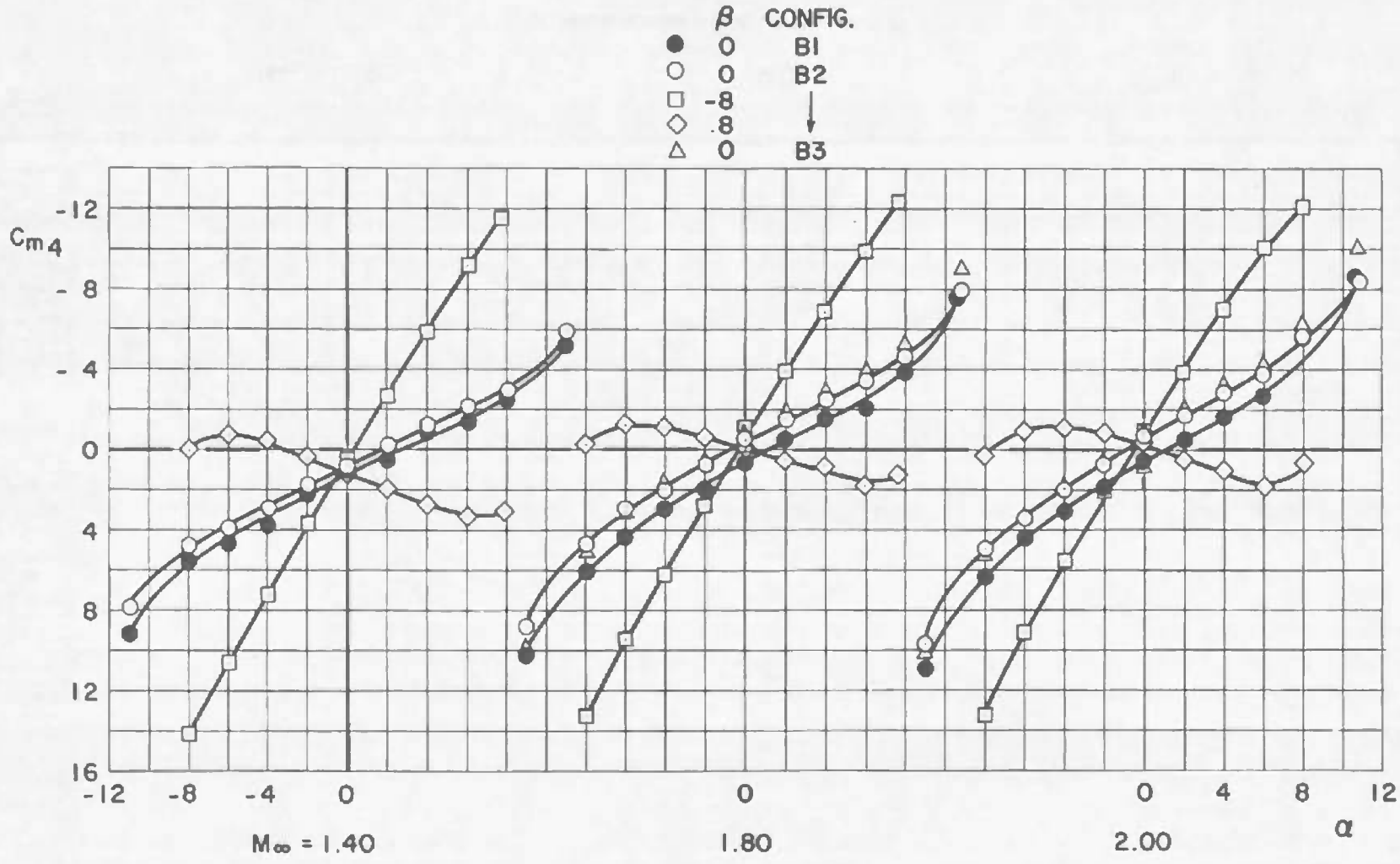

c. Mach Numbers 1.40, 1.80, and 2.00

Fig. 49 Continued

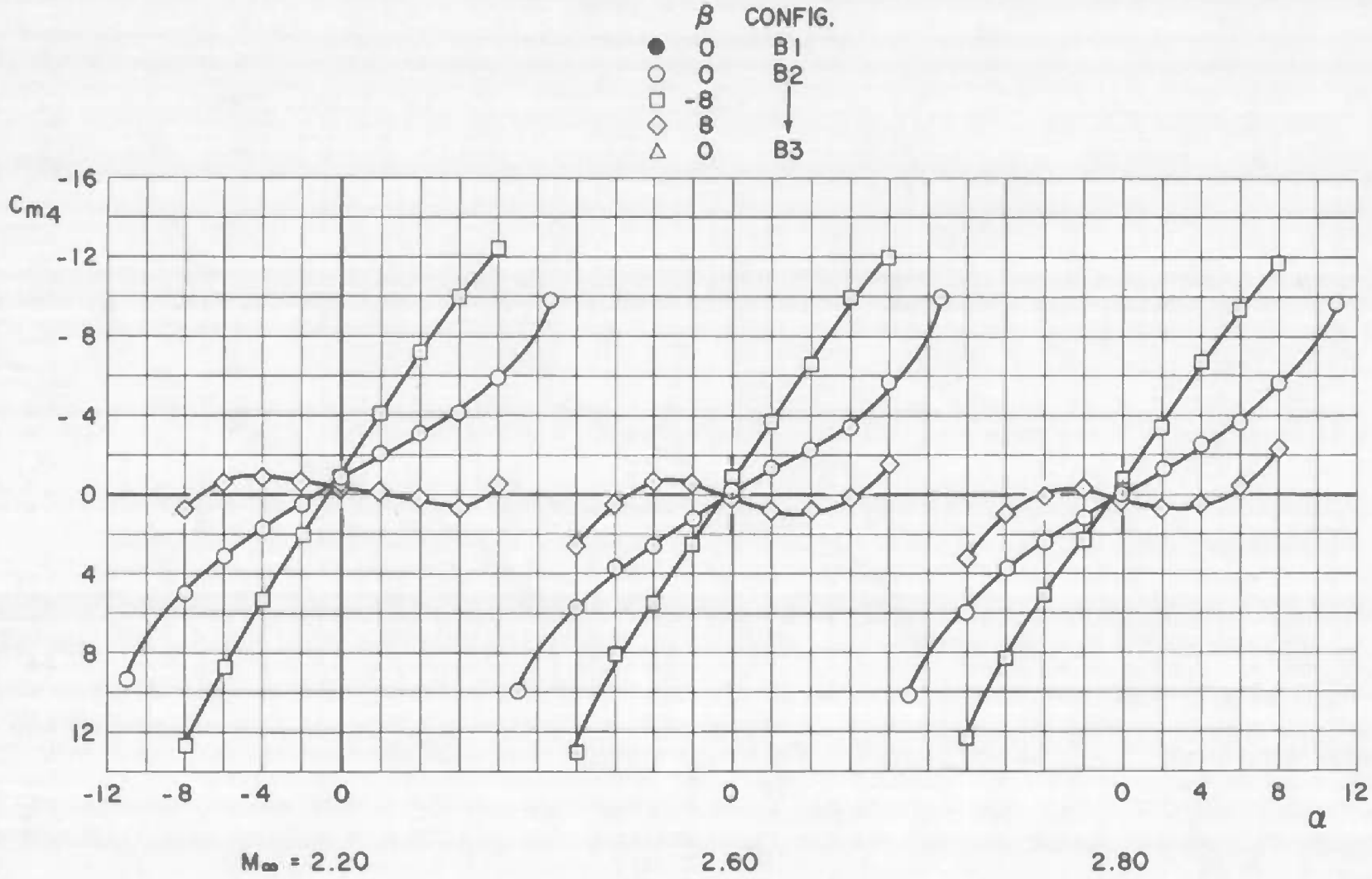

d. Mach Numbers 2.20, 2.60, and 2.80

Fig. 49 Continued

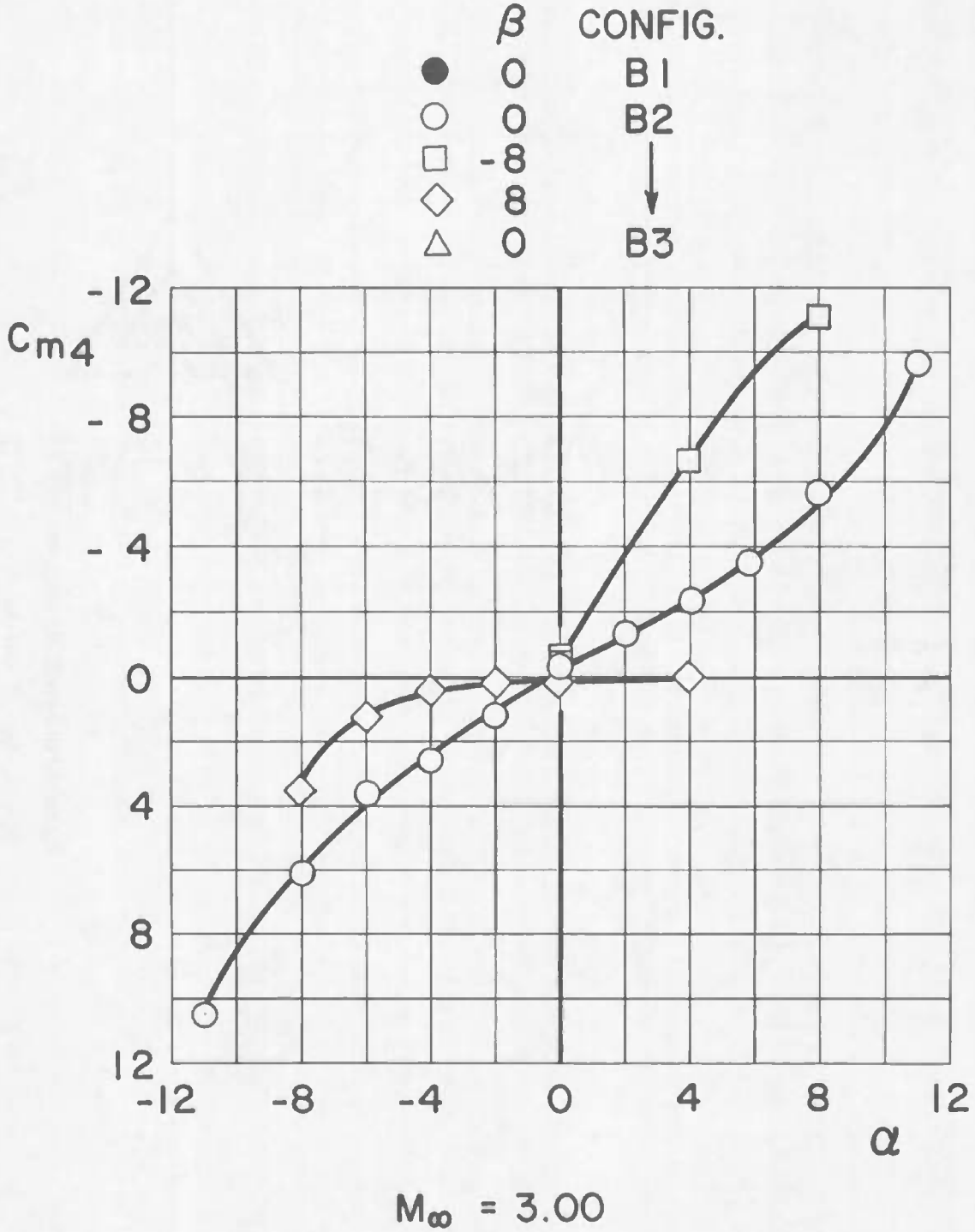

$M_\infty = 3.00$

e. Mach Number 3.00

Fig. 49 Concluded

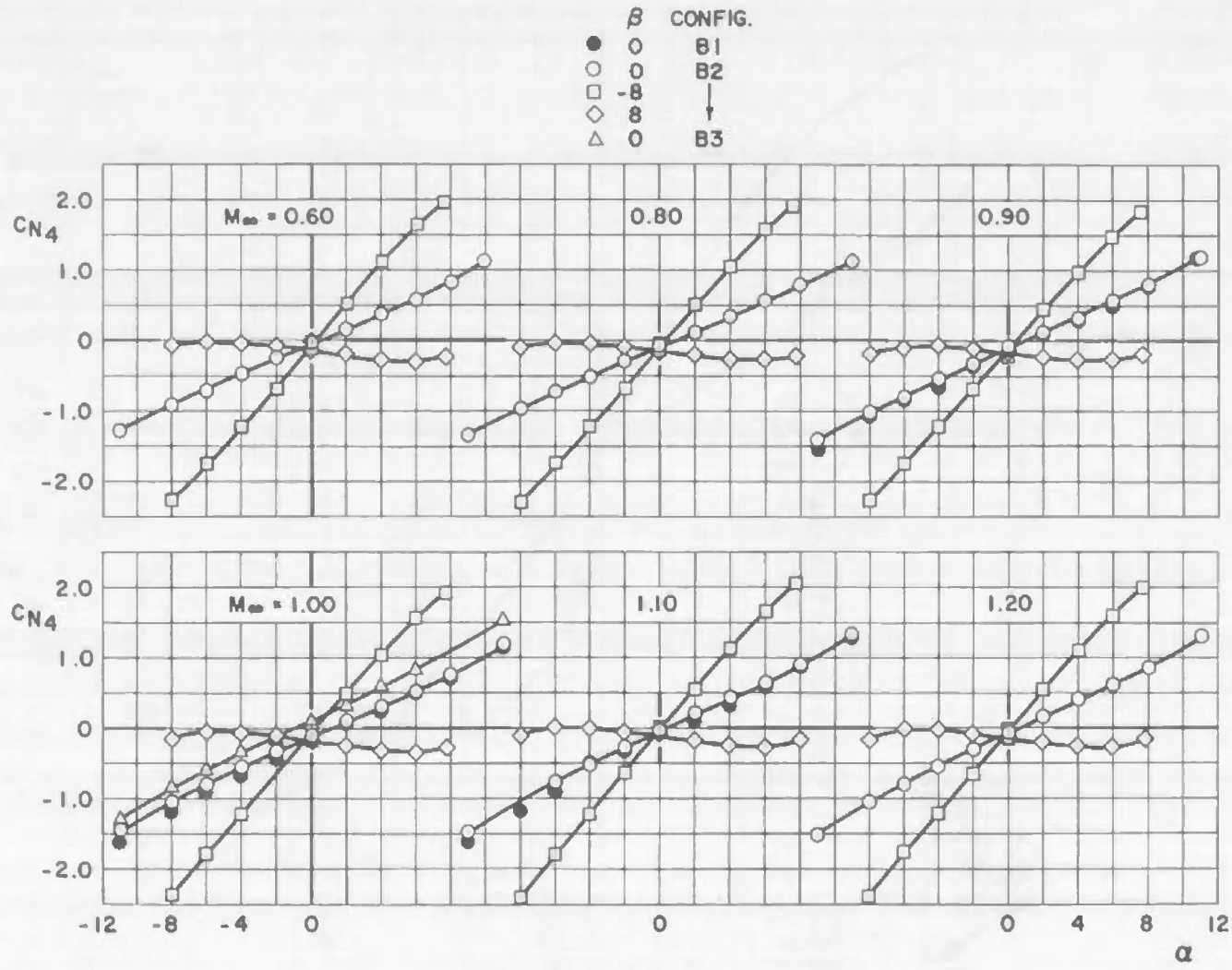

a. Mach Numbers 0.60 through 1.20

Fig. 50 Variation of SRM Normal-Force Coefficient with Angle of Attack for Configurations B1, B2, and B3

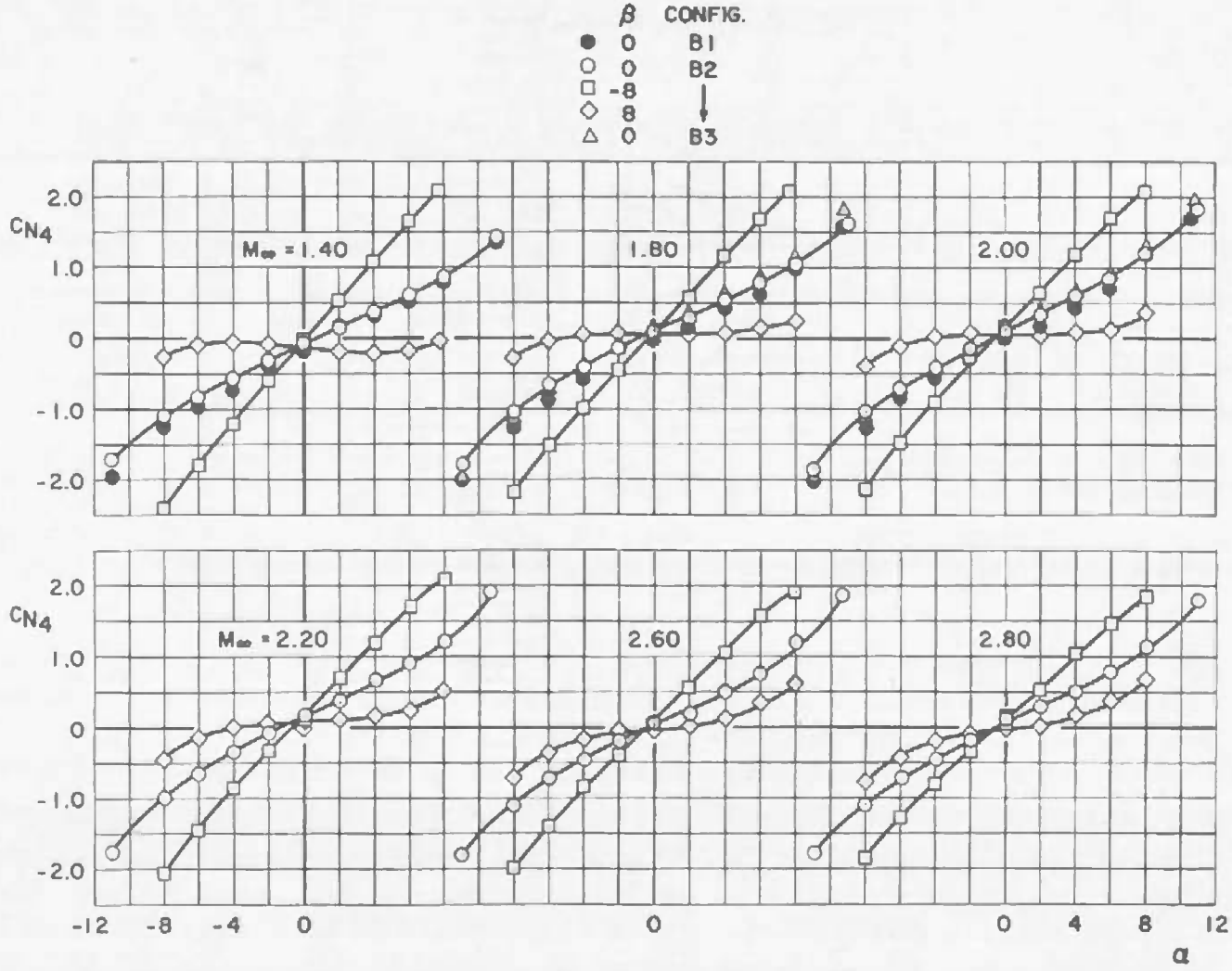

b. Mach Numbers 1.40 through 2.80

Fig. 50 Continued

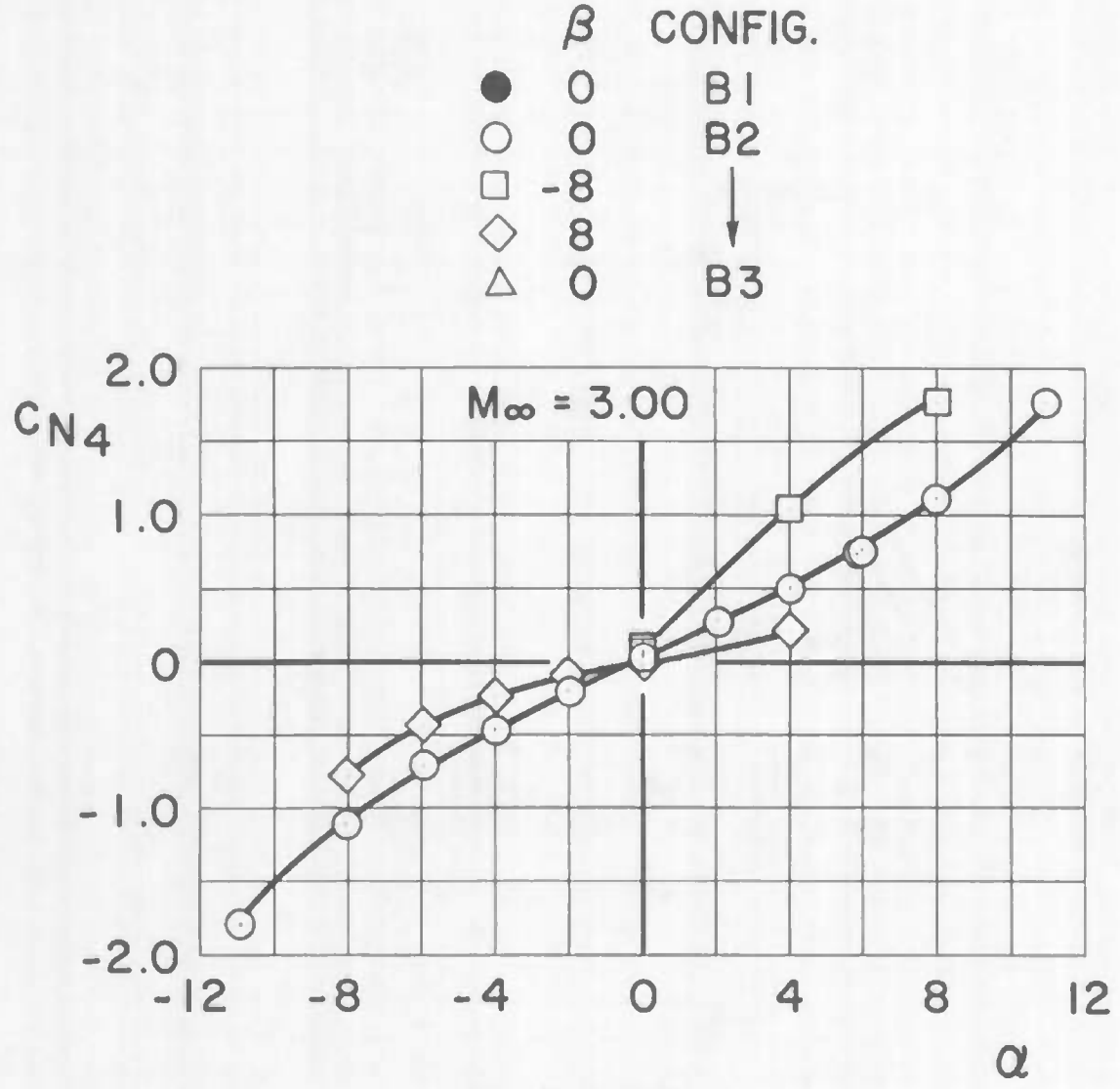

c. Mach Number 3.00

Fig. 50 Concluded

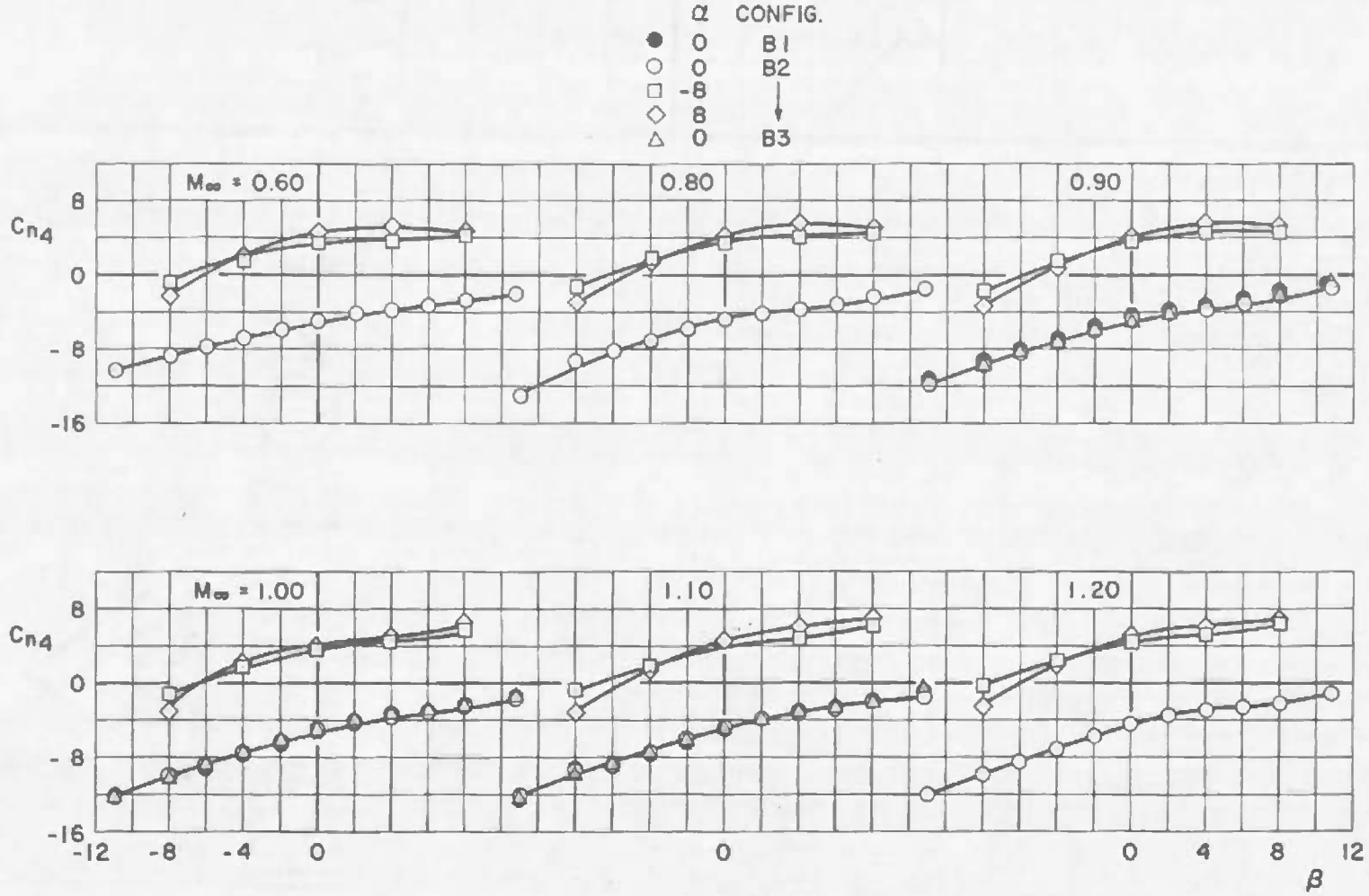

o. Mach Numbers 0.60 through 1.20

Fig. 51 Variation of SRM Yawing-Moment Coefficient with Sideslip Angle for Configurations B1, B2, and B3

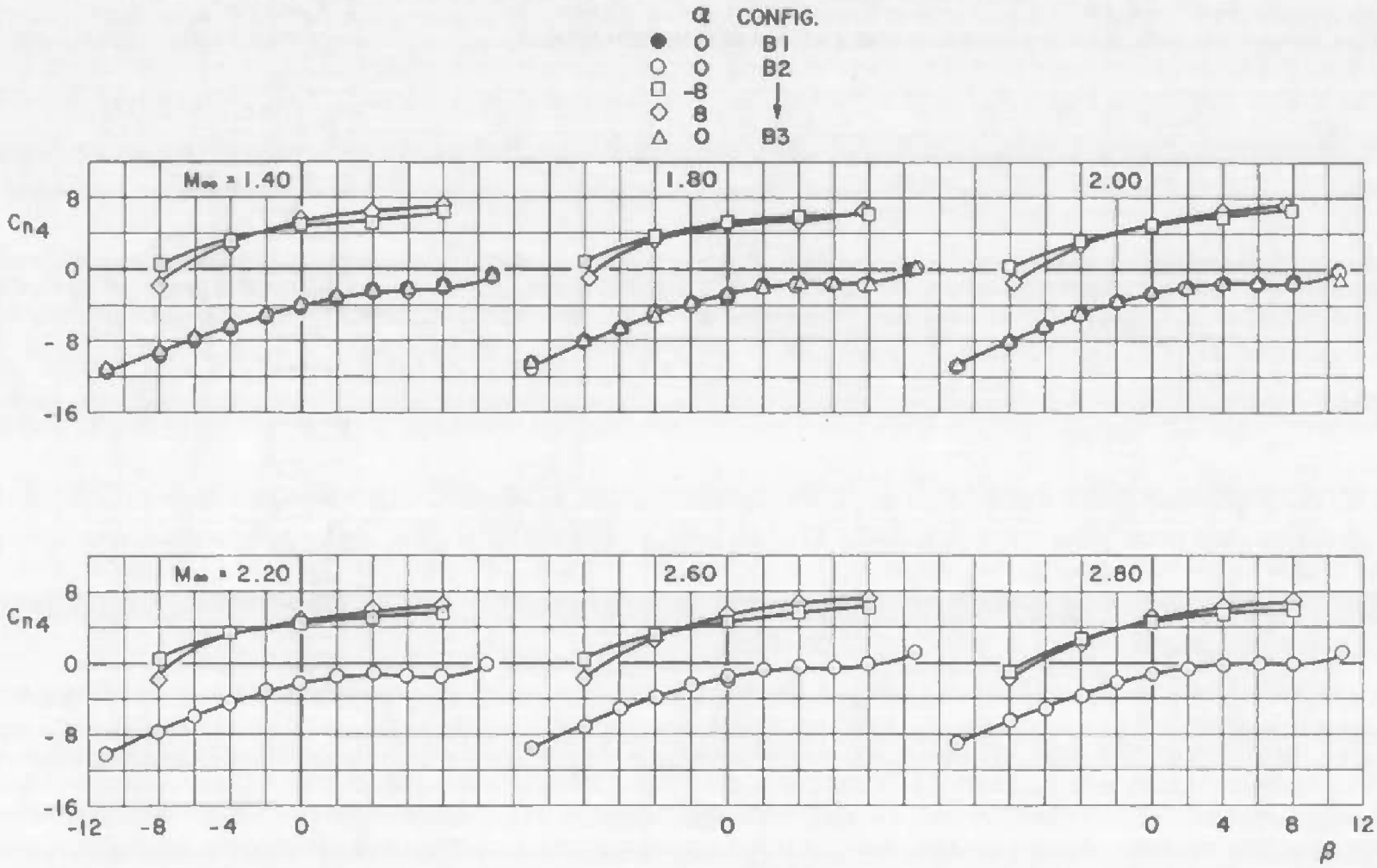

b. Mach Numbers 1.40 through 2.80

Fig. 51 Continued

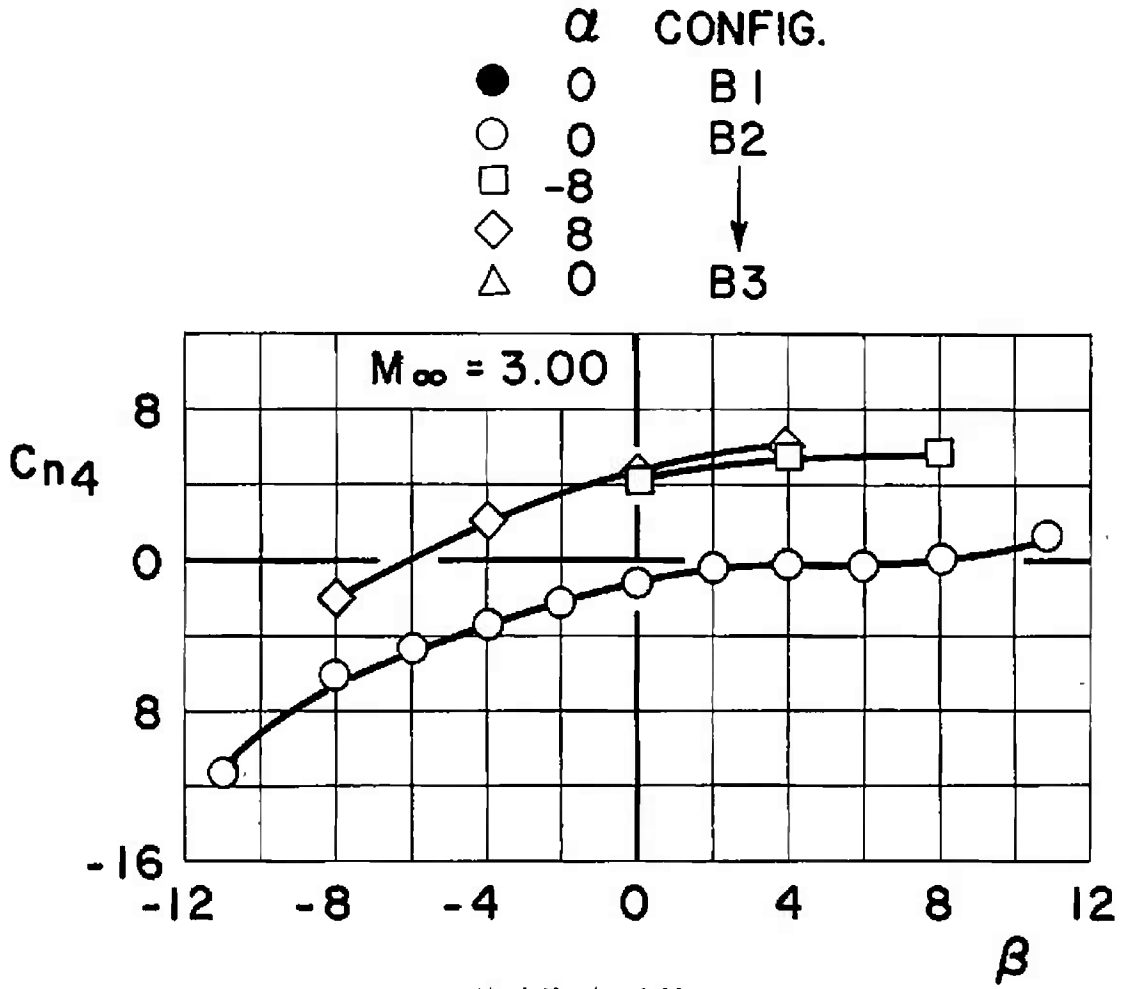

c. Mach Number 3.00

Fig. 51 Concluded

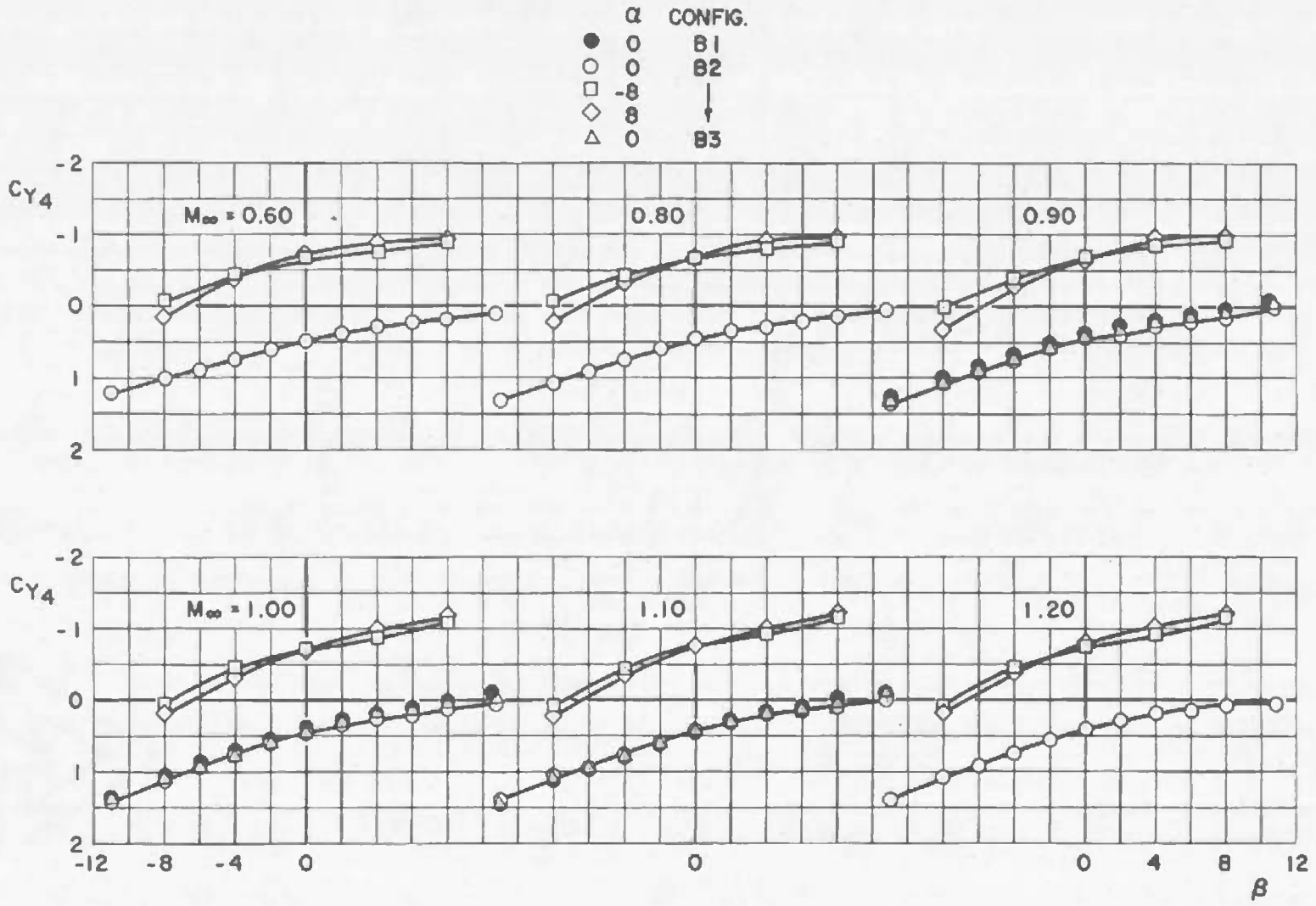

a. Mach Numbers 0.60 through 1.20

Fig. 52 Variation of SRM Side-Force Coefficient with Sideslip Angle for Configurations B1, B2, and B3

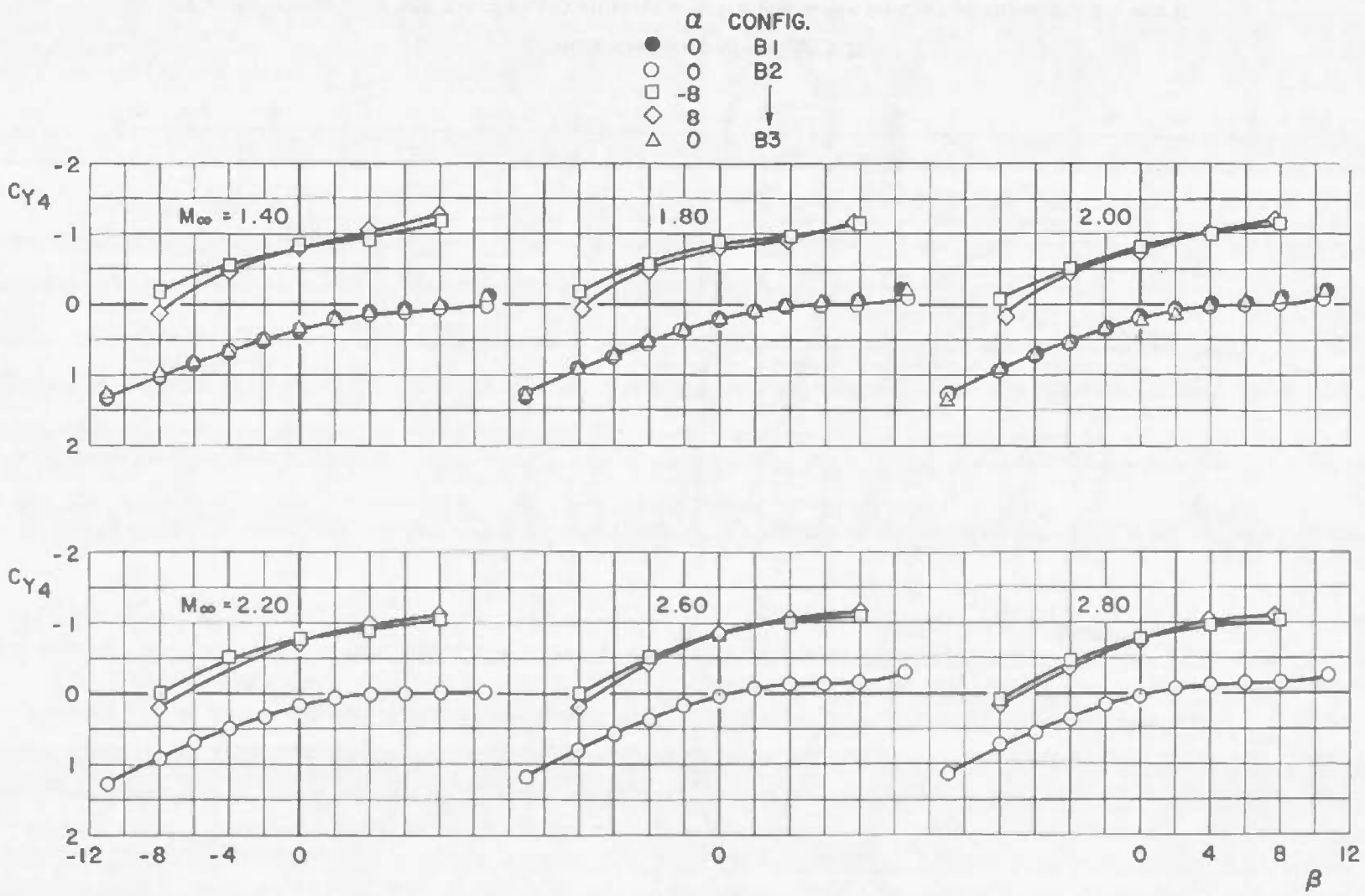

b. Mach Numbers 1.40 through 2.80

Fig. 52 Continued

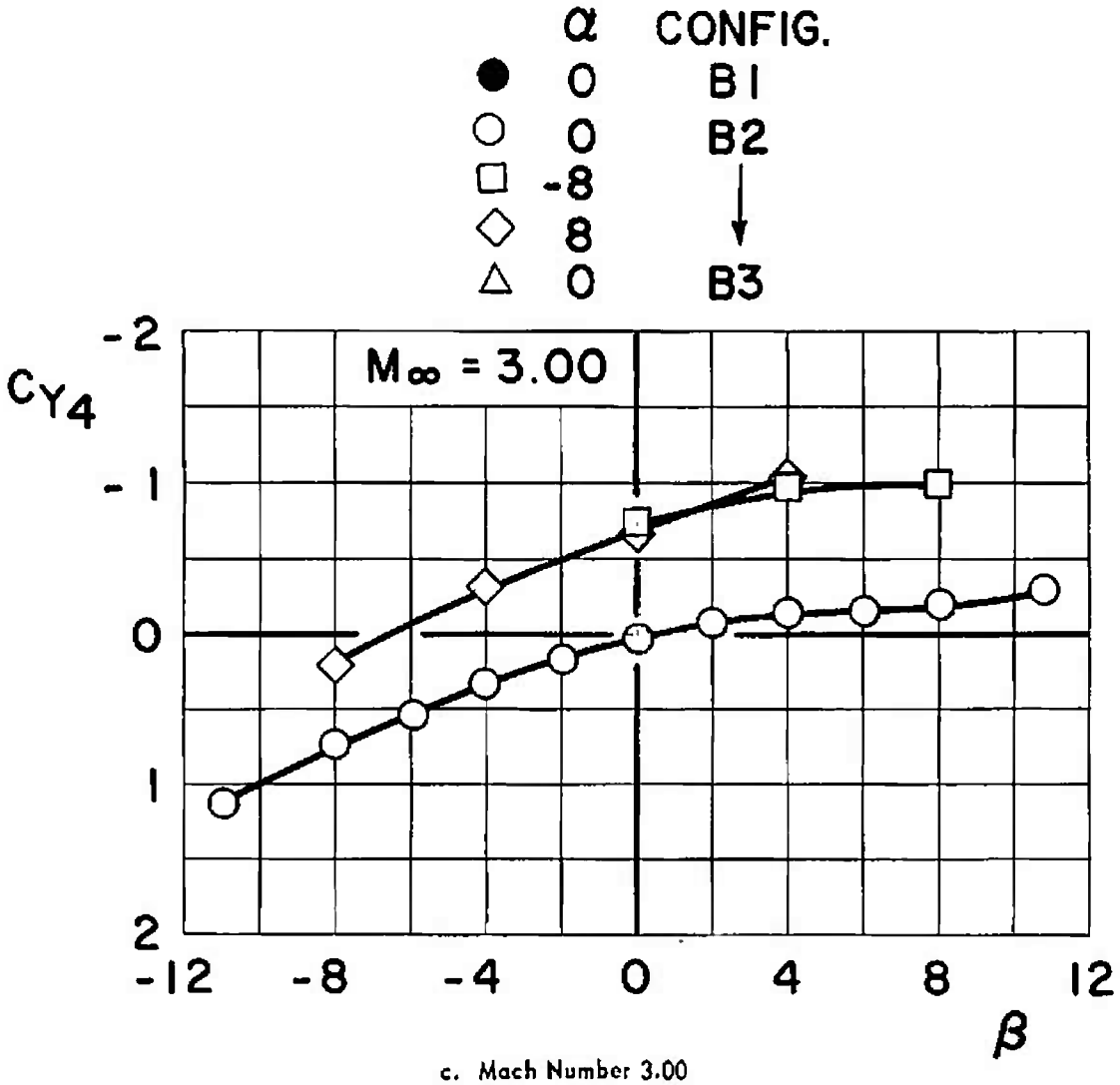

c. Mach Number 3.00

Fig. 52 Concluded

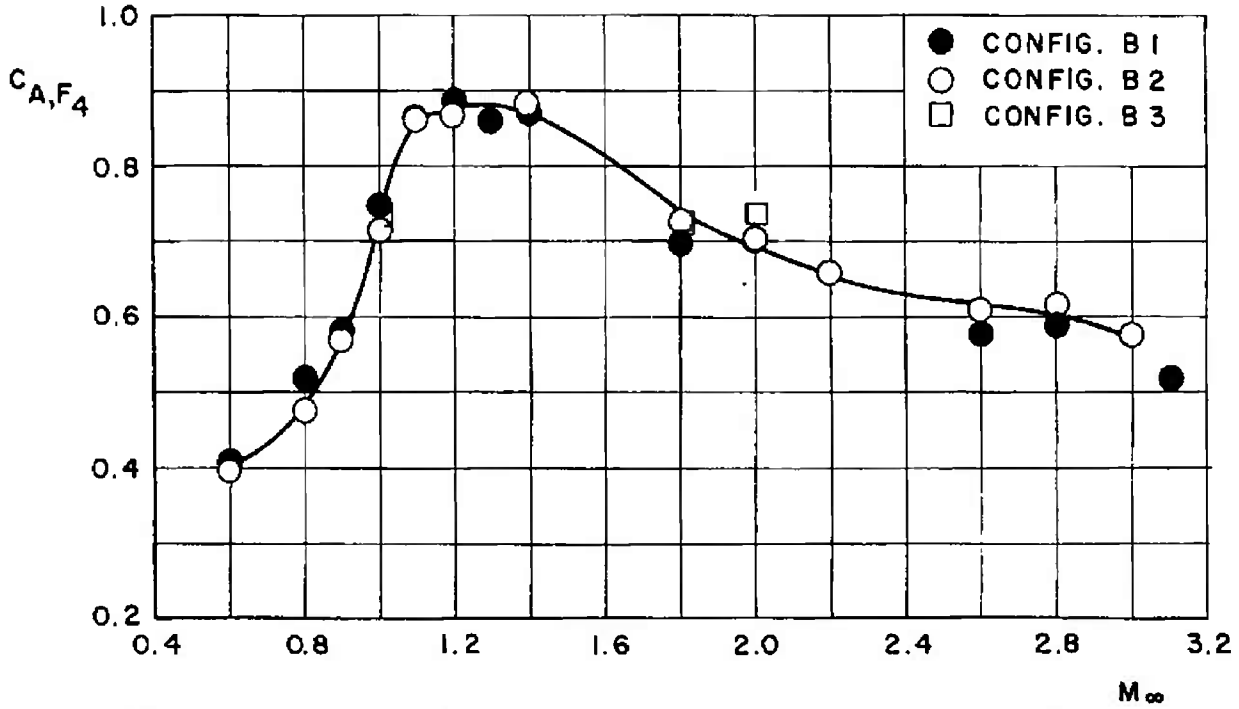

Fig. 53 Variation of SRM Forebody Axial-Force Coefficient with Mach Number for Configurations B1, B2, and B3 at α, β = 0

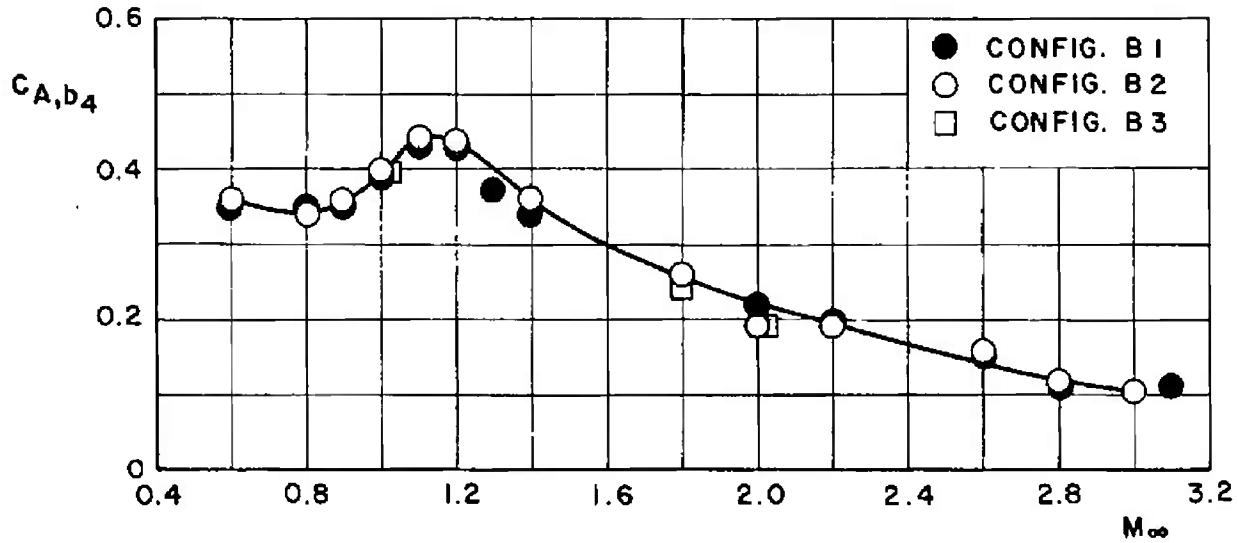

Fig. 54 Variation of SRM Base Axial-Force Coefficient with Mach Number for Configurations B1, B2, and B3 at α, β = 0

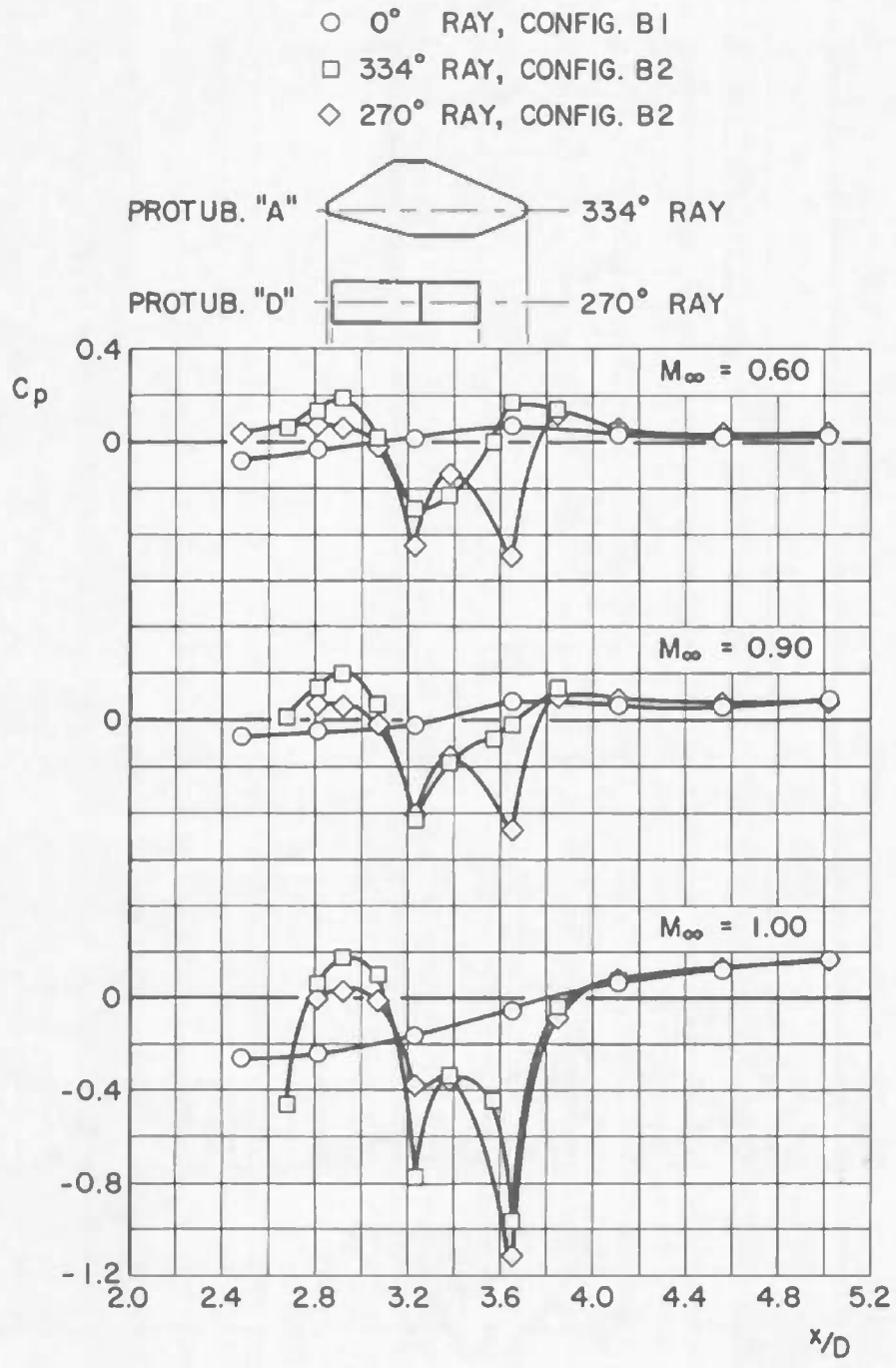

a. Mach Numbers 0.60, 0.90, and 1.00

Fig. 55 Variation of Centerbody Surfoce Pressure Coefficient with Model Stotion for Configurotions B1 ond B2 at α, β = 0

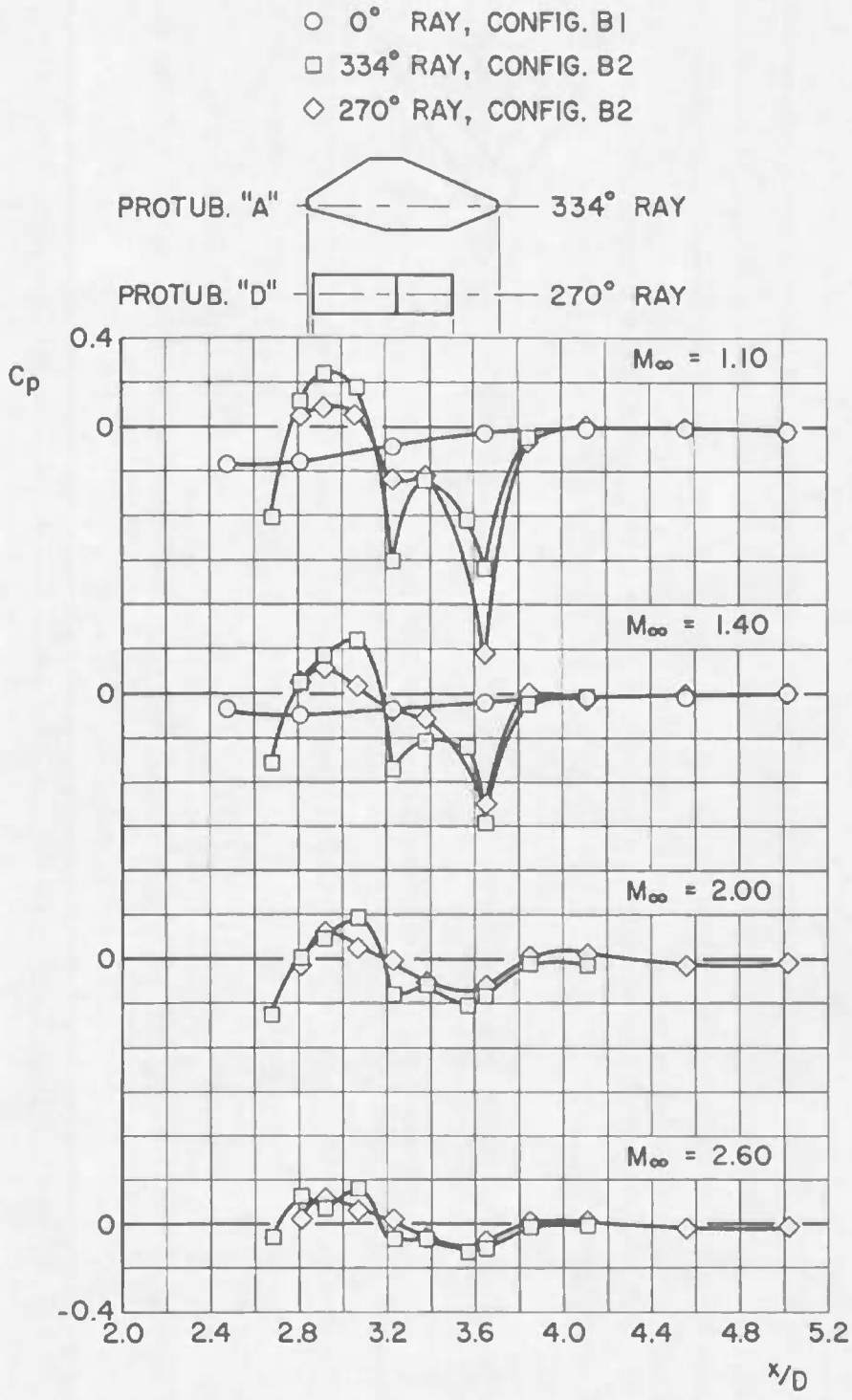

b. Mach Numbers 1.10, 1.40, 2.00, and 2.60

Fig. 55 Concluded

TABLE I
MACH NUMBER INDEX

Mach Number	Configuration				
	M1	M2	B1	B2	B3
0.60	P	F		F,P	
0.80	P	F,P	F	F,P	P
0.90	F,P	F,P	F	F,P	F,P
1.00	F,P	F,P		F,P	F,P
1.10	F,P	F,P	F	F,P	F,P
1.20	P	F,P		F,P	P
1.40	F	F,P	F	F,P	F,P
1.80	F	F,P	F	F,P	F,P
2.00	F	F,P	F	F,P	F,P
2.20	F	F,P		F,P	P
2.60		P		F,P	P
2.80				F	
3.00				F	

Legend: F - Force Data

P - Pressure Data

TABLE II
UNCERTAINTIES

a. Calibration Uncertainties

M_∞	Component	$\pm\delta C_m$	$\pm\delta C_N$	$\pm\delta C_n$	$\pm\delta C_Y$	$\pm\delta C_{A,F}$	$\pm\delta C_{A,b}$	$\pm\delta C_P$
0.60	MOL-Gemini	.056	.016	.055	.013	.016	.015	.019
1.00		.039	.011	.038	.009	.011	.010	.013
1.40		.039	.009	.033	.008	.011	.010	.012
2.00		.044	.017	.057	.016	.016	.014	.017
2.60		.068	.017	.060	.016	.016	.014	.018
0.60	Composite	.219	.067	.122	.026	.031	.019	
1.00		.171	.046	.101	.019	.028	.013	
1.40		.159	.040	.083	.017	.026	.011	
2.00		.288	.071	.142	.031	.033	.015	
2.60		.318	.074	.148	.033	.027	.014	
0.60	SRM	.332	.053	.193	.027	.031	.016	
1.00		.234	.037	.139	.019	.023	.011	
1.40		.203	.032	.117	.017	.020	.010	
2.00		.380	.059	.209	.031	.033	.013	
2.60		.394	.062	.219	.032	.034	.014	

TABLE II (Concluded)

b. Total Uncertainties

M_∞	Component	$\pm\delta C_m$	$\pm\delta C_N$	$\pm\delta C_n$	$\pm\delta C_Y$	$\pm\delta C_{A,F}$	$\pm\delta C_{A,b}$	$\pm\delta C_P$
0.60	MOL-Gemini	.153	.047	.106	.032	.017	.015	.019
1.00		.106	.033	.074	.022	.012	.010	.013
1.40		.094	.029	.064	.019	.050	.010	.012
2.00		.169	.052	.118	.037	.024	.014	.017
2.60		.177	.054	.124	.038	.024	.014	.018
0.60	Composite	2.063	.387	.478	.089	.157	.019	
1.00		1.437	.269	.337	.062	.111	.013	
1.40		1.249	.234	.291	.054	.096	.011	
2.00		1.012	.192	.723	.133	.160	.015	
2.60		1.064	.200	.756	.140	.166	.014	
0.60	SRM	1.137	.178	.383	.059	.071	.016	
1.00		.792	.124	.269	.041	.050	.011	
1.40		.687	.107	.231	.035	.044	.010	
2.00		.799	.125	.515	.080	.044	.013	
2.60		.834	.131	.539	.083	.046	.014	

Security Classification

DOCUMENT CONTROL DATA - R&D

(Security classification of title, body of abstract and indexing annotation must be entered when the overall report is classified)

1 ORIGINATING ACTIVITY (Corporate author) Arnold Engineering Development Center ARO, Inc., Operating Contractor Arnold Air Force Station, Tennessee	2a REPORT SECURITY CLASSIFICATION UNCLASSIFIED 2b GROUP N/A

3 REPORT TITLE

WIND TUNNEL STUDY OF THE EFFECT OF MOL PROTUBERANCES ON STATIC-STABILITY AND PRESSURE DISTRIBUTION CHARACTERISTICS FOR SMALL-SCALE MODELS OF THE TITAN III/MOL LAUNCH VEHICLE

4 DESCRIPTIVE NOTES (Type of report and inclusive dates)

N/A

5 AUTHOR(S) (Last name, first name, initial)

Riddle, Charles D and Shadow, Tommy O., ARO, Inc.

6 REPORT DATE April 1967	7a TOTAL NO OF PAGES 102	7b NO OF REFS 2
8a CONTRACT OR GRANT NO. AF 40(600)-1200 b PROJECT NO c Program Elements 63409404/632A and 64409404/624A d	9a ORIGINATOR'S REPORT NUMBER(S) AEDC-TR-67-59 9b OTHER REPORT NO(S) (Any other numbers that may be assigned this report) N/A	

10 AVAILABILITY/LIMITATION NOTICES

This document is subject to special export controls and each transmittal to foreign governments or foreign nationals may be made only with prior approval of Space Systems Div. (SSBDM) Los Angeles, Calif.

11 SUPPLEMENTARY NOTES Available in DDC	12 SPONSORING MILITARY ACTIVITY Space Systems Division Air Force Systems Command Los Angeles, Calif.

13 ABSTRACT

Force, pressure, and acoustical data were obtained for the Titan III/MOL (Manned Orbiting Laboratory) launch vehicle in Tunnels 16T and 16S of the Propulsion Wind Tunnel Facility. The primary objective of the test was to determine the effect of MOL protuberances on stability and axial-force coefficients and on surface pressure distributions. The force data were measured using three balances which sensed aerodynamic loads separately on the MOL-Gemini section, on the composition vehicle, and on one solid rocket motor. Mach number was varied from 0.60 to 3.00. Protuberance variations produced measurable changes in stability and axial-force characteristics for the MOL-Gemini section only. Surface pressures near the protuberances returned to protuberance-free trends within approximately 0.5-core diameters downstream of a protuberance trailing edge.

(AFR 310-2, Statement 2)

DD FORM 1 JAN 64 1473

Security Classification

14 KEY WORDS	LINK A		LINK B		LINK C	
	ROLE	WT	ROLE	WT	ROLE	WT
Titan III launch vehicle MOL Protuberances stability pressure distribution characteristics						

6. Missiles -- Titan III
1. Space vehicles -- Protuberance effects
2. " -- Pressure distribution
3. " -- Effects
4. Space vehicles -- Stability
5. Manned orbiting laboratory (MOL)

INSTRUCTIONS

1. ORIGINATING ACTIVITY: Enter the name and address of the contractor, subcontractor, grantee, Department of Defense activity or other organization *(corporate author)* issuing the report.

2a. REPORT SECURITY CLASSIFICATION: Enter the overall security classification of the report. Indicate whether "Restricted Data" is included. Marking is to be in accordance with appropriate security regulations.

2b. GROUP: Automatic downgrading is specified in DoD Directive 5200.10 and Armed Forces Industrial Manual. Enter the group number. Also, when applicable, show that optional markings have been used for Group 3 and Group 4 as authorized.

3. REPORT TITLE: Enter the complete report title in all capital letters. Titles in all cases should be unclassified. If a meaningful title cannot be selected without classification, show title classification in all capitals in parenthesis immediately following the title.

4. DESCRIPTIVE NOTES: If appropriate, enter the type of report, e.g., interim, progress, summary, annual, or final. Give the inclusive dates when a specific reporting period is covered.

5. AUTHOR(S): Enter the name(s) of author(s) as shown on or in the report. Enter last name, first name, middle initial. If military, show rank and branch of service. The name of the principal author is an absolute minimum requirement.

6. REPORT DATE: Enter the date of the report as day, month, year, or month, year. If more than one date appears on the report, use date of publication.

7a. TOTAL NUMBER OF PAGES: The total page count should follow normal pagination procedures, i.e., enter the number of pages containing information.

7b. NUMBER OF REFERENCES: Enter the total number of references cited in the report.

8a. CONTRACT OR GRANT NUMBER: If appropriate, enter the applicable number of the contract or grant under which the report was written.

8b, 8c, & 8d. PROJECT NUMBER: Enter the appropriate military department identification, such as project number, subproject number, system numbers, task number, etc.

9a. ORIGINATOR'S REPORT NUMBER(S): Enter the official report number by which the document will be identified and controlled by the originating activity. This number must be unique to this report.

9b. OTHER REPORT NUMBER(S): If the report has been assigned any other report numbers *(either by the originator or by the sponsor)*, also enter this number(s).

10. AVAILABILITY/LIMITATION NOTICES: Enter any limitations on further dissemination of the report, other than those imposed by security classification, using standard statements such as:

(1) "Qualified requesters may obtain copies of this report from DDC."

(2) "Foreign announcement and dissemination of this report by DDC is not authorized."

(3) "U. S. Government agencies may obtain copies of this report directly from DDC. Other qualified DDC users shall request through _____."

(4) "U. S. military agencies may obtain copies of this report directly from DDC. Other qualified users shall request through _____."

(5) "All distribution of this report is controlled. Qualified DDC users shall request through _____."

If the report has been furnished to the Office of Technical Services, Department of Commerce, for sale to the public, indicate this fact and enter the price, if known.

11. SUPPLEMENTARY NOTES: Use for additional explanatory notes.

12. SPONSORING MILITARY ACTIVITY: Enter the name of the departmental project office or laboratory sponsoring *(paying for)* the research and development. Include address.

13. ABSTRACT: Enter an abstract giving a brief and factual summary of the document indicative of the report, even though it may also appear elsewhere in the body of the technical report. If additional space is required, a continuation sheet shall be attached.

It is highly desirable that the abstract of classified reports be unclassified. Each paragraph of the abstract shall end with an indication of the military security classification of the information in the paragraph, represented as *(TS), (S), (C), or (U)*

There is no limitation on the length of the abstract. However, the suggested length is from 150 to 225 words.

14. KEY WORDS: Key words are technically meaningful terms or short phrases that characterize a report and may be used as index entries for cataloging the report. Key words must be selected so that no security classification is required. Identifiers, such as equipment model designation, trade name, military project code name, geographic location, may be used as key words but will be followed by an indication of technical context. The assignment of links, rules, and weights is optional.